Glasnik hemičara i tehnologa Bosne i Hercegovine

Bulletin of the Chemists and Technologists of Bosnia and Herzegovina

Print ISSN: 0367-4444
Online ISSN: 2232-7266

48

June 2017.

Prirodno-matematički fakultet Sarajevo
Faculty of Science Sarajevo

Glasnik hemičara i tehnologa Bosne i Hercegovine

Bulletin of the Chemists and Technologists of Bosnia and Herzegovina

Print ISSN: 0367-4444
Online ISSN: 2232-7266

48

June 2017.

Prirodno-matematički fakultet Sarajevo
Faculty of Science Sarajevo

Glasnik hemičara i tehnologa Bosne i Hercegovine

Bulletin of the Chemists and Technologists of Bosnia and Herzegovina

Print ISSN: 0367-4444
Online ISSN: 2232-7266

Zmaja od Bosne 33-35, BA-Sarajevo
Bosnia and Herzegovina
Phone: +387-33-279-918
Fax: +387-33-649-359
E-mail: glasnik@pmf.unsa.ba
glasnikhtbh@gmail.com

REDAKCIJA / EDITORIAL BOARD

Časopis izlazi polugodišnje, a kompletna tekst verzija objavljenih radova je dostupna na http://www.pmf.unsa.ba/hemija/glasnik.

The journal is published semiannual, and full text version of the papers published are available free of cost at http://www.pmf.unsa.ba/hemija/glasnik.

Citiran u *Chemical Abstracts Service*.

Cited by *Chemical Abstracts Service*.

www.cas.org

Citiran u EBSCO Host.

Cited by EBSCO Host.

Glasnik hemičara i tehnologa Bosne i Hercegovine

Print ISSN: 0367-4444
Online ISSN: 2232-7266

Bulletin of the Chemists and Technologists of Bosnia and Herzegovina

2017
Issue *48*

CONTENT

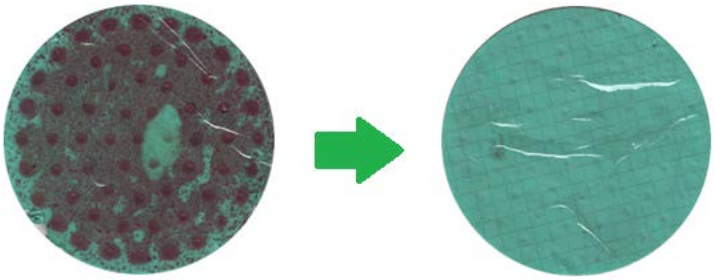

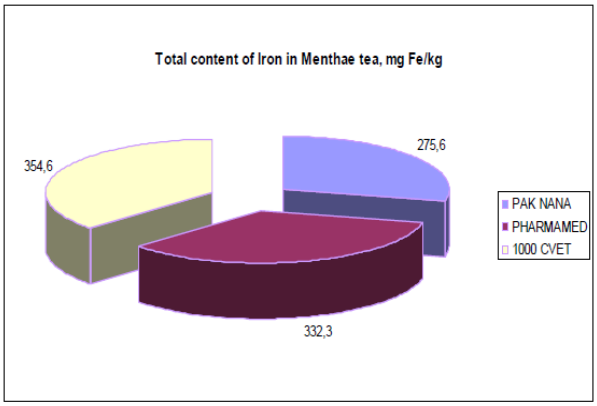

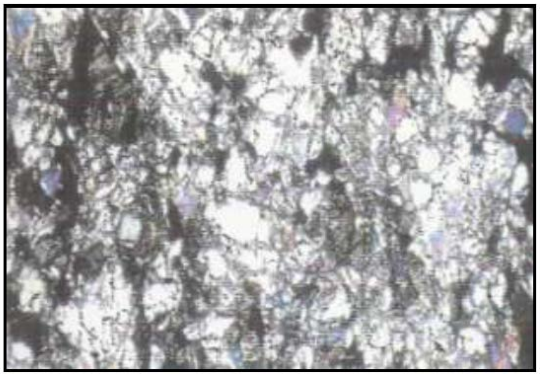

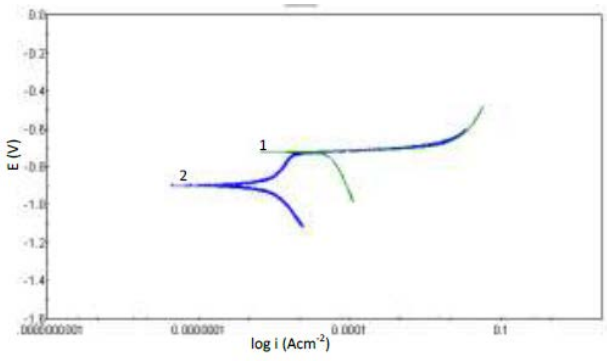

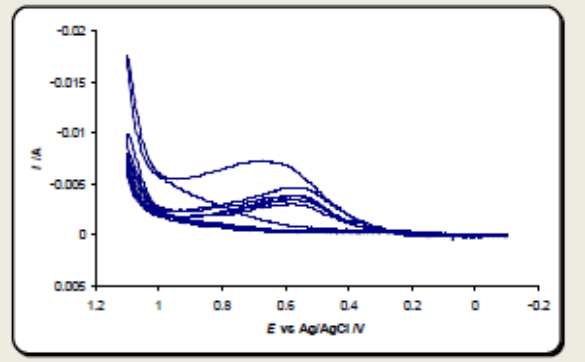

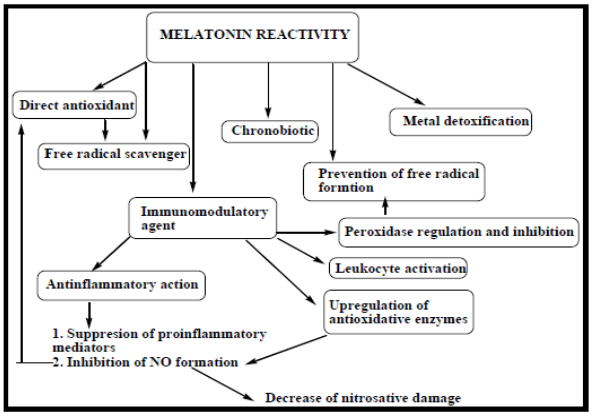

Editorial

6th Regional Symposium on Electrochemistry of South-East Europe was held from 11th to 15th June 2017. in Balatonkenese, Hungary with the organizational support of chemical and electrochemical societies from 17 countries. The scientific theme of the meeting was "Renaissance of Electrochemistry in the 21th century and its effect on the development of South-East Europe".

This, now already well established meeting of electrochemists was organized for the first time in Rovinj, Croatia in 2008, followed by meetings in Belgrade, Serbia (2010), Bucharest, Romania (2012), Ljubljana, Slovenia (2013), Pravets, Bulgaria (2015) and Balatonkense, Hungary this year. Location of the 7th Symposium in 2019 will be Zadar, Croatia. Proceedings of the meeting are published in the open access Journal of Electrochemical Science and Engineering (http://www.jese-online.org/).

Society of Chemists and Technologists of Canton Sarajevo joined organizing societies in the organization of 5th meeting in Bulgaria, 2015. During that meeting, the Association of South-East European Electrochemists (ASEE) was established by a Common Decision of the Scientific Committee (SC) of the Symposium (http://www.rse-see.eu/index.php/about-asee). Mission of the Association is to:

- contribute to the advancement of the fundamental and applied research in the field of electrochemistry
- enhance the regional scientific communication and cooperation in electrochemistry
- help the bridging of the regional electrochemical science and industry
- accelerate regional with international networking in the broad area of electrochemistry
- support, facilitate and rationalize the dissemination and exploitation of knowledge and innovations in electrochemistry and its applications
- organize traditional meetings in the field of electrochemical research, technologies and innovations

Editors

Glasnik hemičara i tehnologa Bosne i Hercegovine

Bulletin of the Chemists and Technologists of Bosnia and Herzegovina

2017

48

1-4

Print ISSN: 0367-4444
Online ISSN: 2232-7266

UDC: _____

Original Scientific paper

Influence of deposition parameters on pulsed laser deposition of $K_{0.3}MoO_3$ thin films

Đekić M.*, Salčinović Fetić A., Hrvat K., Lozančić M.

Faculty of Science, Zmaja od Bosne 33, Sarajevo, Bosnia and Herzegovina

Article info
Received: 19/04/2017
Accepted: 29/05/2017

Keywords:
Pulsed laser deposition
Potassium blue bronze
Thin films
Deposition parameters

***Corresponding author:**
E-mail: majadeki@gmail.com
Phone: +387-33-279891

Abstract: Pulsed laser deposition (PLD) has become the most important technique for the production of new materials with complex stoichiometry and multilayered structures. In this paper we present parameters that influence the production of $K_{0.3}MoO_3$ (KBB) thin films by PLD. KBB is a quasi-one-dimensional (q-1D) conductor that exhibits transition to a new ground state of charge density wave (CDW) below a transition temperature *Tp*. It is considered to be a "canonical" CDW system and its properties have been extensively researched in bulk. In recent years, production of KBB thin films has enabled investigation of CDW properties in the conditions of reduced dimensionality. Choice of deposition parameters highly influences production of the films and therefore it is essential to investigate it in order to obtain high quality films. This investigation enables one to determine optimal conditions for the production of KBB thin films by PLD.

INTRODUCTION

Metals with a chain-like structure which are highly anisotropic and therefore can be considered as quasi-one-dimensional (q-1D) exhibit a transition to a new ground state of charge density wave (CDW). Potassium blue bronze (KBB) is a commonly researched inorganic system with CDW, but it has not been produced in thin film form until recently (Starešinić et al., 2012; Dominko et al., 2011; Đekić et al., 2015; Đekić et al., 2013). It has a deep blue color hence the name "potassium blue bronze". Our main motivation for KBB thin films production was the investigation of reduced dimensionality effects on CDW properties of the material (Borodin, 1986; Zaitsev-Zotov et al., 1992; Zaitsev-Zotov et al., 2010; Schneemeyer et al., 1984; McCarten, et al., 1992).

Properties of the obtained films depend on production parameters such as: ambient gas and pressure, substrate temperature, incident laser fluence, deposition geometry and repetition rate. Deposited films were characterized using several standard characterization techniques: ultraviolet-visible (UV-vis) spectroscopy, atomic force microscopy (AFM), scanning electron microscopy (SEM), time-of-flight elastic recoil detection (TOF-ERDA), electrical transport measurements and femtosecond time-resolved spectroscopy (fs-TRS). Investigation of the influence of deposition conditions on the quality of the films enabled us to determine optimal conditions for further depositions.

EXPERIMENTAL PROCEDURE

In pulsed laser deposition (PLD) technique (Willmott and Huber, 2000; Christen and Eres, 2008; Schou, 2009; Marla et al., 2011), substrate and target are mounted in a vacuum chamber at a certain distance and a laser pulse is used to ablate the material from the target. Following ablation, plasma is created and material from the plasma is deposited on the substrate. Generally, deposition can be performed either in a gas atmosphere or vacuum.

Thin films of KBB were produced out of a polycrystalline $K_{0.3}MoO_3$ powder which was pressed in tablets of 20 mm diameter. The target was mounted on a rotating holder opposite to a substrate. Depositions were performed on (1-102) Al_2O_3 (ALO) and (510) $SrTiO_3$ (STO) substrates of 10 x 10 x 1 mm^3 and 5 x 5 x 0.5 mm^3 dimensions. These substrates were chosen because they have suitable parameters for epitaxial growth (J. van der

Zant, 1996). Depositions were performed with an excimer KrF* laser (COMPexPro) of a wavelength 248 nm, pulse duration ≥7 ns, repetition rate 2-50 Hz and fluence 0.2-10 J/cm^2. Substrate was mounted on a heater at a typical distance of 5 cm away from the target. Number of pulses was usually 6000, with several attempts at 3000, 9000, 10000 and 15000. After a series of trials we have fixed fluence to 2.4 J/cm^2 and repetition rate to 5 Hz. Depositions were performed in an oxygen atmosphere with pressure (p_{O2}) varying between 1-10 Pa and a substrate temperature (Ts) between 375-450°C. Here, we will present the influence of the number of pulses, Ts and p_{O2} on thickness, stoichiometry and texture of the films on two different types of substrates

Table 1: Thickness d, stoichiometry, substrate temperature T_S, oxygen pressure p_{O2}, number of pulses and errors ΔK and ΔO due to measuring technique in K and O fraction of several KBB films from the 7th batch. Some thickness values exceeded limitations of the measuring method.

Film	d (nm)	Stoichiometry	Ts (°C)	p_{O2} (mbar)	No. of pulses	ΔK	ΔO
BB6 ALO	336	$K_{0.24}MoO_{2.86}$	375	0.06 O_2	6000	0.03	0.35
BB5 STO	392	$K_{0.29}MoO_{3.20}$	400	0.08 O_2	6000	0.04	0.40
BB2 ALO	336	$K_{0.28}MoO_{2.82}$	450	0.06 O_2	6000	0.03	0.35
BB9 ALO	294	$K_{0.29}MoO_{3.24}$	450	0.08 O_2	6000	0.04	0.40
BB8 ALO	340	$K_{0.30}MoO_{3.00}$	425	0.08 O_2	6000	0.04	0.42
BB7 ALO	468	$K_{0.19}MoO_{3.15}$	375	0.08 O_2	6000	0.03	0.44
BB2 STO	468	$K_{0.31}MoO_{3.31}$	450	0.06 O_2	6000	0.04	0.46
BB6 STO	468	$K_{0.30}MoO_{3.13}$	375	0.06 O_2	6000	0.04	0.44
BB3 STO	>524	$K_{0.28}MoO_{3.40}$	400	0.04 O_2	9000	0.04	0.48
BB5 ALO	397	$K_{0.27}MoO_{3.39}$	400	0.08 O_2	6000	0.04	0.48
BB11 ALO	>524	$K_{0.31}MoO_{3.25}$	400	0.04 O_2	15000	0.04	0.45
BB12 ALO	184	$K_{0.29}MoO_{3.03}$	400	0.04 O_2	3000	0.04	0.42
BB4 ALO	>524	$K_{0.28}MoO_{3.07}$	400	0.04 O_2	10000	0.04	0.43

Thickness and stoichiometry of some of the deposited films were determined by TOF-ERDA. The films were irradiated with 20 MeV $^{127}I^{6+}$ ion beam and two detectors registered energy of recoiled ions and time of flight of each recoil. Analysis of the results revealed distribution of elements in the examined films and part of the substrate as well as possible contamination of the film.

Imaging using AFM was performed by NanosurfFlex AFM (NorFarb). Linear scanning rate was optimized between 1.5 and 2 Hz with scan resolution of 512 samples per line. Images were acquired in contact mode with silicon and silicon-nitride tips.

RESULTS AND DISCUSSION

In recent years, we have produced seven batches of KBB thin films comprising more than 100 samples by PLD in different conditions.

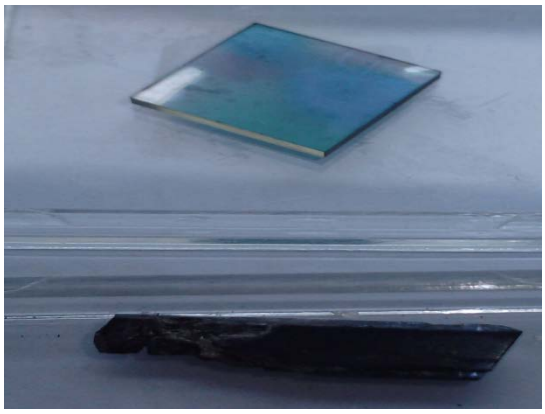

Figure 1: KBB film (above) and crystal (below).

Comparison between a KBB film and crystal is presented in Figure 1.

Results of TOF-ERDA revealed that thickness of the deposited films varied between 100 nm and >524 nm. The results are presented in Table 1 for some of the films. Exact thickness for the thicker films (>524 nm) could not be determined because of the limitations of TOF-ERDA method. As expected, thickness increases with the number of pulses as presented in Figure 2. Atomic ratio of K/Mo and O/Mo in stoichiometry of the produced films does not change significantly with the number of pulses, as presented in Figure 3.

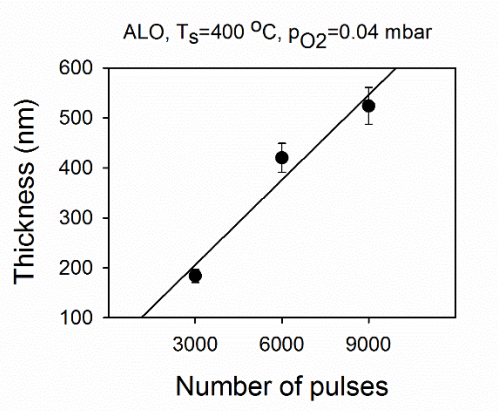

Figure 2: Film thickness versus number of pulses. Line is just guide for the eye. Bars indicate uncertainty in value.

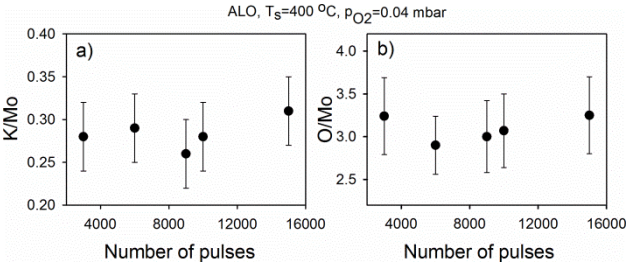

Figure 3: Stoichiometry of deposited films vs. number of pulses for ALO substrate: a) ratio of K/Mo and b) O/Mo atoms. Bars indicate uncertainty in value.

Influence of p_{02} on stoichiometry of the deposited films is presented in Figure 4. We notice that ratios of K and O to Mo follow the same trend for different substrate temperatures *Ts*. Ratio of K/Mo atoms increases up to 0.04 mbar and then it starts to decrease while the ratio of O/Mo atoms increases with p_{02} in the entire range. Similar trend was noticed in (Mantel et al., 1997) for $Rb_{0.3}MoO_3$ films produced by PLD.

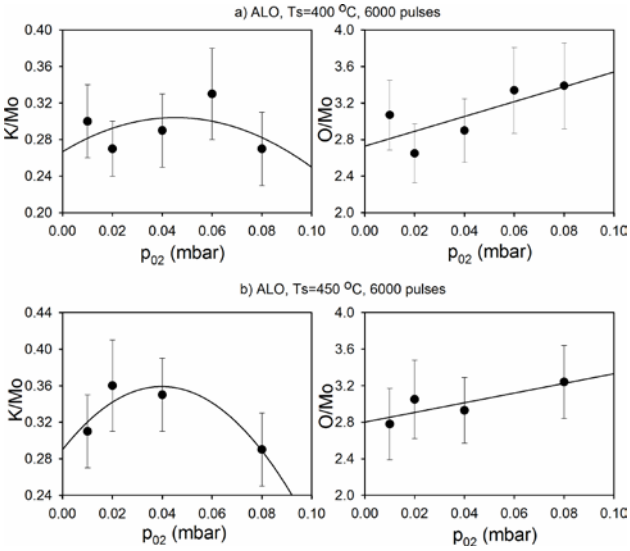

Figure 4: Atomic ratios of K and O to Mo vs. p_{02} for ALO substrate at a) *Ts*=400 °C and b) *Ts*=450 °C. Lines are just guide for the eye. Bars indicate uncertainty in value.

Influence of *Ts* on stoichiometry of the deposited films is presented in Figure 5. Atomic ratios of K/Mo and O/Mo increase with *Ts* for the films deposited on STO substrate in the entire range, while for the films grown on ALO substrate atomic ratios of these elements start to decrease at 420 °C.

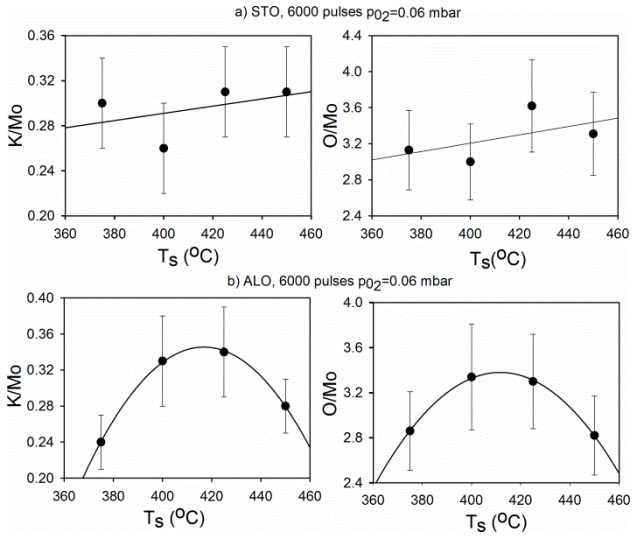

Figure 5: Ratio of K/Mo and O/MO atoms vs. *Ts* for a) STO and b) ALO substrate. Lines are just guide for the eye. Bars indicate uncertainty in value.

AFM revealed that the films were comprised of nanometer sized grains with lengths between 100 and 450 nm and widths between 50 and 150 nm. The films grown on STO substrate exhibited better ordering of the grains than those grown on ALO. Figure 6 represents length of the grains versus *Ts* and p_{02} for different substrates.

The length of the grains decreases with *Ts* down to 425 °C and then it starts to increase for both substrates. For ALO substrates at two different *Ts* the grain length increases with p_{O2} up to 0.06 mbar and then it starts do decrease.

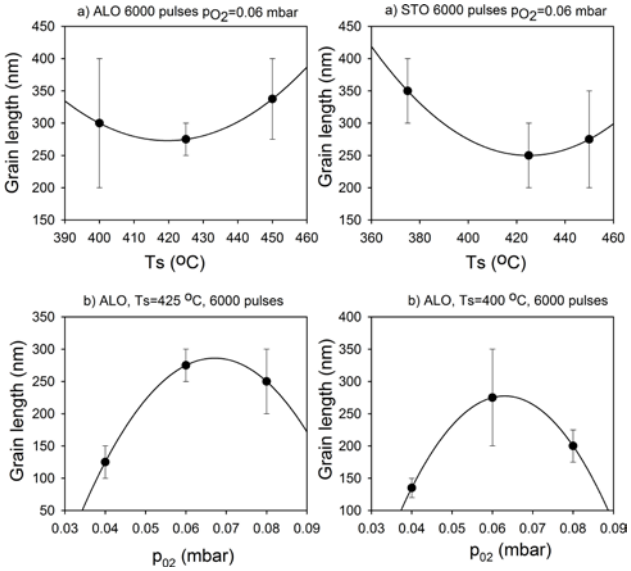

Figure 6: Dependence of the grain length on a) *Ts* for ALO and STO substrates and b) p_{O2} for ALO substrate. Lines are just guide for the eye. Bars indicate uncertainty in value.

CONCLUSION

Based on the analysis of the influence of p_{02} and *Ts* on the quality of the deposited films we were able to determine optimal conditions for the production of KBB films. Other characterization techniques like electrical transport measurements and fs-TRs enabled us to detect transition to CDW state in some of the films. We concluded that the optimal conditions for the production of KBB films are *Ts*=425 °C and p_{02}=0.06 mbar. Further production of KBB thin films is on the way but this time with a completely different PLD system. New system required optimization of p_{02} and *Ts* all over again because every vacuum chamber is unique. However, our preliminary results showed that deposition conditions in a new chamber were not that far from our previously established values and we were able to determine optimal p_{02} and *Ts* very fast. Preliminary results show that we have managed to produce better quality films than before. Further investigation will include the influence of other deposition parameters like repetition rate on the deposited films.

Acknowledgements

This work was supported by the Federal Ministry of Education and Science under contract no. 05-39-3948-1/15.

REFERENCES

Borodin, D.V. (1986). Jumps between metastable states of the quasi-1D conductor TaS_3 with submicron transverse dimensions, *JETP Letters, 43*, 625.

Christen H. M., Eres, G. (2008). Recent advances in pulsed-laser deposition of complex oxides, *Journal of Physics: Condens. Matter*, 20, 264005.

Dominko, D., et al. (2011). Detection of Charge Density Wave Ground State in Granular Thin Films of Blue Bronze $K_{0.3}MoO_3$ by femtosecond spectroscopy. *Journal of Applied Physics, 110 (1)*,

Đekić, M., et al. (2013). Nanocrystalline thin films with charge density wave ground state, *Vacuum, 98*, 93-99.

Đekić, M., et al. (2015). Variable range hopping conductivity in nanocrystalline films of $K_{0.3}MoO_3$, *Thin Solid Films, 591*, 210-214.

J. van der Zant, H. S. (1996). Thin-film growth of the charge-density-wave oxide $Rb_{0.3}MoO_3$, *Appl. Phys. Lett., 68*, 3823.

Mantel, O.C., et al. (1997). Thin films of the charge-density-wave oxide Rb0.3MoO3 by pulsed-laser deposition, *Physical Review B, 55,7.*

Marla, D., et al. (2011). Critical assessment of the issues in the modeling of ablation and plasma expansion processes in the pulsed laser deposition of metals, *J. Appl. Phys.*, ***109***, 021101.

McCarten, J., et al. (1992). Charge-density-wave pinning and finite-size effects in $NbSe_3$, *Physical Review B, 46*, 4456

Schneemeyer, L. F., et al. (1984). Dramatic impurity effects on the charge-density wave in potassium molybdenum bronze, *Physical Review B, 30*, 15.

Schou, J. (2009). Physical aspects of the pulsed laser deposition technique: The stoichiometric transfer of material from target to film, *Applied Surface Science, 255*, 5191.

Starešinić, D., et al. (2012). Charge density waves in nanocrystalline thin films of blue bronze $K_{0.3}MoO_3$. *Physica B, 407*, 1889.

Willmott, P. R., Huber, J. R. (2000). Pulsed laser vaporization and deposition, Review of Modern Physics, 72, 315–328

Zaitsev-Zotov, S. V. et al. (1992). Mesoscopic behavior of the threshold voltage in ultra-small specimens**,** *Journal of Physics I (France), 2*, 111.

Zaitsev-Zotov, S. V., et al. (2010). *New phenomena in CDW systems at small scales*, in Book of abstracts of Collaborative workshop on Charge density waves: Small scales and ultrashort times, Vukovar, Croatia.

Summary/Sažetak

Pulsna laserska depozicija (PLD) je postala najvažnija tehnika za proizvodnju novih materijala sa kompleksnom stehiometrijom i višeslojnih struktura. U ovom radu su predstavljeni parametri koji utiču na proizvodnju tankih filmova $K_{0.3}MoO_3$ (KBB) pomoću PLD tehnike. KBB je kvazi-jednodimenzionalni (q-1D) provodnik koji prelazi u novo osnovno stanje sa valom gustoće naboja (CDW) i to na temperaturama nižim od temperature prelaza (*Tp*). Ovaj sistem se smatra "kanonskim" CDW sistemom i njegova svojstva se intenzivno proučavaju u bulk (masivnim) uzorcima. Proizvodnja tankih KBB filmova posljednjih godina omogućila je istraživanje svojstava CDW –a u uslovima smanjene dimenzionalnosti. Izbor parametara depozicije ima veliki uticaj na proizvodnju filmova te ga je stoga neophodno istražiti da bi se proizveli visoko kvalitetni filmovi. Ovo istraživanje omogućava da se odrede optimalni uslovi za depoziciju KBB tankih filmova PLD tehnikom.

Glasnik hemičara i tehnologa Bosne i Hercegovine

Bulletin of the Chemists and Technologists of Bosnia and Herzegovina

2017

48

5-8

Print ISSN: 0367-4444
Online ISSN: 2232-7266

UDC: _____

Original Scientific Paper

The Correlation between C-Reactive Protein and Regulation of Glycemia in Type-2 Diabetic Patients

Mandal Š.[a*], Čaušević A. [b]

[a] *Department of Natural Sciences in Pharmacy, Faculty of Pharmacy, University of Sarajevo, B&H*

[b] *Department of Biochemistry and Clinical Analysis, Faculty of Pharmacy, University of Sarajevo, B&H*

Article info
Received: 28/02/2017
Accepted: 05/06/2017

Keywords:
C –reactive protein
inflammation
Type 2 diabetes

***Corresponding author:**
E-mail: shakira.mandal@gmail.com
Phone: +387 61 614 203

Abstract: Inflammation plays a significant role in the development of Type 2 diabetes mellitus (T2D). Studies have indicated that C-reactive protein (CRP) as inflammatory marker is an important risk factor for insulin resistance (IR) and T2D. The purpose of this study was to determine concentrations of fasting C-reactive protein, glucose, and hemoglobin A1c (HbA1c) in a total of 40 adults with Type 2 diabetes (40-60 years of the age) and 40 healthy subjects as control group (the same ages). We found that C–reactive protein concentrations in diabetic subjects were higher than those in control group. Also, our results have shown the significant association between CRP and hemoglobin A1c levels ($p<0.05$) and positive association with glucose concentrations ($p>0.05$) in T2 diabetics. A negative, but not significant correlation of CRP with glucose and hemoglobin A1c levels was demonstrated in controls. Therefore, our findings suggest an association between glycemic control and systematic inflammation in people with diagnosed diabetes.

INTRODUCTION

The prevalence of Type 2 diabetes mellitus (T2D) as a metabolic disease with inappropriate hyperglycemia either due to deficiency of insulin secretion or reduction in the biologic effectiveness of insulin, is rapidly raising worldwide. Elevated inflammatory markers and altered adipokine concentrations have been observed in obese T2 diabetic patients. The main physiological abnormalities in Type 2 diabetic are insulin resistance (IR) and impaired insulin secretion but specific underlying mechanisms for the disease remain uncertain yet (Pradhan et al., 2001; Sattar et al., 2003; Luft et al., 2013). Some studies suggest that inflammation has a crucial intermediary role in pathogenesis of T2D, thereby linking diabetes with a number of commonly coexisting conditions thought to originate through inflammatory mechanisms. Chronic systemic inflammation an induce IR and is a key mechanism linking obesity and diabetes. As a nonspecific marker of systemic inflammation, commonly elevated in human insulin resistant states, C-reactive protein (CRP) is an acute-phase reactant synthesized in the liver in response to cytokine, especially interleukin-6 (IL-6). As such it has been associated with hyperglycemia, IR and overt type 2 Diabetes and its complications (Qi et al., 2009; Bandyopadhyay et al., 2013; Sah et al., 2015).

C-reactive protein belongs to the pentraxin family of calcium dependent ligand-binding plasma proteins. The human CRP molecule is composed of five identical non-glycosylated polypeptide subunits each containing 206 amino acid residues. Most functions of CRP are easily understood in the context of the body´s defenses to pathogen. Despite structural differences with immunoglobulin molecule, CRP shows similar functional properties with the immunoglobulins. Importantly, acute-phase CRP values show no relationship to fasting state or

diurnal patterns and have a long half-life. Analysis of serum concentration of CRP, may be performed using different instrumental methods of quantitative chemical analysis. ELISA (enzyme-linked immunosorbent assay), immunoturbidimetry, nephelometry, rapid immunodiffusion, and visual agglutination are methods used to measure of concentration of C-reactive protein. However, mostly used method nowdays is the method of immunoanalysis i.e. turbidimetry or nephelometry.

CRP, a robust clinical marker is easily measured and standardized in high-sensitivity immunoassay (detecting of CRP concentration <5mg/L), therefore providing similar results in fresh, stored, or frozen serum/plasma. Serum levels of CRP are independent of age and ethnicity. All of these factors make it a relatively stable serum protein compared with many other markers which can be used in screening for organic diseases; in monitoring the response to the treatment of inflammation and infection and detection of intercurrent infection in immune-compromised individuals, and in the few specific diseases characterized by modest or absent acute-phase responses (King et al., 2003; Bandyopadhyay et al., 2013; Mohammed et al., 2015).

Therefore, the objective of this study was to determine the concentration of C-reactive protein in Type 2 diabetes and examine the relationship between CRP with glucose and hemoglobin A1c levels.

EXPERIMENTAL

Subjects

A total of 80 participants (40 control and 40 diabetic) have been screened for serum C-reactive protein (CRP), glucose, and hemoglobin A1c (HbA1c) after obtaining informed consent. Participants involved in this study were free of evidence of hepatitis B or C viral infection or active liver and kidney damage and were selected on the basis of presence of history of diabetes for more than five years.

Initial diagnosis of T2D was established by a specialist of internal medicine who used World Health Organization (WHO) criteria for diagnosis of the disease. All research involving human subjects and material derived from human subjects in this study was done in accordance with ethical principles outlined in World Medical Association Declaration of Helsinki – Ethical Principles for Medical Research Involving Human Subjects (initiated in June 1964, last amendment in October 2000). Nondiabetic controls were of approximately same age (40-60 years old), with normal glucose tolerance (fasting plasma glucose less than 6.2 mmol/l and two hours postprandial glycemia less than 7.8 mmol/l).

Sample Analysis

Blood samples from all of the participants in the study were collected into siliconized tubes (BD Vacutainer Systems, Plymouth, UK).

Blood samples were withdrawn by using sterile syringe from the 12 to 14 hours of overnight fasting diabetic and control patients in the morning. All samples, after collection in sterile tubes were centrifuged at 3000 rpm for 10 minutes and serum was stored at 4°C. Fasting blood glucose concentration was measured by an enzymatic glucose hexokinase method while ion-exchange high-performance liquid chromatography was used for measurement of hemoglobin A1c (HbA1c). C-reactive protein (CRP) was measured by Sandwich Enzyme Linked Immunosorbent Assay Method (immunoturbidimetric method) applied on BT PLUS 2000-Biotechnic Instruments Bioanalyzer (Rome, Italy).

Immunoturbidimetric assay for CRP

Briefly, the test samples were treated with a specific antibody to human CRP in a suitable buffer. The turbidity induced by the formation of immune complexes was measured at 546 nm, and the values were then calculated automatically from a known standard. All the assay steps were performed automatically by the instrument. A commercial control serum was used to verify the assay performance.

Statistical analysis

All statistical analyses were done by SPSS (version 17.0 for Windows, SPSS Inc; Chicago, IL, USA). *P* values smaller than 0.05 were accepted as significant.

Within the programme, nonparametric Mann-Whitney U-test was used in order to estimate differences in glucose, hemoglobin A1c, insulin, and CRP concentration between groups. Spearman's correlation coefficient was calculated in order to analyze the relationships between the study variables.

RESULTS AND DISCUSSION

The study was conducted on 80 participants of both genders and od similar age. In our study, C-reactive protein concentrations, in Type 2 diabetes patients were slightly higher when compared to control subjects (6.33mg/L and 5.55 mg/L, respectively). Fasting serum concentrations of glucose and hemoglobin A1c (HbA1c), as expected, were significantly higher in T2D group of patients compared to controls. Results for tested clinical parameters in study participants are presented in Table I.

Table 1. Concentrations of testing parameters in studied participants.

Parameter	Controls	Type 2 Diabetics	*P* values	Normal range
Fasting glucose, mmol/L	5.3	10.3	*p<0.001*	3.9-7.2 mmol/L
C-reactive protein, mg/L	5.55	6.33	*p<0.05*	*Low risk* ≤2mg/L *Moderate risk* 2-6mg/L *High risk* ≥6 mg/L
Hemoglobin A1c, %	4.5	6.9	*p<0.001*	6.0%

C-reactive protein a marker of systemic inflammation is emerging as an independent risk factor for insulin resistance, and cardiovascular disease. Elevated CRP levels have also been linked to an increased risk of later development of diabetes. Furthermore, CRP levels are higher in people with diabetes compared with those without diabetes. These findings are in line with our results (King et al., 2003; Sattar et al., 2003; Luft et al., 2013).

One of the goals of the study was to investigate the relation between CRP and hemoglobin A1c (HbA1c) in adults with diabetes. Recent research evidence supports a link between hyperglycemia and inflammation. Such evidence is consistent with the findings in the current study, which further documented the association between hyperglycemia and inflammation in adults with diabetes (Figures 1 and 2).

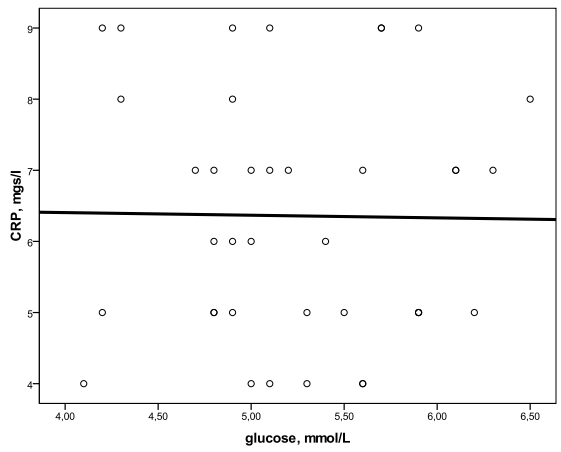

Figure 1a

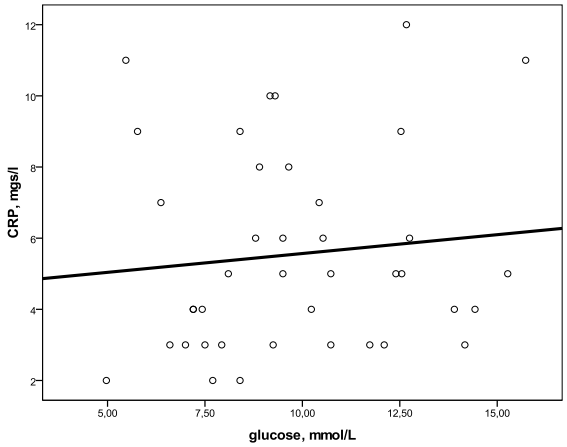

Figure 1b

Figure 1. Spearman´s correlation coefficient between glucose and CRP levels in studied patients (1a controls: *r = - 0.007, p>0.05*; 1b diabetics: *r = 0.179, p>0.05*)

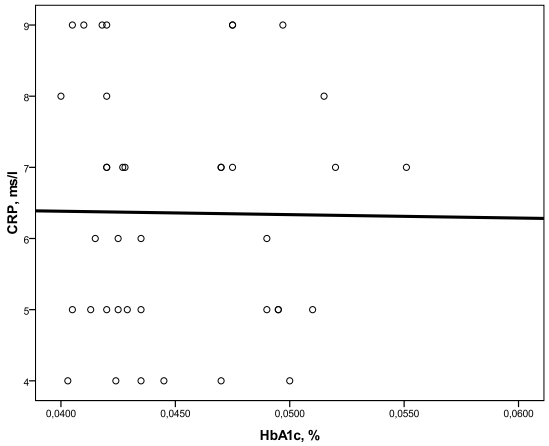

Figure 2a

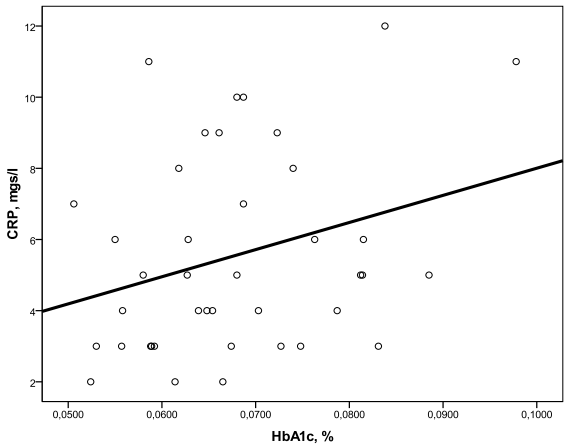

Figure 2b

Figure 2. Spearman´s correlation coefficient between hemoglobin A1c and CRP levels in studied patients (1a controls: *r = - 0.073, p>0.05*; 1b diabetics: *r = 0.371, p<0.05*)

CRP is known to be higher in people with impaired glucose tolerance and frank diabetes. Furthermore, increased CRP has been found to be a risk factor for later development of diabetes. De Luca et al., 2008; Ehiaghe et al., 2013 and Rajkovic et al., 2014, found links between CRP and insulin resistance. Other studies have related hyperglycemia to inflammation by demonstrating simultaneous inflammation, endothelial dysfunction, and insulin resistance at the physiologic level. In this study, the likelihood of elevated CRP levels increased with increase in hemoglobin A1c levels.

CONCLUSION

This is one of the first studies addressing state of hyperglycemia and its correlation to C–reactive protein levels. The study indicated that concentrations of the CRP, as a pro-inflammatory cytokine, were higher in diabetic patients compared to controls. In addition, we observed that CRP concentration significantly correlated with glycemic control i.e. hemoglobin A1c in these patients. However, due to possible influence other factors on inflammation, further studies should be observed this problem more clearly and include of high number of patients.

REFERENCES

Bandyopadhyay, R., Paul, R., Basu, K. A., Chakraborty, P., Mitra, S. (2013). Study of C Reactive Protein in Type 2 Diabetes and its Relation with Various Complications from Eastern India. *Journal of Applied Pharmaceutical Science, 3(7)*, 156-159.

De Luca, C., Olefsky, M. J. (2008). Inflammation and insulin resistance. *Federation of European Biochemical Societies Letters, 582*, 97-105.

Ehiaghe, F. A., Agbonlahor, E. D., Tatfeng, M. Y., Onikepe, F., Oviasogie, E. F., Ehiaghe, I. J. (2013). Serum C reactive protein level in type 2 diabetes mellitus patients attending diabetic clinic in Benin City, Nigeria. *Journal of Diabetes Mellitus, 3*, 168-171. King, E. D., Buchanan, A. T., Mainous, G. A., Pearson, S. W. (2003). C-reactive protein and glycemic control in adults with diabetes. *Diabetes Care, 26*, 1535–1539.

Luft, C. V., Schmidt, I. M., Pankow, S. J., Couper, D., Ballantyne, M. C., Young, H. J., Duncan, B. B. (2013). Chronic inflammation role in the obesity-diabetes association: a case-cohort study. *Diabetology & Metabolic Syndrome, 5(31)*, 1-8.

Mohammed, S. M. Alnour., Mahdi, H. A. Abdalla. (2015). A study of fibrinogen level and C-reactive protein in Type 1 and Type 2 diabetes mellitus and their relation to glycemic control. *American Journal of Medicine and Medical Sciences, 5(5)*, 201-203.

Pradhan, D. A., Manson, E. J., Rifai, N., Buring, E. J., Ridker, M. P. (2001). C–reactive protein, interleukin 6, and risk of developing Type 2 diabetes mellitus. *JAMA, 86(3)*, 327-334.

Qi, L., Rifai, N., Hu, B. F. (2009). Interleukin-6 receptor gene, plasma C-reactive protein, and diabetes risk in women. *Diabetes, 58*, 275–278.

Rajkovic, N., Zamaklar, M., Lalic, K., Jotic, A., Lukic, Lj., Milicic, T., Singh, S., Stosic, Lj., Lalic, M. N. (2014). Relationship between Obesity, Adipocytokines and Inflammatory Markers in Type 2 Diabetes:Relevance for Cardiovascular Risk Prevention. *Int. J. Environ. Res. Public Health, 11*, 4049-4065.

Sah, P. J., Yadav, K. C. (2015). Assessment of hs-Crp with serum uric acid in Type-2 diabetic patients in western region of Nepal. *Quest Journals Journal of Medical and Dental Science Research, 2(3), 01-05.*

Sattar, N., Perry, G. C., Petrie, R. J. (2003). Type 2 diabetes as an inflammatory disorder. *Br J Diabetes Vasc Dis, 3*, 36-41.

Summary/Sažetak

Inflamacija ima značajnu ulogu u razvoju Tip 2 diabetes mellitusa (T2D). Istraživanja su pokazala da je C-reaktivni protein (CRP) kao inflamatorni marker važan faktor rizika za insulinsku rezistenciju (IR) i T2D. Cilj ovog rada bio je odrediti koncentraciju natašte C-reaktivnog proteina, glukoze i hemoglobina A1c (HbA1c) kod ukupno 40 odraslih osoba s Tip 2 dijabetesom (40-60 godina starosti) i 40 zdravih ispitanika kao kontrolne grupe (iste starosne dobi). Nađeno je da je koncentracija C-reaktivnog proteina kod dijabetičara veća od izmjerene koncentracije u kontrolnoj grupi. Također, naši su rezultati pokazali i statistički značajnu korelaciju između CRP i vrijednosti hemoglobina A1c ($p < 0,05$) i pozitivnu asociranost s koncentracijama glukoze ($p > 0,05$) kod T2 dijabetičara. Pokazana je negativna korelacija ali ne i statistički značajna između CRP i vrijednosti glukoze i hemoglobina A1c u kontrolama. Dakle, naši rezultati ukazuju na povezanost regulacije glikemije i sistemske inflamacije kod osoba s dijagnosticiranim dijabetesom.

Glasnik hemičara i tehnologa Bosne i Hercegovine

Bulletin of the Chemists and Technologists of Bosnia and Herzegovina

2017

48

9-14

Print ISSN: 0367-4444
Online ISSN: 2232-7266

UDC: _____

Original Scientific Paper

Inhibitory effects of selected phenolic acids on the oscillations of the Briggs-Rauscher reaction

Džomba, E., Gojak-Salimović, S.*

University of Sarajevo, Faculty of Science, Department of Chemistry, Zmaja od Bosne 33-35, 71000 Sarajevo, B&H

Article info
Received: 13/04/2017
Accepted: 14/06/2017

Keywords:
Briggs-Rauscher reaction
Phenolic acids
Inhibition time
Oscillation

***Corresponding author:**
E-mail: sgojak@pmf.unsa.ba
Phone: 00-387-33-279-907
Fax: 00-387-33-649-359

Abstract: Phenolic acids are secondary metabolites of aromatic plant that possess prominent antioxidant activity. When an antioxidant is added to an active oscillating Briggs-Rauscher reaction mixture, there is an immediate cessation of the oscillations, an inhibition time that linearly depends on the concentration of the antioxidant added, and a subsequent regeneration of oscillations. In this study, the effects of concentration of the ethanol solutions of selected phenolic acids (gallic, caffeic, chlorogenic, rosmarinic, *p*-coumaric and *m*-coumaric acids) on the oscillatory system Briggs-Rauscher reaction were investigated. The reaction was performed in a constantly stirred reactor, with accurately defined concentrations of reactants, at constant temperature of 25°C. Flow oscillations in the Briggs-Rauscher reaction mixture were monitored as a change in potential between the platinum electrode and silver/silver chloride reference electrode. Relative antioxidant activities of phenolic acids were determined in three ways on the basis of inhibition times. The obtained results showed that the gallic and *p*-coumaric acids have much less antioxidant activity than the caffeic, chlorogenic and rosmarinic acids. The ability to inhibit oscillations of the Briggs-Rauscher reaction mixture is not showed for *m*-coumaric acid.

INTRODUCTION

Phenolic acids are widespread plant secondary metabolites. They belong to the subclass of polyphenols with more than 8000 of natural compoundsthat possess one common structural feature, a phenol (an aromatic ring bearing at least one hydroxyl group). According to the basic structure they are divided into hydroxybenzoic and hydroxycinnamic acids.

Caffeic, vanillic, ferulic and *p*-coumaric acids are found in almost all plants. Other acids are found in selected plants or foods (Robbins, 2003). The hydroxycinnamic acid class, which includes *p*-coumaric, caffeic and ferulic acids, occur most frequently as simple esters with hydroxy carboxylic acids or D-glucose. In contrast, the hydroxybenzoic acid class, such as *p*-hydroxybenzoic, gallic and ellagic acids, is present mainly in the form of glucosides (Ota *et al*., 2011).

Although the role of phenolic acids as secondary metabolites in plants is not fully clarified, it is considered to participate in many processes such as nutrient, protein synthesis, enzyme activity, photosynthesis and others.

Phenolic acids have prominent antioxidant activity. Hydroxycinnamic acids has better antioxidant properties than most hydroxybenzoic acids (Rice-Evans *et al*., 1996; Robards *et al*., 1997).

Gallic acid and its derivatives have potential for combating oxidative damages, cancer manifestations and microbial infestations. Large number of research studies are available to show its ability for the treatment of diabetes, ischemic heart diseases, ulcer and other ailments (Nayeem *et al*., 2016).

Caffeic acid, one of the most prominent naturally occurring cinnamic acids, is known to selectively block the biosynthesis of leukotrienes, components involved in immunoregulation diseases, asthma and allergic reactions (Robbins, 2003).

Chlorogenic acid is an ester formed between caffeic acid and quinic acid, and is one of major polyphenol compounds found in numerous plant species, including coffee beans, apples, and blueberries. Chlorogenic acid protects cells from oxidative stress induced by UVB radiation (Cha *et al*., 2014). Moreover, chlorogenic acid protects mesenchymal stem cells against oxidative stress (Li *et al*., 2012).

Rosmarinic acid has antioxidant and anti-inflammatory effects and is used for the treatment of asthma and reactive airway diseases, allergic disorders such as allergic rhinitis, otitis media, chemical sensitivity and multiple allergen reactivity (Stansbury, 2014).

The *p*-coumaric acid has beneficial effects on human health through their prevention of degenerative pathologies, such as cardiovascular disease and cancer (Ota *et al.*, 2011).

The *m*-coumaric acid is a polyphenol metabolite from caffeic acid, formed by the gut microflora and the amount in human biofluids is diet-dependant (Konish and Kobayashi, 2004; Mennen *et al*., 2016).

All the methods for measurements of the antioxidant activity are based on the generation of free radicals in a reaction mixture and the effects of added antioxidants on some properties of the radical or of the mixture: absorbance, quenching of chemiluminescence, electric potential, ect. These properties change depending on the amount of antioxidants added with respect to those of a reference mixture (Cervellati *et al*., 2002; Shalaby and Shanab, 2013). The Briggs-Rauscher oscillating reaction method is relatively new and inexpensive method for meausuring antioxidant activity. This method is based on the inhibitory effects by antioxidants on the oscillations of the Briggs-Rauscher reaction mixture. When antioxidants are added to an active oscillating Briggs-Rauscher reaction mixture, some of which cause an immediate cessation of the oscillations, an inhibition time that linearly depends on the concentration of the antioxidant added in a wide range of concentration, and a subsequent regeneration of the oscillations (Cervellati *et al*., 2001; Cervellati *et al*., 2002; Furrow *et al*., 2004). The inhibition time (t_{inhib}) is defined as the time elapsed between the end of the addition of the antioxidant and the first regenerated oscillation. Relative antioxidant activity with respect to a substance chosen as standard can then be determined on the basis of inhibition time (Hönor and Cervellati, 2002; Hönor *et al*., 2002).

In this study, the inhibitory effects of concentration of the ethanol solutions of selected phenolic acids (gallic, caffeic, chlorogenic, rosmarinic, *p*-coumaric and *m*-coumaric acids) on the oscillatory system Briggs-Rauscher reaction, which consisted of hydrogen peroxide, malonic acid, manganese(II) sulfate monohydrate, potassium iodate, sulfuric acid and starch as indicator, were investigated.

EXPERIMENTAL

Reagents

All used reagents were of analytical grade. Potassium iodate, sulfuric acid, hydrogen peroxide and ethanol were obtained from Semikem (Sarajevo, BiH), malonic acid, manganese(II) sulfate monohydrate and starch were obtained from Merck (Darmastadt, Germany), chlorogenic acid was obtained from Acros Organics, (Geel, Belgium), gallic acid, caffeic acid, rosmarinic acid, *p*-coumaric acid and *m*-coumaric acid were obtained from Sigma (St. Louis, USA).

Preparation of the solutions for the Briggs-Rauscher reaction

For the Briggs-Rauscher oscillating reaction (Marković and Talić, 2013; Dacić and Gojak-Salimović, 2016) the following mixture should be prepared: 0.067 mol/L potassium iodate, 1.5 mol/L hydrogen peroxide, 0.0267 mol/L sulfuric acid, 0.050 mol/L malonic acid, 0.0067 mol/L manganese(II) sulfate monohydrate and 0.01% fresh starch. In our study, for achieving the Briggs-Rauscher oscillating reaction, three stock solutions were prepared daily. **Solution A**: 43 g potassium iodate and 4.5 mL 96% sulfuric acid were dissolved in distilled water and diluted to 1 L; **Solution B**: 15.6 g malonic acid, 3.4 g manganese(II) sulfate monohydrate and 3 g starch were dissolved in distilled water and diluted to 1 L; **Solution C**: 500 mL of 30% hydrogen peroxide was diluted to 1 L.

Preparation of the solutions of selected phenolic acids

In the concentration range used in this work all of selected phenolic acids are ethanol soluble.

Apparatus

Oscillations of the Briggs-Rauscher reaction were monitored potentiometrically by recording the potential of the reaction mixture using a platinum electrode and $Ag/AgCl/KCl_{(sat)}$ reference electrode (+197 mV vs. SHE). The electrodes were connected to a pH multimeter (Phywe, Model 13702.93). The accuracy of the multimeter was ±1 mV. All measurements were conducted at constant temperature (25±0.5°C) using a thermostating system. The reaction mixture was stirred by a magnetic stirrer (600 rpm).

Procedure

The Briggs-Rauscher reaction mixture was prepared by mixing the appropriate amounts of stock solutions of reagents. For each measurement 10 mL of each solution A and B were mixed into the double-wall thermostated beaker equipped with a magnetic stir bar and placed on a stirring plate. The 10 mL of solution C was used to initiate the oscillations. After the third oscillation, 1 mL of ethanol solution of phenolic acid at corresponding concentration was added to an active Briggs-Rauscher reaction mixture. Typical potentiometric recordings for a non-inhibited and an inhibited Briggs-Rauscher reaction mixture are shown in Figure 1 and Figure 2. The inhibition times were then measured from the recordings.

The addition of 1 mL of ethanol, without phenolic acid does not interrupt the oscillations. All samples were run at least in duplicate and results were expressed as mean values.

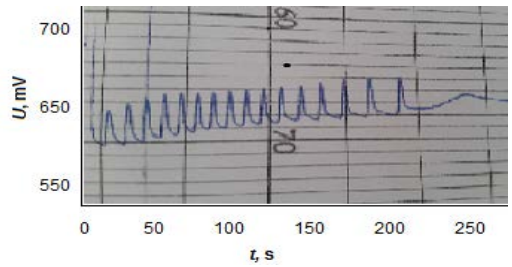

Figure 1: Recording of the potential versus time of non-inhibited Briggs-Rauscher reaction

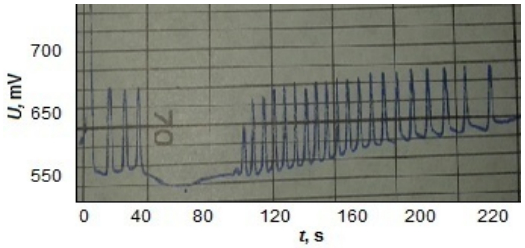

Figure 2: Recording of the potential versus time when 1 mL of a solution of gallic acid (100 mg/L) was added to 30 mL of an active Briggs-Rauscher reaction mixture after the third oscillation

RESULTS AND DISCUSSION

Our previous work showed the ability of chlorogenic acid to inhibited oscillations of the Briggs-Rauscher reaction mixture at room temperature (Dacić and Gojak-Salimović, 2016). In this study, the effects of various concentration of the ethanol solutions of selected phenolic acids (gallic, caffeic, chlorogenic, rosmarinic, *p*-coumaric and *m*-coumaric acids) on the oscillatory system Briggs-Rauscher reaction were evaluated at 25°C.

In all samples except *m*-coumaric acid, the inhibition times increased with increased concentration, and linearity was found in a wide concentration range of phenolic acid added (Figure 3). Below a certain concentration of phenolic acid added (different for each phenolic acid), the behavior deviates from linearity. At low concentrations of phenolic acids added, the inhibition times become too low to be measured as well for some other antioxidants (Cervellati *et al*., 2000). There is a threshold under which inhibition time cannot be detected and we believe that the straight-lines curve toward zero under these lower limits. At high concentrations of phenolic acids the amplitudes of resumed oscillations becomes too low, until up to a given concentration (different for each phenolic acid) oscillations do not restart.

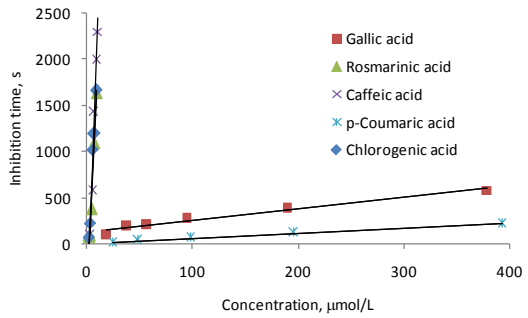

Figure 3: Straight lines of inhibition time versus concentration for the phenolic acids studied

As shown in Figure 3, the slopes of the straight lines are different, so the calculation of the relative antioxidant activity will depend on the substance chosen as standard and the concentration of the sample. The parameters of the straight lines and *R*-squared values are reported in Table 1.

Table 1: Parameters of straight-lines equations (t_{inhib}= *m*(antioxidant) + *q*) and *R*-squared values

Antioxidant	*m* (μmol/L)$^{-1}$ s	*q* (s)	R^2
Caffeic acid	326.0	–1055	0.978
Chlorogenic acid	228.7	–419.4	0.955
Rosmarinic acid	230.8	–480.1	0.970
Gallic acid	1.156	148.6	0.995
p-Coumaric acid	0.551	4.125	0.997

The relative antioxidant activity were calculated as relative activity with respect to concentrations (*rac*), relative activity with respect to slopes (*ras*) and relative activity with respect to inhibition times (*rat*) (Cervellati *et al*., 2001). Caffeic acid was chosen as standard.

Relative antioxidant activity with respect to concentrations (*rac*) is the ration between concentrations of the chosen standard and samples that give the same inhibition time:

$$rac = [std]/[smp]$$

The concentration of standard that should give the same inhibition time of the sample was calculated from the straight-line equation of the chosen standard.

Relative antioxidant activity with respect to slopes (*ras*) is the ratio between the slope of the straight line of the sample and that of the standard:

$$ras = \text{slope(smp)}/\text{slope(std)}$$

Relative antioxidant activity with respect to inhibition times (*rat*) is the ratio between the inhibition time of the sample and that of the standard at the same concentration:

$$rat = t_{inhib}(\text{smp})/t_{inhib}(\text{std})$$

The chosen concentration must be specified together with the *rat* values and must be in the linear concentration range of the standard and of all the examined substances. The obtained *rac*, *ras* and *rat* values are reported in Table 2.

Table 2: Relative antioxidant activities with respect to concentrations, slopes and inhibition times

Antioxidant	Concentration (μmol/L)	*rac*	*ras*	*rat*
Caffeic acid	3.85	1	1	1
Chlorogenic acid	2.71	1.420	0.700	0.872
Rosmarinic acid	2.95	1.305	0.707	0.850
Gallic acid	44.5	0.086	0.035	0.085
p-Coumaric acid	355	0.011	0.017	0.005

The *rac* values were calculated at an inhibition time of 200 s. On the basis of *rac* values, the order of antioxidant activity of the studied phenolic acids is: chlorogenic acid > rosmarinic acid > caffeic acid > gallic acid > *p*-coumaric acid. When possible, it is convenient to calculate a mean value of *rac* in the linear concentration range of the sample and the standard. The value $(rac)_m$ is more significant than the *rac* value calculated at only one inhibition time (Cervellati*et al*., 2002).

On the basis of *ras* values, the order of antioxidant activity of the studied phenolic acids is: caffeic acid > rosmarinic acid ≈ chlorogenic acid > gallic acid > *p*-coumaric acid. This method of relative activity calculation is useful for comparison of the effect of changes in sample concentration with the effect of changes in the reference concentration, within the linear ranges (Cervellati *et al*., 2001).

The *rat* values were calculated at concentration 9 μmol/L. On the basis of *rat* values, the order of antioxidant activity of the studied phenolic acids is: caffeic acid > chlorogenic acid > rosmarinic acid > gallic acid >*p*-coumaric acid. This method of relative activity calculation has the same limitations asthe *rac*. The advantage is that the activity is reffered to a given specified concentration (Cervellati *et al*., 2001).

The ability to inhibit oscillations of the Briggs-Rauscher reaction mixture is not showed for *m*-coumaric acid. Recording of the potential versus time when 1 mL of a solution of *m*-coumaric acid (2500 mg/L) was added to 30 mL of active Briggs-Rauscher reaction mixture after the third oscillation are reported in Figure 4.

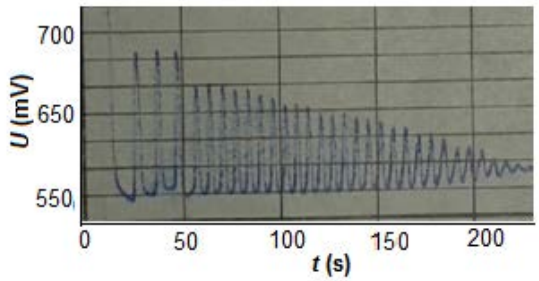

Figure 4: The effect of the *m*-coumaric acid on the active Briggs-Rauscher reaction mixture

The oscillatory time (the duration of the oscillatory regime) and numbers of oscillations depends on the concentration of studied phenolic acids. Variation of oscillations parameters in the Briggs-Rauscher reaction mixture with concentration of *m*-coumaric acid are reported in Table 3.

Table 3: Variation of oscillations parameters in the Briggs-Rauscher reaction mixture with concentration of *m*-coumaric acid

Concentration (μmol/L)	Oscillations	
	Duration (s)	Number
0	220	16
24.6	255	22
49.1	420	31
73.7	460	40
122.8	490	53
245.6	420	52
358.6	285	36
491.2	210	28

The largest number of oscillations (60) caused addition 1 mL of *p*-coumaric acid concentration of 500 mg/L to the 30 mL active Briggs-Rauscher reaction mixture. The lowest number of oscillations (23) caused addition 1 mL of gallic acid concentration of 300 mg/L to the 30 mL active Briggs-Rauscher reaction mixture.

The ranking order of the antioxidant activity of antioxidants components of secondary plant products differed from assay to assay. The Briggs-Rauscher reaction method can give useful *in vitro* information on the antioxidant activity at low pH values and has many advantages. Milos and Makota (2012) demonstrated some new possibilities of this method for determine the synergistic or antagonistic effects in mixture of compounds, which often poses a problem when using traditional methods.

CONCLUSIONS

The Briggs-Rauscher oscillating reaction is suitable as an analytical method to determine relative activity of antioxidants. In this study, the effects of concentration of the ethanol solutions of selected phenolic acids (gallic, caffeic, chlorogenic, rosmarinic, *p*-coumaric and *m*-coumaric acids) on the oscillatory system Briggs-Rauscher reaction were investigated. In all samples except *m*-coumaric acid, the inhibition time increased with increased concentration, and linearity was found in a wide concentration range of phenolic acid added. Relative antioxidant activities with respect to concentrations, slopes and inhibition times were calculated. The obtained results showed that the gallic acid and *p*-coumaric acid have much less antioxidant activity than the caffeic acid, chlorogenic acid and rosmarinic acid. The ability to inhibit oscillations of the Briggs-Rauscher reaction mixture is not showed for *m*-coumaric acid. Our future investigation will be focused on the antioxidant synergisms and antagonisms among selected phenolic acids.

REFERENCES

Cervellati, R., Crespi-Perellino, N., Furrow, S.D., Minghetti, A. (2000). Inhibitory effects by soy antioxidants on the oscillations of the Briggs-Rauscher reaction. *Helvetica Chimica Acta*, 83(12), 3179-3190.

Cervellati, R., Höner, K., Furrow, S.D., Neddens, C., Costa, S. (2001). The Briggs-Rauscher Reaction as a Test to Measure the Activity of Antioxidants. *Helvetica Chimica Acta*, 84(12), 3533-3547.

Cervellati, R., Renzulli, C., Guerra, M.C., Speroni, E. (2002). Evaluation of Antioxidant Activity of Some Natural Polyphenolic Compounds Using the Briggs-Rauscher Reaction Method. *Journal of Agricultural and Food Chemistry*, 50(26), 7504-7509.

Cha, J.W., Piao, M.J., Kim, K.C., Yao, C.W., Zheng, J., Kim, S.M., Hyan C.L., Ahn, Y.S., Hyun, J.W. (2014). The Polyphenol Chlorogenic Acid Attenuates UVB-mediated Oxidative Stress in Human HaCaT Keratinocytes. *Biomolecules and Therapeutics*, 22(2), 136-142.

Dacić, M., Gojak-Salimović, S. (2016). The effect of chlorogenic acid on the Briggs-Rauscher oscillating reaction. *Glasnik hemičara i tehnologa Bosne i Hercegovine/Bulletin of the Chemists and Technologists of Bosnia and Herzegovina*, 46, 51-54.

Furrow, S.D., Höner, K., Cervellati, R. (2004). Inhibitory Effects by Ascorbic Acid on the Oscillations of the Briggs-Rauscher Reaction. *Helvetica Chemica Acta*, 87(3), 735-741.

Höner, K., Cervellati, R., Neddens, C. (2002). Measurements of the in vitro antioxidant activity of German white wines using a novel method. *European Food Research and Technology*, 214(4), 356-360.

Höner, K., Cervellati, R. (2002). Measurements of the antioxidant capacity of fruits and vegetables using the BR reaction method. *European Food Research and Technolology*, 215(5), 437-442.

Konishi, Y., Kobayashi, S. (2004). Microbial metabolites of ingested caffeic acid are absorbed by the monocarboxylic acid transporter (MCT) in intestinal Caco-2 cell monolayers. *Journal of Agricultural and Food Chemistry*, 52(21), 6418-6424.

Li, S., Bian., H., Liu, Z., Wang, Y., Dai, J., He, W., Liao, X., Liu, R., Luo, J. (2012). Chlorogenic acid protects MSCs against oxidative stress by altering FOXO family genes and activating intrinsic pathway. *Europaen Journal of Pharmacology*, 674(2), 65-72.

Marković, M., Talić, S. (2013). Antioksidacijska aktivnost odabranih hercegovačkih vina. *Kemija u industriji*, 62(1-2), 7-12.

Mennen, L.I., Sapinho, D., Ito, H., Bertrais, S., Galan, P., Hercberg, S., Scalbert, A. (2006). Urinary flavonoids and phenolic acids as biomarkers of intake for polyphenol-rich foods. *British Journal of Nutrition*, 96(1), 191-198.

Milos, M., Makota, D. (2012). Investigation of atioxidant synergisms and antagonisms among thymol, carcacrol, thymoquinone and *p*-cymene in a model system using the Briggs-Rauscher oscillating reaction. *Food Chemistry*, 131(1), 296-299.

Nayeem, N., Asdaq, S.M.B., Salem, H., Ahel-Alfqy, S. (2016). Gallic Acid: A Promising Lead Molecule for Drug Development. *Journal of Applied Pharmacy*, 8(2), 213-216.

Ota, A., Abramović, H., Abram, V., Poklar-Ulrih, N. (2011). Interactions of *p*-coumaric, caffeic and ferulic acids and their styrenes with model lipid membranes. *Food Chemistry*, 24(4), 1256-1261.

Rice-Evans, C.A., Miller, N.J., Paganga, G. (1996). Structure-antioxidant activity relationship of flavonoids and phenolic acid. *Free Radical Biology and Medicine*, 20(7), 933-956.

Robards, K., Prenzler, P.D., Tucker, G., Swatsitang, P., Glover, W. (1999). Phenolic compounds and their role in oxidative processes in fruits. *Food Chemistry*, 66(4), 401-436.

Robbins, R.J. (2003). Phenolic Acids in Food: An Overview of Analytical Methodology. *Journal of Agricultural and Food Chemistry*, 51(10), 2866-2887.

Shalaby, E.A., Shanab, S.M.M. (2013). Antioxidant compounds, assays of determination and mode of action. *African Journal of Pharmacy and Pharmacology*, 7(10), 528-539.

Stansbury, J. (2014). Rosmarinic Acids a Novel Agent in the Treatment of Allergies and Asthma. *Journal of Restorative Medicine*, 3(1), 121-126.

Summary/Sažetak

Fenolske kiseline su aromatski sekundarni biljni metaboliti koji posjeduju značajnu antioksidacijsku aktivnost. Kada se antioksidans doda u aktivnu Briggs-Rauscher reakcijsku smjesu dolazi do neposrednog gašenja oscilacija. Vrijeme inhibicije oscilacija je u proporcionalnom odnosu s količinom i svojstvima dodanog antioksidansa. U ovom radu ispitivan je uticaj koncentracije etanolnih rastvora odabranih fenolskih kiselina (galna, kafena, hlorogenska, ruzmarinska, *p*-kumarinska i *m*-kumarinska kiselina) na oscilirajući sistem Briggs-Rauscher reakcije. Reakcija je izvođena u reakcionom sudu, uz stalno miješanje tačno definisanih koncentracija reaktanata, pri konstantnoj temperaturi od 25°C. Tok oscilacija Briggs-Rauscher reakcijske smjese praćen je potenciometrijskom metodom uz platinsku elektrodu i srebro/srebro hloridnu referentnu elektrodu. Relativne antioksidacijske aktivnosti bazirane na vremenima inhibicije izračunate su na tri načina. Rezultati ispitivanja su pokazali da galna i *p*-kumarinska kiselina imaju mnogo manju antioksidacijsku aktivnost od kafene, hlorogenske i ruzmarinske kiseline. Sposobnost inhibicije oscilacija Briggs-Rauscher reakcijske smjese nije pokazala *m*-kumarinska kiselina.

Glasnik hemičara i tehnologa Bosne i Hercegovine

Bulletin of the Chemists and Technologists of Bosnia and Herzegovina

2017

48

Print ISSN: 0367-4444

Online ISSN: 2232-7266

UDC: ___

Original Scientific Paper

15-20

Electrochemical treatment of leather industry wastewater

Halilović, N.[a*], Krdžalić, E.[b,c], Bašić, A.[d,e], Dacić, M.[d,e], Avdić, N.[a]

[a]*University of Sarajevo, Faculty of Science, Department of Chemistry, Zmaja od Bosne 33-35, 71000 Sarajevo, B&H*

[b]*University of Zenica, Faculty of Metallurgy and Materials Science, Department of Chemistry, Travnička Cesta 1, 72000 Zenica, B&H*

[c]*Factory of glues, facades, inks KOMOCHEM, Donja Zimča 68, 71300 Visoko, B&H*

[d]*Faculty of Pharm and Health, University in Travniku, Dolac na Lašvi, Polje Slavka Gavrančića 17C, 72270 Travnik, B&H*

[e]*Institute for Biomedical Research and Diagnostics GENOM, Dolac na Lašvi, Polje Slavka Gavrančića 17C, 72270 Travnik, B&H*

Article info
Received: 20/04/2017
Accepted: 14/06/2017

Keywords:
Aluminum
Escherichia Coli
Copper
Chlorides
Electrocoagulation
Leather industry wastewater

***Corresponding author:**
E-mail: namir.halilovic@live.com
Phone: 00-387-61-495311

Abstract: Leather industry wastewater is contaminated with bacteria including *Escherichia Coli*. In this paper, results obtained from analysis of leather industry wastewater samples with use of copper electrodes are presented and compared with the results of use of aluminum electrodes and mixed metal oxide electrodes. In all experiments the same materials were used as anode and cathode except the two last where anode of the mixed metal oxides and steel cathode was used. Electrodes with platinum group metals or their oxides as active coatings are generally the best suited for electrochemical water disinfection. After 7 min of electrolysis at only 0.018 A/dm^2, Cl^- was reduced using both tested electrodes, the efficiency of microorganisms removal followed the order: Cu > Al. The electrochemical treatment of wastewater resulted in the production of chlorine gas and hypochlorite, which is microorganisms deactivator. Also, electrocoagulation by aluminum anode was used for water purification to reduce all pollutants, including chlorides and microorganisms.

INTRODUCTION

At the phase boundary between the electrodes and the water, the electric current leads to the electrochemical production of disinfecting species from the water itself (for example, ozone), or from species dissolved in the water (for example, chloride is oxidised to free chlorine). If electrochemical disinfection is applied to drinking water, industrial water, seawater or other solute-containing water, its effect is mainly based on the electrochemical production of hypochlorite and/or hypochlorous acid from the chloride content of the water (Kraft, 2008).

First, chlorine is electrochemically produced from chloride ions dissolved in the water (Mendia, 1982):

$$2Cl^- \rightarrow Cl_2 + 2e^-$$

The gas in low concentrations is an irritant to the mucous membranes, the respiratory system, and the eyes (Harms and O'Brien, 2010).

Chlorine hydrolyses in water and hypochlorous acid (HClO) is formed:

$$Cl_2 + H_2O \rightarrow HClO + HCl$$

In the nomenclature of water disinfection, the sum of hypochlorous acid and hypochlorite concentrations is usually termed *free chlorine* or *active chlorine*. The disinfecting effect of free chlorine is based on the release of atomic oxygen according to (Chen, 2004):

$$HClO \rightarrow O + Cl^- + H^+$$

$$ClO^- \rightarrow O + Cl^-$$

Our goal was find the best anode-cathode material for electrochemical disinfection and removal of chloride from leather industry wastewater.

EXPERIMENTAL

Chemicals and instruments

Sodium thiosulfate, p.a. (Merck); potassium iodide, p.a. (Merck); starch, p.a. (Merck); hydrochloric acid, p.a. (Merck); sodium chloride, p.a. (Merck); conductivity meter (Iskra); pH meter (PHYWE); constanter (PHYWE); amperemeter (PHYWE); digital multimeter (DT9205A); magnetic stirrer (TEHTNICA ŽELEZNIKI); analytical balance (Mettler); thermometer; copper anode and cathode, aluminum anode and cathode (see Fig. 1 (a), (b), (c)), anode of the mixed metal oxides - MMO (RuO_2, IrO_2) and cathode of steel and laboratory glassware were used for the experiment process.

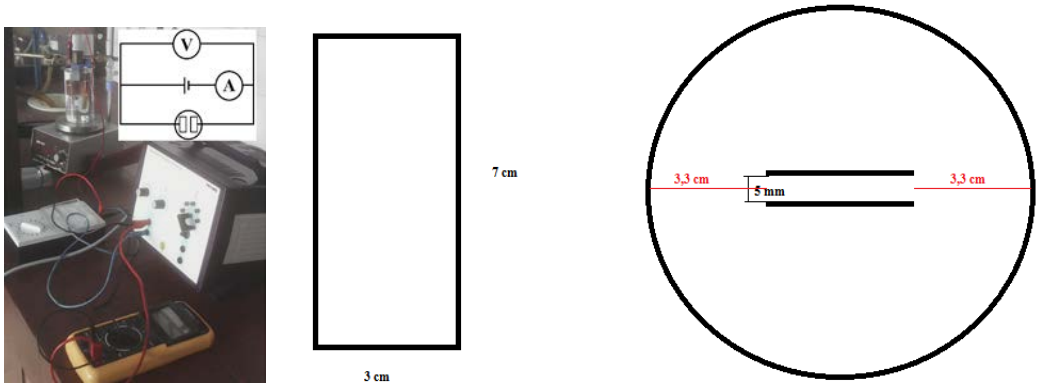

Figure 1: **(a)** Scheme and apparatus for electrolysis using Al and Cu electrodes. **(b, c)** Dimensions of used electrodes and position in laboratory glass.

Procedure

Electrolysis duration for all experiments was 7 min. Dimension of used electrodes was 7 cm × 3 cm and the distance between the electrodes was 5 mm as shown by Fig. 1 (b, c). Scheme for electrolysis using aluminum, copper and MMO electrodes is given in Fig. 1 (a). The volume of the tested samples was the same, 0,4 dm^3. Experiments were carried out at 500 rpm on a magnetic stirrer.

The determination of hypochlorite in standard solution of chloride after electrolysis

Hypochlorous acid reacts with iodide when the solution is acidic:

$$HOCl\ (aq) + HCl\ (aq) + 3I^-\ (aq) \rightarrow I_3^-\ (aq) + 2Cl^-\ (aq) + H_2O(l)$$

Tridiodide, I_3^-, is a dark red complex. A dark blue complex is formed when triiodide is combined with starch.

$$I_3^- + starch \rightarrow [I_3^-][starch]$$

As result of these three reactions a dark blue complex formation is observed. Its concentration is proportional to the amount of sodium hypochlorite in the solution. In the next step, the starch-triiodide product is titrated by sodium thiosulfate to form a colorless solution of iodide, dithionate, and uncomplexed starch (Chang, 2010):

$$[I_3^-][starch] + 2S_2O_3^{2-} \rightarrow 3I^- + S_4O_6^{2-} + starch$$

Copper anode and cathode, aluminum anode and cathode, anode of the mixed metal oxides - MMO (RuO_2, IrO_2) and cathode of steel are used in determining hipohloritne acid as a product of electrolysis of Cl- standard solution, which concentration was 0,05 mol/dm^3(this concentration was detected in leather industry wastewater). Apparatus for electrolysis is shown in Fig. 1 (a).

The determination of chloride in sample of leather industry wastewater by Mohr method

Determination of the chloride in the wastewater before and after electrolysis is carried out by titration method. The Mohr method uses chromate ions as an indicator in the titration of chloride ions with a silver nitrate standard solution (Skoog et all., 1996). The reactions are:

$$Ag^+ + Cl^- \leftrightarrow AgCl(s)$$
$$2Ag^+ + CrO_4^{2-} \leftrightarrow Ag_2CrO_4(s)$$

By knowing the stoichiometry and moles consumed at the end point, the amount of chloride in an unknown sample can be determined.
The decrease in total chloride is presented:

$$\omega(\%) = \frac{c_{Cl^-(before\ electrolysis)} - c_{Cl^-(after\ electrolysis)}}{c_{Cl^-(before\ electrolysis)}} \cdot 100$$

The determination of *Escherichia Coli* and total bacterias in sample of leather industry wastewater

The nutrient pads are made of biologically inert cellulose cardboard that does not bind the nutrient medium chemically or physically. Growth of microorganisms can therefore develop freely. All equipment must be sterile.
We used two standards:
Endo-NPS: Medium selective for *Escherichia Coli* and coliform bacteria in water (DIN EN ISO 9001, 2008).
and is used white membrane filter with pores of 0,45 mm. Application of bacteria are carried out by filtering 100 mL of sample on a Buchner funnel using white membrane filter. The filter is transferred by pincette to an inert bacterial surface. Before transporting the filter, it is necessary to add water on the dehydrated base, 3 to 5 ml of distilled water. Incubation of the seeded filtrate sample takes 24 hours at 37°C or 42-44°C. E. coli develops dark red colonies on green metallic shiny surface.

Standard *TTC-NPS*: For colony count determinations of water and waste water for pure cultures (DIN EN ISO 9001, 2008).
Standard is designed for the determination of the bacteria: *Escherichia Coli, Pseudomonas aeruginosa, Staphylococcus aureus*. Application of bacterias is carried out by filtering 100 mL of sample on a Buchner funnel using a membrane filter with pores of 0,45 microns, and then the filter is transferred by pincette to an inert bacterial surface. Incubation of the seeded filtrate sample takes 48 hours at 30°C or 48-72 hours at 20°C. Bacterias develope pink colonies on the surface. These points are visible to the eye.

The determination of conductivity and pH of NaCl standard solution and sample of leather industry wastewater

These parameters were determined before and after electrolysis with copper, aluminum and MMO electrodes for samples of wastewater and for standard samples of NaCl (c = 0,05 mol/dm^3) because of comparison.

RESULTS AND DISCUSSION

Results of experiments are showed in Table 1 and Figure 2, 3, and 4.

Table 1: Results of determination of hypochlorite, pH and conductivity of NaCl standard solution and sample of leather industry wastewater. Minus(-) refers to the reduction of the initial value of the parameter after experiment.

Electrode pair (A, K)	Cl^- standard samples of NaCl = 0,05 mol/dm^3			Leather industry wastewater				
	HOCl [mol/dm^3]	ΔpH (pH_0=7,14)	Δκ (mS/cm)	ΔpH (pH_0=8,43)	Δκ (mS/cm)	Reduction of chloride [%]	Destruction of *E. coli* [%]	Destruction of all bacterias [%]
$Cu_{500\ o/min}$	$86,7 \cdot 10^{-5}$	3,84	0,152(-)	x	3,168	17,8	100	100
$Al_{500\ o/min}$	$2,3 \cdot 10^{-5}$	1,11	0,159	0,67(-)	0,022	75,8	>90	>80
MMO	$90 \cdot 10^{-5}$	1,91	0,25	x	x	x	x	x

(a) (b)

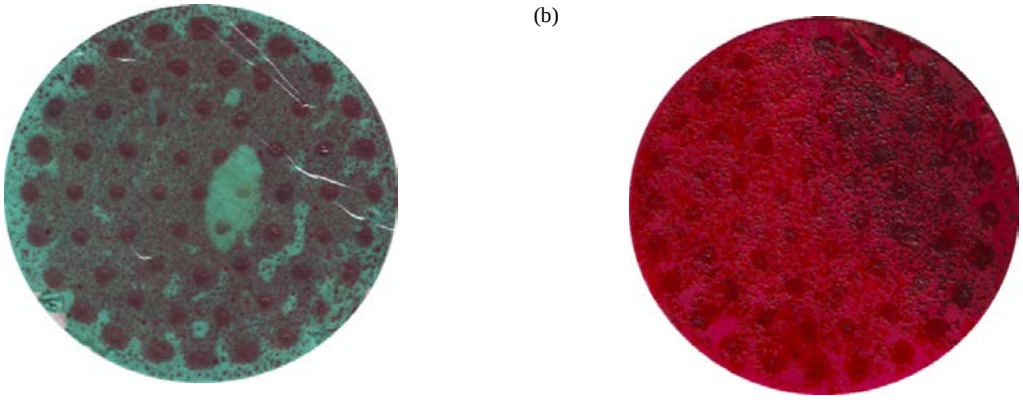

Figure 2: **(a)** A test for total bacteria in wastewater before experiment. **(b)** A test for *E.coli* in wastewater before experiment. Each red dot on nutrient pad is a colony of bacteria.

(a) (b)

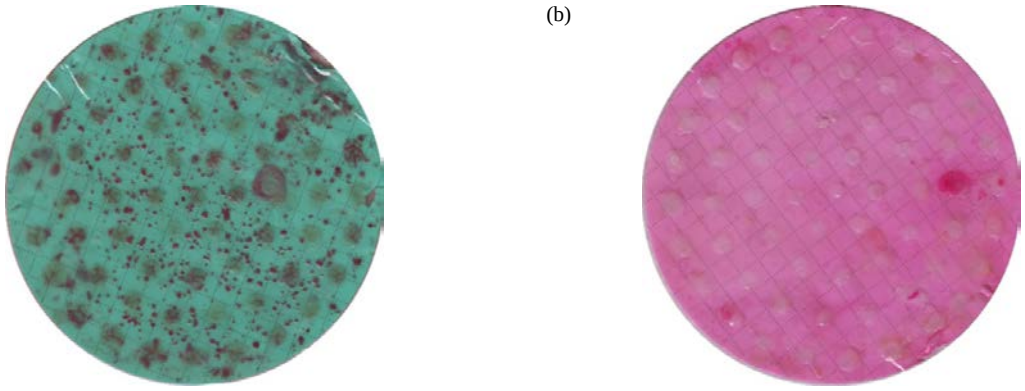

Figure 3: **(a)** A test for total bacteria after experiment with Al anode-cathode pair. **(b)** A test for *E. Coli* after treatment with Al anode-cathode pair. Each red dot on nutrient pad is a colony of bacteria.

(a) (b)

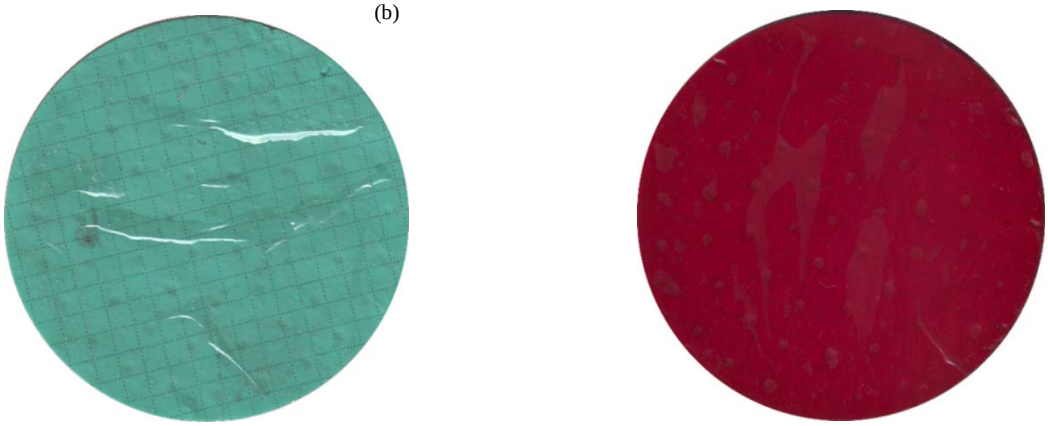

Figure 4: **(a)** A test for total bacteria after treatment with Cu anode-cathode pair. **(b)** A test for *E. Coli* after treatment with Cu anode-cathode pair.

Electrodes with platinum group metals or their oxides as active coatings are generally the best suited for electrochemical water desinfection as shown by the results in Tab. 1. ($c_{HOCl} = 90 \cdot 10^{-5}$ mol/dm^3). MMO comes before aluminum and copper electrodes because in this experiment formed hydroxide does not react with the metal ion of MMO electrodes.

MMO electrodes are very expensive, so we will not discuss them for use in wastewater treatment but can be used for the production of HOCl.

After 7 min of electrolysis at 0,018 A/dm^2, Cl^- was reduced and, using both tested electrodes, the efficiency of microorganisms removal followed the order: Cu>Al (comparison of the number of red dots on Fig. 2, Fig. 3 and Fig 4 showed in Tab 1).

While microbial inactivation mechanisms have not been clearly explained, it is evident that there exist synergistic effects on water disinfection when Cu^{2+} and Ag^+ are provided simultaneously (Younggy, 2014).

After the electrolysis with Cu, pH of NaCl standard solution is measured, and its value was 10,98 (see ΔpH=3,84 for NaCl solution in Tab. 1), so it is important to mention the following reaction is not favored and OH^- ions do not accumulate to a significant extent:

$$Cu^{2+} + 2OH^- \rightarrow Cu(OH)_2\ (s)$$

The anode is surrounded by an acidic medium and the primary reaction is the formation of the dichloride. NaOH, which accumulate, increases the pH.

During the electrolysis in NaCl solution, a copper anode is oxidized froming the protective layer (Naumczyk et all., 1996; Antonijević, et all., 2009):

$$2Cu^+ + H_2O \rightarrow Cu_2O + 2H^+$$
$$2Cu + H_2O \rightarrow Cu_2O + 2H^+ + 2\ e^-$$

followed by the reaction:

$$Cu^+ + Cl^- \rightarrow CuCl$$
$$2CuCl \rightarrow Cu + CuCl_2$$
$$CuCl + Cl^- \rightarrow CuCl_2^-$$

Cu^{2+} inactivate microorganisms, including pathogens, as an active disinfectant which are shown in Fig 5 (see Fig. 4).

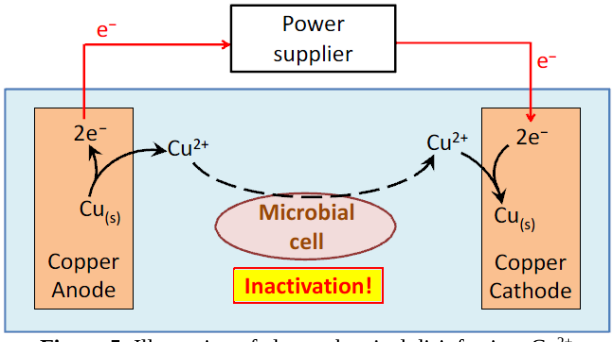

Figure 5: Illustration of electrochemical disinfection. Cu^{2+} released at the anode inactivates microorganisms. Simultaneously, Cu^{2+} is recovered as metallic copper at the cathode (Vepsäläinen, 2012)

At the anode, metallic copper is oxidized to aqueous Cu^{2+} ions (Fig. 5). The aqueous Cu^{2+} ions released from the anode inactivate microorganisms (including pathogens) as an active disinfectant. Simultaneously, Cu^{2+} ions migrate toward the cathode where Cu^{2+} is reduced to metallic copper (reaction below). With this recovery of Cu^{2+} ions at the cathode, the disinfected water from the reactor will have sufficiently low Cu^{2+} concentration that are safe for human consumption (Halilović and Avdić, 2015) (this is reason for destruction of bacterias showed in Fig. 4).

$$Cu(s) \rightarrow Cu^{2+} + 2e^-$$
$$Cu^{2+} + 2e^- \rightarrow Cu(s)$$

In experiment with NaCl standard solution, κ (mS/cm^3) decreased primary because of reaction between Cu^{2+} and chlorides from solution (Δκ for NaCl standard solution in Tab. 1).

In experiment with aluminum electrodes, pH decreased and come close to zero (0,67(-) in Tab.1) because of reaction OH^- with metal ions in sample of leather industry wastewater. Also, the additional reasons for this kind of behavior are processes as electrocoagulation,

electroflotation and electroflocculation that affects metal ions that are released from the anode.

Electrocoagulation process involves the separation of solid particles from the solution. The process takes place with the formation of coagulants by electrolytic dissolution of electrodes made of aluminum. Aluminium seems to be a more suitable electrode material for electrocoagulation applications because it produces Al(III) species (Kraft, 2008; Vepsäläinen, 2012) (this is reason for reduction of bacteria showed in Fig. 3, the other reason is the formation of HOCl).

Electrocoagulation: $Al^{3+} + 3OH^{-} \rightarrow Al(OH)_3$

The reduction of pH in alkaline effluents is the result of hydroxide being precipitated and the formation of $Al(OH)_4^-$ by the equation (Gardić, 2007):

$$Al(OH)_3 + OH^- \rightarrow Al(OH)_4^-$$

In the case of electrolysis of NaCl standard solution, the acidic environment is formed around anode, but during the mixing of the solution pH rises. In the end of the experiment pH was 8,25; and at the end the pH rises as in the previous examples. It is evident that in electrolysis with Al lower pH is observed when compared with other electrode materials, Cu and MMO (see Tab. 1).

The explanation is in the reaction of OH^- ions with Al^{3+} ions to form a particle coagulant. It acts as a seed for the removal of solid particles from the solution. Aluminum ions in a water solution will give a large number of compounds of the mesh patterns of Al-O-Al-OH structure, which are capable of adsorbing the chemical pollutants such as F-, or similar ions. Aluminum is commonly used in the treatment of drinking water, and the iron in the treatment of waste water (Chen et al., 2000).

CONCLUSIONS

The electrochemical treatment of wastewater produced in a leather industry resulted in the production of chlorine gas and hypochlorite, which is a microorganisms deactivator. Also, electrocoagulation by Al and Cu anode has been in use for water production or wastewater treatment to reduce all pollutants, including chlorides and microorganisms. With this technology, metal cations are produced on the electrodes through electrolysis and these cations form various hydroxides in the water depending on the water pH.

Apparaently the Cu and Al act directly or indirectly to the bacteria and Cu is dominant with direct action of Cu^{2+} ions with respect to Al^{3+} ions. On the other hand, aluminum is better and more suitable coagulant as anodic-cathode material. The efficiency of microorganisms removal followed the order Cu>Al, but because of price and electrocoagulation effect, Al anode-cathode pair is good candidate for use in purification of leather industry wastewater.

The highest concentration of certain hypochlorous acids formed by electrolysis following order:

$$MMO\ (IrO_2, RuO_2) > Cu > Al$$

and increased compared to the theoretically expected, because of the mixing, the influence of the base, the temperature and the participation of secondary reactions.

Due to the large loss of Cu^{2+} ions to be separated by electrolysis from the anode and the same is not reduced at the cathode due to the mixing of the solution, a copper electrode is not applicable to the waste water purification at high current densities.

REFERENCES

Antonijević, M. M., Gardić, V., Milić, S. M., Alagić, S. Č., Stamenković, A. T., Jojić, M. (2009). *Protection of materials*, Technical Faculty Bor, Beograd, Serbian, p. 28.

Chen, G. (2004). *Separation and Purification Technology*, 38, 11–41.

Chang, N. (2010). *Chemistry*, TCU of New York Winter, New York, USA, p. 8.

Chen, X., Chen, G.H., Yue, P.L. (2000). *Separation and Puriication Technology*, 19, 65–76.

DIN EN ISO 9001: Endo-NPS (2008).

DIN EN ISO 9001: Standard TTC-NPS (2008).

Gardić, V. (2007). *The application of electrochemical methods for wastewater treatment,* Protection of materials, 48, 49-58.

Halilović, N., Avdić, N. (2015). *The electrochemical removal of chloride and disinfection of leather industry wastewater*, Master thesis, Sarajevo: Natural-Matematics Faculty, Department of Chemistry, p. 29.

Harms, L. L., O' Brien, W. J. (2010). *White's handbook of chlorination and alternative disinfectants*, Wiley, Hoboken, New Jersey, p. 28.

Kraft, A. (2008). *Platinum Metals Review*, 52 177–185.

Mendia, L. (1982). *Wat. Sci. Tech*., 14, 331-344.

Naumczyk, J., Szpyrkowicz, L., Zilio-Grandi, F. (1996). *Wat. Sci. Tech.* 34, 17-24.

Skoog, D. A., West, D. M., Holler, F. J. (1996). *Fundamentals of Analytical Chemistry*, Thomson Learning, Inc, USA.

Vepsäläinen, M. (2012). *Electrocoagulation in the treatment of industrial waters and wastewaters*, VTT SCIENCE 19, Espoo, Finland, p. 77.

Younggy, K. (2014). *Safe drinking water*, McMaster University, Hamilton, Ontario, p. 1-3.

Summary/Sažetak

Otpadna voda kožarske industrije je zagađena bakterijama uključujući Ešerihiju Koli. Ovaj rad sadrži rezultate prikupljene tretiranjem uzoraka otpadne vode elektrodama od bakra, aluminija i metalnih oksidnih elektoda. U svim eksperimentima su korišteni parovi elektroda istog sastava, osim u poslednjem u kome je korištena anoda od metalnih oksida i čelična katoda. Elektrode platinske grupe metala i njihovi oksidi kao aktivne prevlake su se pokazali naučinkovitijim za dezinfekciju vode. Poslije 7 min elektrolize pri 0.018 A/dm^2, koncentracija Cl^- jona je smanjena koristeći obe vrste elektroda, a uklanjanje mikroorganizama prati red Cu > Al. Elektrohemijskom obradom otpadne vode nastaje gas hlorin i hipohlorit, koji je inaktivator mikroorganizama. Također, elektrokoagulacija izazvana aluminijumskom anodom je iskorištena za pročišćavanje vode za smanjenje svih zagađivača, uključujući hloride i mikroorganizme.

Glasnik hemičara i tehnologa Bosne i Hercegovine

Bulletin of the Chemists and Technologists of Bosnia and Herzegovina

2017

48

21-26

Print ISSN: 0367-4444
Online ISSN: 2232-7266

UDC: _____

Original Scientific Paper

The determination of iron levels in Menthae tea (*Mentha piperita* L.)

Mandal Š.[a*], Keškić N. [b], Marevac N.[b]

[a] *Department of Natural Sciences in Pharmacy, Faculty of Pharmacy, University of Sarajevo, Bosnia and Herzegovina*

[b] *Faculty of Pharmacy, University of Sarajevo, Bosnia and Herzegovina*

Article info
Received: 28/02/2017
Accepted: 14/06/2017

Keywords:
iron, menthae tea, dry digestion

***Corresponding author:**
E-mail: shakira.mandal@gmail.com
Phone: +387 61 614 203

Abstract: Menthae tea (*Mentha piperita* L.) is one of the most widely consumed herbal teas. This tea is recognized as a drink that may have several health benefits, primarily due to the presence of nutritional elements especially essential micro and ultramicro elements. In this study, we investigated the content of iron in mentha tea samples found in a local market in Sarajevo. The preparation of the samples was done by dry digestion in triplicate while levels of iron were analyzed by spectrophotometry. The amounts of iron were ranged from 275.6 mg Fe/kg to 354.6 mg Fe/kg. The used spectrophotometric method is simple and sensitive method that can be applied for the determination of total Fe content in plant material.

INTRODUCTION

People around the world use medicinal plants as herbal tea and for the health reasons. World Health Organization (WHO), reported that, about 80% of population in peripheral communities use only medicinal herbs for the treatment of many diseases. Chemical compositions of different medicinal and aromatic plants contain proteins, lipids, carbohydrate and mineral elements. Because of that, many plants are consumed as spices, dietary supplements, or serve as herbal teas. Recently, it has been a lot of scientific interest for the determination of composition i.e. nutrient contents of plants, especially for the determination of the micro and ultra microelements in plants (Szentmihályi et al., 2008; Remigius, 2012; Mihaljev et al., 2014; Živkov-Baloš et al., 2014). Additionally, minerals and trace metals are partially recognised for their medicinal and nutritional properties, as well as their toxic ones. Microelements are known as nutrients for which there are RDA (Recommended Dietary Allowances) values available. Based on this set values consuming 1L of tea, in some cases will cover 10% or more of the daily requirement for several elements. However rganic components of the plant parts may change and the microelement content of the different parts of plant drugs are also different (Szentmihályi et al., 2008; Gogoasa et al., 2013; Mihaljev et al., 2014). Therefore, the phytotherapeutic effect of medicinal plants may also differ according to the plant species and plant parts.

Among the other essential elements, iron is an indispensable microelement for living organisms because of its participation in metabolic processes, such as transport of oxygen, DNA synthesis, and electron transfers. It is also possible that medicinal plant raw materials may supply this element for humans with iron deficiency. This issue is extremely important for pregnant and lactating women. Several medicinal plants are also traditionally used against anemia.

Number of studies focusing on determination of concentrations of micro and ultra-microelements in medicinal plants; have established that iron occur in the range of concentration from several tens to several hundreds/thousands of mg/kg of dry plant weight, and that its level in many cases depends on genetic factors and on the morphological part of a plant. The levels of essential elements in plant vary according to the geographical region, geochemical soil characteristics, and the ability of plants to selectively accumulate some of these elements. Generally, these elements are absorbed through the root systems and dispersed throughout the plant body (Korfali et al., 2013).

Mentha piperita L. (Family: Lamiaceae), commonly known as peppermint, is an important medicinal herb

worldwide. “Medicinal plant of the year 2004”; oldest known medicinal plant species in Eastern and Western traditions although first described in 1753 by Carolus Linnacus,It is used as flavoring agent, in cosmetics preparations , and as pharmaceutical products amongst others. The trace elements present in Menthae may play a direct or indirect role in their biological activities: anti-inflammatory, antioxidant, antimicrobial, antifungal activities. Provided studies show antioxidant and antimicrobial properties of the Menthae leaves which are locally available (Gonçalves et al., 2009; Kızıl et al., 2010; Pramila et al., 2012; Saeed et al., 2014; Siddig et al., 2015). Some investigators found that its antifungal activity is comparable to that of synthetic fungicides. As a significant trace element, iron is necessary for all living organisms and essential element in cell metabolism (involved in photosynthesis, respiratory, etc.). Since elements are able to pass through different membranes, essential elements get into the cells and organs of human body that cases favorable or non-favorable processes. Therefore, increasing focus on the importance of dietary minerals in the prevention of disease justifies need for more serious studies on the mineral content of plants (Saeed et al., 2014; Stanojkovic et al., 2015).

The aim of this study is to determine of total content of iron in some brand Menthae tea samples, using dry digestion as method for preparation herbal samples (biological materials) and spectrophotometric analysis as method of quantification.

EXPERIMENTAL

Biological material

Plant samples (mint teas-Menthae folium) were taken from different manufactures from a local market in Sarajevo: PAK NANA (Bosnia and Herzegovina), 1000 CVET (Slovenia) and Pharmamed (Bosnia and Herzegovina).

Sampling and sample preparation

The preparation of Menthae tea samples was carried out by dry digestion. The herbal samples were prepared with mass of 1.0000± 0.0002 g in crucible and heated during 4 hours at temperature of 500^0C in furnace. After cooling, ashes were dissolved in concentrated nitric acid (1ml), crucible washed with mixture of nitric and hydrochloric acids (concentration of 0.05 $moldm^{-3}$), and filtrated (blue filtered paper) in volumetric flask (100 cm^3), then diluted to mark with same mixture of acids. Digestion of each tea samples were done in triplicate.

Reagent and standard solutions

All reagents were analytical grade (p.a.) while distilled water (Milli-Q, Millipore), used for samples dilution and labware washing.

Instruments

- Spectrofotometer “Spectronic Genesys 2“ (Spectronic Instruments, Milton Roy Company, Champaign, Illionois, USA)
- The device for the production of ultrapure water (Arium® 611, Sartorius Mechatronics, Germany)
- Analytical balance (AX 250 Delta Range®, Mettler Toledo Inc., USA), Sartorius analytical balance
- Technical scales (BL 1500, Sartorius Mechatronics, Germany)
- Magnetic mixer with heater (Heidolph Instruments GmbH & Co.KG Lab Equipment Sales Walpersdorfer Str. 12 D-91126 Schwabach, Germany)
- Furnace (Nabertherm 30-3000°C, Lilienthal, Germany)

Spectrophotometric method

Spectrophotometric method was performed with a *Spectronic Genesys 2* spectrophotometer. Solutions of each of nine samples were red to red pale color. Before spectrophotometric analysis, intensity of color, increases by the addition of a reagent, potassium thiocyanate (5 $moldm^{-3}$), for complexation of iron ions and formation of red complex with different composition, from $[FeSCN(H_2O)_5]^{2+}$ to $[Fe(SCN)_6]^{3-}$, and intensity of color solutions. Potassium thiocyanate is an inexpensive, available reagent that forms iron (III)-ions with a stable complex. This reaction is favorable in acidic medium and takes place at a temperature of 50^0C, and with acid that will not complexe iron (III) ions. For this reaction nitric acid was used, with concentration of 5 $moldm^{-3}$.

The calibration solutions were prepared over a concentration range of 1.40 and 69.81 $\mu g/cm^3$ Fe .Absorbance was measured at 481,0 nm for working and analyzed solutions (the calibration curves demonstrated adequate linearity, R^2 = 0.9999). Calibration curve is presented in Figure 1.

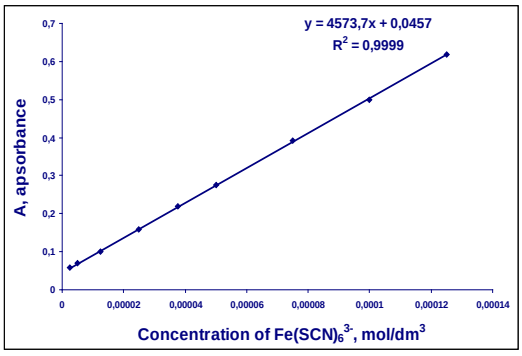

Figure 1. The calibration curve for spectrophotometric analysis of Menthae tea samples

Statistical analysis

All the assays were carried out in triplicates. The experimental results were expressed as mean ± standard deviation. The data were analyzed using Microsoft Office Excel.

RESULTS AND DISCUSSION

Preparation of tea samples was done by dry digestion, while the quantitative analysis and determination of the concentration of iron was performed spectrophotometrically, using the thiocyanate method. Results showing concentrations of iron (total content of iron of leaf of mentha herbs) in three different Menthae tea samples, produced by different manufactures and purchased at a local market in Sarajevo are presented in Table I. The content of studied metal is expressed in mg/kg of dry matter (d.m.). Range of iron levels varies from 275.6 to 354.6 mg/kg d.m. with average value of 320.8 mg/kg d.m.

Table 1. Content of iron in Menthae tea samples
Data are expressed as mean ±SD. A, Apsorbance; d.m., dry mass

Tea sample	A	mean of Apsorbance	mean of Concentration $[Fe(SCN)_6]^{3-}$, (mol/dm^3)	Content of Fe (mg/kg of d.m.)
Sample 1		0.6273	$1.27 \cdot 10^{-4}$	354.6±6.8
I	0.701			
II	0.615			
III	0.566			
Sample 2	0.487	0.4973	$9.87 \cdot 10^{-5}$	275.6±6.6
I				
II	0.437			
III	0.568			
Sample 3	0.577	0.5893	$1.19 \cdot 10^{-4}$	332.3±5.7
I				
II	0.540			
III	0.651			

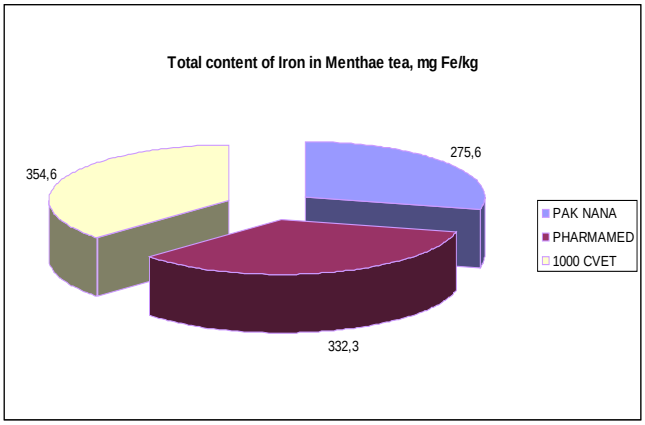

Figure 2. The total content of iron in analyzed Menthae tea samples

Our results are in line to previously provided studies and demonstrated that levels of iron in most of mentha species are highest when compared to other mineral elements. Concentrations of iron (mg Fe/kg of d.m) were from 358 mg Fe/kg, 293 mg Fe/kg, 260 mg Fe/kg and 489 mg Fe/kg, to 1068 mg Fe/kg and 11841mg Fe//kg (Arzani et al., 2007; Bielicka-Giełdoń and Ryłko, 2013; Ebrahimzadeh et al., 2011; Szymczycha-Madeja et al., Maghrabi, 2014; Faiku and Haziri, 2015, respectively) or 129 mg Fe/kg and lowest when compared to mean of 320.8 mg Fe/kg, obtained in this study. Data obtained in study Živkov-Baloš et al., (2014) for content of iron in *Mentha piperita* of 274.83 mg Fe/kg d.m. are similar to our results for sample tea *1*.

Contents of microelements in medicinal plants are influenced by genetically-determined properties of a plant as well as by external factors, including geographic location, soil type and profile, fertilization, availability of water, pollution by pesticides or dusts, and gases. Moreover, highest iron a concentration was found from locality were menthe plant grows and cultivated as organic species (Faiku and Haziri, 2015; Maghrabi, 2014). Concentrations of some elements as well as iron are also affected by technological processes, duration and storage conditions.

Leaves of mentha plant are frequently used in herbal teas and for culinary purpose to add flavor and aroma. Also, mentha spices are rich sources of iron among others trace elements which play important role in human nutrition.

Mentha as medicinal plant and raw material may be used as a supplement in cases of iron deficiency. However, it is also known from the literature (Lozak et al., 2002; Konieczynski and Wesolowski, 2008; Szymczycha-Madeja et al., 2013; Mirzaei et al., 2015), that only a small percentage of iron present in medicinal plants is bioavaible, when considering its water-soluble species.

Taking this into account, total content concentration of iron in some medicinal plants as well as in menthe depends on or is influenced by pH. At concentration of iron species in aqueous solutions, at the characteristic pH of saliva (pH6.5), stomach juice (pH1.2), and intestine juice (pH7.8) could help to answer the questions whether and what amounts iron species can be potentially absorbed in specific segments of the digestive system of humans. Only soluble iron can be absorbed in the human digestive system, thus, only a fraction of iron can be treated as being bioavailable. It has been shown that pH has significant effects on the determined species. Comparing results of iron species determined in all solutions with different pH values, it can be seen that pH significant impact on the amounts of bioavailable iron. These results indicate that only the fractions of iron detected in the particular solutions can be considered bioavailable iron in the neutral aqueous solutions. The reason for this is probably the complex composition of plant material, in which iron is bound by various ligands. Also, brewing time had significant effect on the percentage of microelement extraction to the aqueous phase, such in the case of iron (Dormana et al., 2009; Zijp et al., 2010; Sembratowicz et al., 2014).

Some trace elements are essential for normal growth and functioning of living organisms, but only at low concentrations. They catalyze many biochemical reactions occurring in the organisms that are involved in the formation of red blood cells, hormones, and vitamins, as well as take part in the processes of photosynthesis and the creation of pigments, respiration, oxidation, and reduction. Some of these elements are important in metabolism, and are part of the bone and tissues of living organisms, and participate in the functioning of neural systems. But in too high doses these metals can be toxic (Gonçalves, 2009; Denys, 2012; Bielicka-Giełdoń et al., 2013; Mirzaei et al., 2015).

Phytopharmaceuticals are gaining popularity worldwide; however, cases of adverse effects and drug interactions have also increased. One reason is in the high metal content both as ingredients but also as contaminants. Metal monitoring in food, like herbal teas, provides basic information on safety aspects in regulatory processes as well as nutritional values. Metal contents varied significantly, depending on the stores the products were purchased in and on tea packaging (loose leaves versus tea bags). Mentha plants are mainly used for treatment of disorders of gastrointestinal tract. They have also been reported to have antioxidant, anti-inflammatory, antimicrobial, analgesic and anticarcinogenic effects (Rubio et al., 2012; Prabu et al., 2015; Siddig et al., 2015). Herbalists consider peppermint as an astringent, antiseptic, antiemetic, carminative, analgetic. The plant extract that possesses radioprotective, antioxidant, anticancerogenic, antitumorgenic, antiandrogenic, antiallergic, antispasmolic properties amongst others. Plant extract can, also, reduce the arsenic-induced toxicity; reduce glucose, total cholesterol, LDL-chol, and triglycerides levels (in diabetic rat). In study Barbalho et al., (2011) results indicate that *Mentha piperita* can be used for therapeutic and preventive affecting biochemical profile, blood pressure and body mass index in humans.

Medicinal plants are the raw material for many herbal formulations and popular supplements. The use of herbal medicines has been on the rise in recent years due to their low prices. The last few decades have witnessed a rapid development in the diet studies focused on the determination of trace elements, which reflect their role in human health and nutrition. Deficiency, excess or imbalance of trace element intake into human body may result in various diseases.

CONCLUSION

The determination of element content in medicinal plant drugs and extracts has several important aspects. Since elements are able to pass through different membranes, essential elements enter into the cells and organs of human body that might be favorable or non-favorable processes. Among the other essential elements, iron is the most important microelement for living organisms because of its participation in metabolic processes, such as transport oxygen, DNA synthesis, and electron transfers.

In our study, all tested Menthae tea samples showed high iron levels, which indicate that dry digestion as method for preparation and spectrophotometric analysis, are applicable for detection and determination of iron concentrations in biological materials.

REFERENCES

Arzani, A., Zein, A. H., Razmjo, K. (2007). Iron and magnesium concentrations of mint accessions (*Mentha* spp.). *Pl. Physiol. Bioch., 45*, 323-329.

Barbalho, S. M., Machado, F. M. V. F., Oshiiwa, M. Abreu, M., Guigeri, E. L., Tomazela, P. (2011). Investigation of the effects of peppermint (*Mentha piperita*) on the biochemical and anthropometric profile of university students. *Ciência e Tecnologia de Alimentos, 31(3),* 584-588.

Bielicka-Giełdoń, A., Ryłko, E. (2013). Estimation of Metallic Elements in Herbs and Spices Available on the Polish Market. *Pol. J. Environ. Stud., 22(4),* 1251-1256.

Denys J. Charles. (2012). Antioxidant Properties of Spices, Herbs and Other Sources. Peppermint**.** pp 469-475.

Dormana, H. J. D., Koşara, M., Başerb, K. H. C., Hiltunen, R. (2009). *Mentha* x *piperita* L. (Peppermint) Extracts. *Natural Product Communications, 4(4),* 535-542.

Ebrahimzadeh, M. A., Eslami, S., Nabavi, M. S., Nabavi, S. F., Moghaddam, A. H., Bekhradina, A. R. (2011). Estimation of Essential and Toxic Mineral Elements in *Mentha* Species. *Asian Journal of Chemistry, 23(4),*1648-1650.

Faiku, F., Haziri, A. (2015). Total lipids, proteins, minerals, essential oils and antioxidant activity of the organic extracts of *Mentha Longifolia* (L.) growing wild in Kosovo. *Eur. Chem. Bull., 4(9),* 432-435.

Food and National Board, Insitute of Medicine (2002) Dietary Reference Intakes for Vitamin A, Vitamin K, Arsenic, Boron, Chromium, Copper, Iodine, Iron, Manganese, Molybdenum, Nickel, Silicon, Vanadium, and Zinc, National Academic Press, Boston, pp 1-773

Gogoasa, I., Jurca, V., Alda, L.M., Velciov, A., Rada, M., Alda, S., Sirbulescu, C., Bordean, D. M., Gergen I. (2013). Mineral Content of Some Medicinal Herbs. *Journal of Horticulture, Forestry and Biotechnology, 17(4),* 65-67.

Gonçalves, R. S., Battistin, A., Pauletti, G., Rota, L., Serafini, L. A. (2009). Antioxidant properties of essential oils from *Mentha* species evidenced by electrochemical methods. *Rev. Bras. Pl. Med., Botucatu, 11(4),* 372-382.

Kızıl, S., Haşimi, N., Tolan, V., KILINÇ, E., Yüksel, U. (2010). Mineral content, essential oil components and biological activity of two mentha species (*M. piperita* L., *M. spicata* L.). *Turkish Journal of Field Crops, 15(2),* 148-153.

Konieczynski, P., Wesolowski, M. (2008). Determination of the water-extractable fraction of iron in selected medicinal plant raw materials: Folium Menthae, Folium Urticae and Folium Salviae. *Chemical Speciation and Bioavailability, 20(4),* 261-266.

Korfali, S. I., Mroueh, M., Al-Zein, M., Salem, R. (2013). Metal concentration in commonly used medicinal herbs and infusion by Lebanese population:health impact. *Journal of Food Research, 2(2),* 70-7.

Lozak, A., Sołtyk, K., Ostapczuk, P., Fijałek, Z. (2002). Determination of selected trace elements in herbs and their infusions. *Sci Total Environ. 22(289),* 33-40.

Maghrabi, A. I. (2014). Determination of some mineral and heavy metals in Saudi Arabia popular herbal drugs using modern techniques. African Journal of Pharmacy and Pharmacology, *8(39),* 1000-1005.

McKay, D. L., Blumberg, J. B. (2006). A review of the bioactivity and potential health benefits of peppermint tea (*Mentha piperita* L.). *Phytotherapy Research, 20,* 619-633.

Mihaljev, Ž., Živkov-Baloš, M., Ćupić, Ž., Jakšić, S. (2014). Levels of some microelements and essential heavy metals in herbal teas in Serbia. *Acta Poloniae Pharmaceutica - Drug Research, 71(3),* 385-391.

Mirzaei, A., Rezanejad, M. T., Mirzaei, N. (2015). Phytochemical and Antiradical Properties of Alcoholic and Aqueous Extracts of Red capsicum and *Mentha Piperita. Research Journal of Pharmaceutical, Biological and Chemical Sciences, 6(3),* 174-179.

Prabu, R., Raksha, S., Suralikerimath, N., Nagulendran, K. R. (2015). Evaluation of hepatoprotective and lipotropic effect of *Mentha piperita* leaf against carbontetrachloride-induced hepatic damage in rats. *Indian Journal of Pharmaceutical Science & Research, 5(1),* 10-13.

Pramila, D. M., Xavier, R., Marimuthu, K., Kathiresan, S., Khoo, M. L., Senthilkumar, M., Sathya, K., Sreeramanan, S. (2012). Phytochemical analysis and antimicrobial potential of methanolic leaf extract of peppermint (*Mentha piperita*: Lamiaceae). *J. Med. Plants Res., 6(2),* 331-335.

Recommended Dietary Allowances (10^{th}Edn) (1989) National Academy Press, NY, Washington DC, pp 1-285

Remigius, Chizzola. (2012). Metallic mineral elements and heavy metals in medicinal plants. *Medicinal and Aromatic Plant Science and Biotechnology, 6(Special Issue 1),* 39-53.

Rita, P., Animesh, D. K. (2011). An updated overview on peppermint (*Mentha piperita* L.). *International Research Journal of Pharmacy, 2(8),* 1-10.

Rubio, C., Lucas, J. R. D., Gutiérrez, A. J., Glez-Weller, D., Pérez Marrero, B., Caballero, J. M., Revert, C., Hardisson, A. (2012). Evaluation of metal concentrations in mentha herbal teas (*Mentha piperita*, *Mentha pulegium* and *Mentha* species) by inductively coupled plasma spectrometry. *Journal of Pharmaceutical and Biomedical Analysis, 71,* 11-17.

Saeed, K., Pasha1, I., Bukhari, H., Butt1, M. S., Iftikhar, T., Shujah-Ud-Din, U. (2014). Compositional profiling of Mentha piperita. *PAK. J. FOOD SCI., 24(3),* 151-156.

Sembratowicz, I., Rusinek-Prystupa, E. (2014). Effects of Brewing Time on the Content of Minerals in Infusions of Medicinal Herbs. *Pol. J. Environ. Stud., 23(1),* 177-186.

Siddig, MA., Elbadawi, AA., Abdelgadir, AE., Siddig, AA., Gibreel, MO. (2015). Structural characterization and physical properties of three different types of peppermint (Mentha cervina). *Int. Journal of Applied Sciences and Engineering Research, 4(3),* 364-370.

Stanojkovic-Sebic, A., Pivic, R., Josic, D., Dinic, Z., Stanojkovic, A. (2015). Heavy metals content in selected medicinal plants commonly used as components for herbal formulations. *Journal of Agricultural Sciences, 25,* 317-325. Szentmihályi, K.,

Hajdú, M., Then, M. Inorganic biochemistry of medicinal plants. Medicinal and Aromatic Plant Science and Biotechnology; 2008, 2(1):57-62.

Szymczycha-Madeja, A., Welna, M., Zyrnicki, W. (2013). Multi-Element Analysis, Bioavailability and Fractionation of Herbal Tea Products. *J. Braz. Chem. Soc.*, *24(5)*, 777-787.

Zijp, IM., Korver, O., Tijburg, LB. (2010). Effect of tea and other dietary factors on iron absorption. *Crit Rev Food Sci Nutr. 40(5)*, 371-398.

Živkov-Baloš, M., Mihaljev, Ž., Ćupić, Ž., Jakšić, S., Apić, J., Ljubojević, D., Prica, N. (2014). Determination of some essential elements in herbal teas from Serbia using Atomic spectrometry (AAS). *Contemporary Agriculture/Savremena poljoprivreda, 63(4-5)*, 394-402.

Summary/Sažetak

Čaj od mente (*Menthae piperita* L.) je jedan od najčešće konzumiranih biljnih čajeva. Ovaj je čaj prepoznat kao napitak sa više zdravstvenih benefita, prije svega usljed prisustva nutritivnih elemenata posebno esencijalnih mikro i ultramikro elemenata. U ovoj studiji ispitali smo sadržaj željeza u uzorcima čajeva od mente iz lokalnih marketa u Sarajevu. Pripremanje uzoraka provedeno je suhom digestijom u triplikatu dok je sadržaj željeza analiziran spektrofotometrijski. Količina željeza bila je u intervalu od 275.6 mg Fe/kg do 354.6 mg Fe/kg. Primjenjena spektrofotometrijska metoda je jednostavna i osjetljiva te se može koristiti za određivanje ukupnog sadržaja željeza u biljnom materijalu.

Glasnik hemičara i tehnologa Bosne i Hercegovine

Bulletin of the Chemists and Technologists of Bosnia and Herzegovina

2017

48

27-34

Print ISSN: 0367-4444
Online ISSN: 2232-7266

UDC: _____

Original Scientific Paper

Contribution to Knowledge of Contains on Peridotite Rocks of the Krivaja-Konjuh Ophiolitic Complex (Massif)

Operta, M.

Department of Geography, Faculty of Science, Zmaja od Bosne 33-35, Sarajevo, Bosnia and Herzegovina

Article info
Received: 31/03/2017
Accepted: 16/06/2017

Keywords:
peridotite,
mineralogical tests,
chemical tests,
optical method,
X-ray fluorescence spectroscopy method
electron microprobe method

***Corresponding author:**
E-mail: opertamevlida@yahoo.com
Phone: +38733 723 754

Abstract: Krivaja-Konjuh ultramafic complex is mainly constructed of ultramafic rocks associated with different varieties of igneous rocks (gabbro, dolerite, diabase, spilite, keratophyres, granitoids) and metamorphic rocks (amphibolites, amphibolite schists and eclogites). This paper presents results of mineralogical and chemical analysis of ultramafite rocks (peridotite-lherzolites) samples in the southern part of Krivaja-Konjuh massif. The samples were examined optically, by using method of X-ray fluorescence spectroscopy and electron microprobe method. Optical results showed that lherzolites have uniform textural characteristics and mineral composition. Results of chemical studies on these rocks demonstrated modal composition with high content of MgO, low content of CaO and high content of MgO:FeO (about 5 and up). Based on CIPW normative system, their composition is uniform with a very small variation in the content of diopside, with a slightly larger variation in the content of olivine. The rhombic pyroxene in composition correspond to enstatite and monoclinic pyroxenes are diopside by the composition. Spinel in peridotites are Al spinels and Al chromium spinels.

INTRODUCTION

Ophiolite zone of Internal Dinarides is a separate tectonic unit and it stretches from Banija in Croatia through Bosnia and western Serbia, to Kosovo on southeast and continues to Hellenides. Within ophiolite zones in Bosnia, there are 6 ophiolite complexes (Krivaja-Konjuh, Ozren, Kozara, Varde and Višegrad area, complex Ljubić, Čavke and Vrbanje, and complex Borje and Mahnjače) mainly of identical composition, although each carries some specific characteristics that makes it different from other complexes. Krivaja-Konjuh complex is located in the central parts of the ophiolite zone of the Dinarides and is elongated in the northwestsoutheast direction. The dominant role in Krivaja-Konjuh massif have ultramafic rocks occupying an area of over 500 km2 and they are associated with different varienties of ingeous rocks and metamorphic rocks. A few ten of samples pf peridotides were microscopic processed, and selected representative samples were examined in detail which will significantly extend our knowledge of peridotite in Krivaja-Konjuh (massif). Based on all acquired field and laboratory data, the mineral and chemical composition of samples have been determined. Determination of the content of macro elements and normative CIPW composition and determination of micro elements is the basis for rock classification and complete definition of the chemical composition of these rocks.

Geological characteristics of the dinaride ophiolite zone

Ophiolite complex rocksare is related to the internal Dinarides and they represent very complex association of rocks among which ultramafites are the most characteristic ones which are associated with different varieties of gabbros, dolerite, diabases, spilite and amphibolites and united in the so-called diabase-chert formation or Jurassic-igneous-sedimentary formation (Katzer, 1906.; Ćirić, 1954.; Pamić, 1964.). Various types of gabbros, dolerites, diabases and spilites constitute about 5-10% ophiolite complex (Pamić, 1964).

Ophiolite zone of the Dinarides has been camouflaged in some parts, with drawn Mesozoic, mainly calcareous and Paleozoic semimetamorphic rocks. In ophiolite complexes of the Dinarides ophiolite zones, prevail ultramafites (lherzolites, harzburgites) and serpentinite. Very rarely one encounters complete preserved ophiolite profiles (Pamić&Desmons, 1989), but more often than chaotic relationships, i.e. ophiolite mélange (Dimitrijević, 1973) is present.

Ophiolite mélange is built of shale-silt matrix in which they are usually fragments of greywackes, radiolarites and exotic limestones of Middle Triassic to Jurassic - Lower-Cretaceous age. In the mélange, there are also fragments and blocks of ophiolites centimeter - decimeter - hectometer - the kilometer in size.

As the most dominant rocks in the ophiolite mélange appear fragments and blocks of peridotites represented by faulted plates, thickness from a few hundred meters to 2000 meters, drawn on ophiolite mélange (Pamić&Desmons, 1989).

So far, in the ophiolite mélange, e.g. in its matrix, typical fossil remains have not been found. Based on uncharacteristic fossils, Jurassic age is assumed, which is consistent with available data on isotopic age 189-136 Mav(Lanphere et al., 1975; Meyer et al., 1979; Lugović et al., 1991).

Over the ophiolite mélange of the Dinarides ophiolite zone lie transgressive Lower Cretaceous formations of Pogarska formation.

Krivaja-Konjuh Ophiolite Complex

There is a large number of works related to certain small areas (Pamić, et al., 1977., Pamić, 1978: Operta et al., 2003., Trubelja et al., 1995., Šegvin, B., 2010., Faul et al., 2014) about Krivaja-Konjuh ophiolite complex,

Krivaja-Konjuh complex extends from the Bosna river valley in the west to the road Sarajevo-Tuzla in the east.

In the north, i.e., the northwest, boundary is not visible, while to the south it extends to Vareš. Through the central part of the ophiolite complex the river Krivaja flows dividing it into two equally sized blocks, after which, together with neighboring mountain Konjuh the complex got its name.

The dominant role in the Krivaja-Konjuh massif have ultramafite rocks occupying an area of over 500 km^2 and they are associated with different varieties of igneous

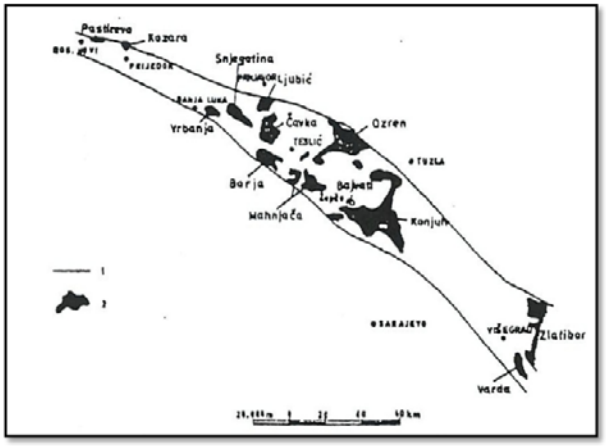

Figure 1. Schematic map of northwestern and middle parts of the Dinaride Ophiolite zone (Pamić et al., 1977). 1. boundary of the Ophiolite zone. 2. larger ultramafic massifs.

rocks and metamorphic rocks (amphibolites, amphibolite schists and eclogites). (Pamić, 1978).

Amphibolites form narrower or wider zones around ultramafite massif and in some areas they exceed ultramafic in size. All these rocks are members of the Jurassic ophiolite mélange with a dominant share of greywacke sandstones and slates. Krivaja-Konjuh ophiolite complex together with ophiolite mélange covers an area of approximately 1000 km^2 (Pamić, 1978).

Over the ophiolite mélange, synclinally lies Pogari Formation of Tithonian-Cretaceous age and over the Krivaja-Konjuh ultramafic massif in the area Sokoline, transgressivelly lie the Upper Jurassic limestones. This suggests that age of ophiolite mèlange falls between the Jurassic and Tithonian.

Phyllite and quartz-sericite schists were spotted in the central part of the southern perimeter of Dubоštica and on the east end at Konjuh to Miljevice, similar in appearance to match the Paleozoic formations. It is concluded that they represent the transformed greywacke sandstones and slates of Jurassic ophiolite mélange.

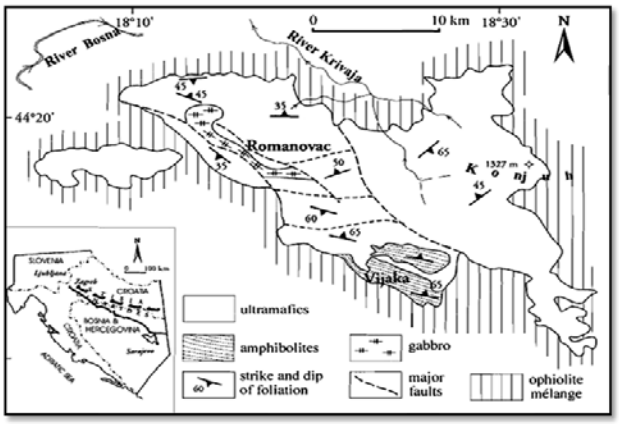

Figure 2. Schematic structural map of Krivaja-Konjuh massif (Pamić et al., 1977).

Ophiolite complexes of various geographical areas mainly have identical composition. Mafic rocks are much subordinated; they occur frequently but in smaller

masses. The relationship between ultramafic and mafitc, including amphibolites, is 9 to 1 (Pamić, 1978).
Rarely one can encounter a fully preserved ophiolite profiles. Usually the complete ophiolite profiles in ophiolite situating are broken, tectonised, and, as smaller or larger fragments, they are included in ophiolite mélange.

EXPERIMENTAL

A few dozen samples of peridotites were selected in the southern part of the Krivaja-Konjuh ultramafic massif, which were optically tested and based on the results of optical tests, seven samples were selected. The samples were labeled and prepared for analysis of macroelements and microelements, by X-ray fluorescence spectroscopy method, and for chemical analysis of mineral phases by electron microprobe. The paper presents in detail the results of those tests.

Optical Methods

To determine mineral composition and structural, textural characteristics of rocks as well as relationships among minerals, microscopic preparates were made with standard thickness from 0.02 to 0.03 mm. As a binding agent and at the same time as an internal standard for refractive index, Canada balsam from the "Semikem"Company was used.
When making microscopic preparates,slides were used, with various sizes, depending on whether they are used for testing the structure and textures, mineral composition, or for determining on universal table.
In microscopic determination, a polarizing Reichart microscope was used with a range of increasing 25-630x at the Faculty of Science in Zagreb, and polarizing Olympus microscope brand PX 40 at the Institute of Mineralogy of Innsbruck.
Samples were microscoped in transmitted light in orthoscopic conditions, without and with the included analyzer, and in conoscopic illumination observations conditions. Standard microscope equipmentwas used.
A polarizing microscope was also used, with the Carl Zeiss Jena universal table (4 + 1 axis) with increases 125-500x. Hemispheres were used, with refractive indexes n-1,516 and n-1,648 depending on the refractive index of the measured minerals. As a light source, "white" light microscope bulb was used.

Chemical Analyzes of Rocks

Analysis of macro elements

The rocks have been chemically analyzed by the method of X-ray fluorescence spectroscopy using wave-dispersive instrument SRS 3000 (TYROLIT Schleifmittelwerk, SWAROVSKI GROUP-SCHWARZ Tyrol) at the Institute of Mineralogy and Petrology in Innsbruck.
Analysis of macroelements was also performed by the method of X-ray fluorescence spectroscopy according to the procedure recommended by Johnson & Matthey.
Proportion of bivalent iron in the sample was determined according to the volumetric method, according to WILSON (1955).
Water in the sample was determined gravimetrically, drying at 110 °C (H_2O^-) and the subsequent sample annealing at 1025 °C to determine H_2O^+.

Analysis of micro elements

Analysis of trace elements was also performed by the method of X-ray fluorescence spectroscopy. For the analysis of trace elements, 35 mm diameter tablets were made by compressing 4 g of finely ground sample. Before pressing, the sample was admixed 1 g binder (Hoechst Wachs C). The sample was pressed in a hydraulic press for ten minutes with pressure to 20 kN and dried at 110°C.

Chemical analyzes of mineral phases

Chemical analyzes of mineral phases were carried out using electron microprobe ARL -SEMQ at the Institute of Mineralogy and Petrology in Innsbruck. This instrument has four WDS spectrometers and Noran-Voayager EDS (energy dispersive system). All analyzes were done at a voltage of 15 kV and current of 20 nA with a nominal diameter of the beam of 1-2 microns. Next standards were used: labradorite (Si, Al, Ca) rutile (Ti), chromite (Cr), diopside (Mg), rodonite (Mn), fayalite (Fe), albite (Na), sanidine (K), V metal (V), metal (V), pyrope (Si analysis with garnets).
Bivalent and trivalent iron in ilmenite, garnet, clinopyroxenes and orthopyroxenes, is calculated based on the stoichiometry.

Method for calculation of chemical analysis to the standard formula

Analysis results were calculated to a number of oxygen and cations.
Analyses of clinopyroxene and orthopyroxene werecalculated according to the Norm recommendations (Wood, 1988) at 6 O.
Analyses of spinel and olivine were calculated according to the recommendations of HYPER - FORM (S.Bjerg et al. 1991). Analyses of spinel were calculated at 32 O, and olivine at 4 O.

RESULTS AND DISCUSSION

In the southern part of Krivaja-Konjuh ultramafic massif, peridotite samples were taken and optically tested,and samples were selected for analysis of macro and micro elements by X-ray fluorescence spectroscopy method as well as for chemical analysis of mineral phases by electron microprobe.
The results of optical tests showed that lherzolites have uniform structural-textural characteristics and mineral composition. They were made of olivine, enstatite and diopside, with a clear domination of olivine. Accessory ingredient is spinel.
The structures of ultramafic rocks are granular and porphyroide. The grain size of the primary constituents

of the granular representatives ranges from 0, 5 to 2 mm, and in ultramafic with porphyroblastic structure, phenocrystic size (typically lamellar enstatite) goes up to 20 mm.Very rarely are fresh, usually are serpentinised. Serpentised ultramafite are fine-ground. Ultramafic textures are massive (rarely) and various parallel (pseudostratification and foliation).

In mineral composition of the optically surveyed lherzolites, one can find primary and secondary minerals. The primary minerals of lherzolites are olivine, enstatite, diopside and spinel. Secondary minerals were following: serpentine, chlorite, amphibole, talc, magnesite, quartz, opal, magnetite, limonite and hematite.

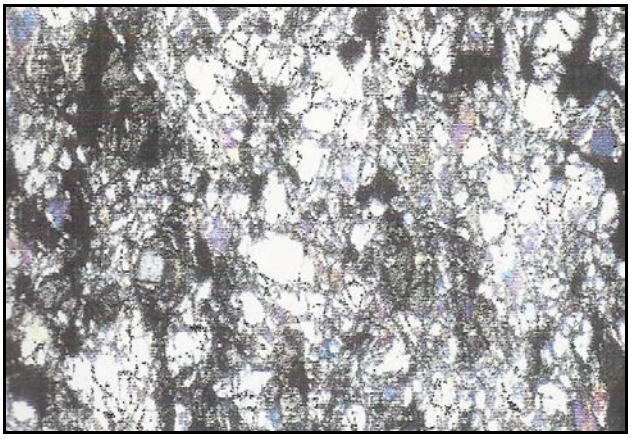

Figure 3: Recrystalization of olivine small grains mixed with pyroxene in lherzolites. N+.

Chemical composition of lherzolites in Vijaka area is very uniform and it stands out with high MgO content (about 40 wt. %), low CaO content about 3% (from 1.96 to 2.86%) and a high ratio of MgO: FeO (about 5 or higher) - table 1.

Table 1. Chemical analysis of macro elements in peridotites-lherzolites (macroelements in wt. %)

Sample	1	2	3	4
SiO_2	41,03	41,75	40,31	39,81
TiO_2	0,15	0,18	0,14	0,12
Al_2O_3	0,92	1,63	1,57	1,08
Fe_2O_3	2,91	2,92	2,96	3,16
FeO	5,83	5,85	5,91	6,33
MnO	0,13	0,12	0,13	0,13
MgO	35,77	38,34	38,89	40,17
CaO	1,96	2,86	2,64	2,42
Na_2O	0,18	0,31	0,22	0,19
K_2O	0,02	0,00	0,00	0,00
P_2O_5	0,02	0,01	0,00	0,01
H_2O^-	0,52	0,59	0,64	0,59
H_2O^+	10,49	6,28	6,88	6,40
total	99,92	100,8	100,2	100,4

1 and 4-lherzolites; 2-serpentinizied lherzolites; 3-porphyroblastic lherzolites.

This, in fact, is in accordance with the contents of the main components which Pamić (1977) got by researching the chemical composition of spinel lherzolites in the Krivaja-Konjuh ultramafic massif.

The whole chemical compositions of the samples analyzed are shown in Table 1. Frey (1984) used calcium for the differentiation of rocks between the Ca rich and Ca poor mantle rocks, since calcium is closely associated with clinopyroxene and this mineral is very often well-preserved in the rocks.

Analyzed samples are affected by serpentinisation, which probably results in changes, of the primary Ca content.

Like Ca, Ti is incompatible element, which is exhausted during melting, in the mantle rocks coming to separation Ti rich phases of the gabrous composition solutions. In contrast to Ca, Ti is an element with low mobility (Pearce & Cann, 1973) and therefore during metamorphism stay in mantle rocks even if Ca is shifted-removed. As trace elements Ni and Co are significantly enriched, both become compatible elements with high distribution relationship between the residue and the partial solution. Usually they are incorporated in olivine crystal lattice replacing Mg. The same route of enrichment must be valid for Cr (2930 ppm) but in research of mantle rocks, this is not fully explored. The content of chromium in the less exhausted and inexhaustible mantle rocks is 2510-3090 ppm (Table 2).

Table 2. Chemical analysis of trace elements in peridotites-lherzolites (trace elements and rare soils in ppm).

Sample	1	2	3	4
Qtz	0,00	0,00	0,00	0,00
Or	0,10	0,00	0,00	0,00
Ab	1,70	2,80	2,00	1,70
An	1,90	3,30	3,60	2,20
Lct	0,00	0,00	0,00	0,00
Ne	0,00	0,00	0,00	0,00
C	0,00	0,00	0,00	0,00
Di	7,10	9,30	8,30	8,30
Hy	28,50	14,20	10,30	6,40
Ol	57,70	67,50	72,90	78,50
Ac	0,00	0,00	0,00	0,00
Mt	2,70	2,60	2,60	2,50
Ilm	0,30	0,00	0,00	0,00
Ap	0,10	0,00	0,00	0,00

1 and 4-lherzolites; 2-serpentinizied lherzolites; 3-porphyroblastic lherzolites.

Most likely it seems that the Cr is incorporated (plugged-annexed) in spinels which are very unevenly distributed in mantle rocks. This explains the variability of Cr in peridotites.

Table 3. provides a lherzolites modal relationship.

Table 3. Normative composition of the CIPW (wt.%)

	1	2	3	4)
Ba	7	9	6	5
Co	119	109	106	117
Cr	2730	2650	3090	2510
Cu	23	25	25	26
Ga	4	4	3	3
Ni	2380	2050	1930	2180
Sc	11	12	14	11
Sr	< 2	12	< 2	< 2
V	59	68	72	63
Y	2	3	3	2
Zn	53	50	52	51
Zr	3	6	2	2
S	230	180	150	200
Cl	790	890	540	580
F	< 50	< 50	< 50	< 50
Pb	4	2	2	2
Rb	< 2	< 2	< 2	< 2
Cs	< 5	< 5	< 5	< 5
La	< 5	< 5	< 5	< 5
Ce	< 10	< 10	< 10	< 10
Pr	< 5	< 5	< 5	< 5
Nd	< 5	< 8	< 5	< 5
Sm	7	< 5	< 5	< 5
As	< 2	< 2	< 2	< 2
Mo	2	2	2	2
Nb	2	2	2	2
Sn	< 3	< 3	< 3	< 3
Th	< 2	< 2	< 2	< 2
U	< 2	< 2	< 2	< 2

1 and 4-lherzolites; 2-serpentinizied lherzolites; 3-porphyroblastic lherzolites

Unified in this way, modal relations conditioned uniform chemical characteristics of lherzolites. The table 3 (normative composition of the CIPW) shows a balanced composition of the main components of which should be pointed out the following: a small variation in the content of the diopside (7.10 to 9.30 wt. %) and slightly larger variations in the content of hyperstene (6.40-28.50) and the content of olivine (57.70 to 78.50%). Converted Niggli parameters (table 4.) indicate the great ratio of magnesium to iron (Niggli value Mg is usually between 0.80 and 0.90), a low content of aluminum and calcium is conditioned by the presence of small amounts of diopside (transition to harzburgite). Usually there is a higher amount of constitutive water, which shows a high degree of serpentinization of these rocks.

Olivine, clinopyroxene, orthopyroxene and spinels

Olivine is a common phase/mineral. It is developed hypidiomorphic to allotriomorphic, often, however, with rounded, egg-shaped contours. The content of fayalite component in lherzolites of Vijaka area varies from 9-11%. The mean content of fayalite in the analyzed lherzolites of Vijaka area is 10.12%. The average results of fayalite are roughly in line with the values of mean content-received by Pamić (1977) for the Vijaka ultramafic area (8% fayalite). Mean Fo content in the analyzed lherzolite rocks is 89% . The values obtained are consistent with the values of mean content received by Pamić et al (1977) for the Vijaka ultramafic area (89% forsterite).

Table 4. Niggli petrochemical classification for analyzed peridotites.

Sample	1	2	3	4
Si	66,05	61,89	59,28	57,06
Al	0,87	1,43	1,33	0,95
Fm	95,45	93,59	94,17	95,09
C	3,38	4,54	4,15	3,70
Alk	0,29	0,45	0,35	0,26
K	0,00	0,00	0,00	0,00
Mg	0,88	0,89	0,89	0,88
Ti	0,19	0,18	0,18	0,17
P	0,00	0,00	0,00	0,00
H	56,29	31,08	33,75	30,55
W	0,31	0,31	0,32	0,31
C/fm	0,04	0,05	0,04	0,04

.

Olivine in lherzolites has high content of MgO and small content of CaO which is unusually low (0.04 to 0.10%). NiO content (from 0.19 to 0.45%) is characteristic of olivines from crust peridotites (Table 5).

Analyzed peridotites-lherzolites in Vijaka area are characterized by quite uniform modal composition, and the main petrogene minerals have uniform chemistry; olivine contains about 89.7% forsterite and orthopyroxene about the same number of percentage enstatite component, which is reflected in very high ratio MgO: (MgO + FeO), which is more than 5 (table 6).

Average compositions in lherzolites are as follows: enstatite is $Fs_{16}En_{83}Wo_1$ and clinopyroxene Fs_6 En_{48} Wo_{46}.

Enstatite is also characteristic one, although much more subordinated ultramafic ingredient. It occurs in discrete grains and sometimes we find in it clinopyroxene lamelle, which cause lamelliform. According to teodolite-microscopic determination (Pamic et al., 1977), the content of ferrosilite component in the Krivaja-Konjuh-ultramafic massif varies from 7 to 16% and the mean content based on the measurements performed 34 granules is 11%. This geochemical tests on lherzolites composition by electron microprobe, have confirmed that the chemical composition of enstatite is uniform: content of ferrosilite component varies from 15 to 18%, and the mean content is 16%.

Diopsides are more subordinated than enstatite. It usually occurs as hypidiomorphic and flattened grains. Often it occurs in lamelli form, which is due to secretion by direction of other pinacoides. Optical tests on 23 grains Pamic et al., 1977, noted the presence of irondiopside in ultramafic. Our tests have shown that in lherzolites, chromium content in diopside varies from 0.21-0.99 wt.%, with the mean content of 0.60% Cr_2O_3, and it represents the emerald green chrome diopside (table 7).

Table 5. Selected chemical analyzes of olivine in peridotite-lherzolites (wt. % and formula calculation based on 4 O).

	1	3-3	3-5	4-3
SiO_2	40,97	40,79	40,79	40,89
Si	1,001	1,002	1,000	1,002
TiO_2	0,00	0,00	0,24	0,00
Al_2O_3	0,00	0,00	0,00	0,00
Cr_2O_3	0,27	0,00	0,00	0,07
FeO	9,77	10,07	10,05	9,55
MnO	0,19	0,20	0,00	0,26
MgO	49,04	48,71	48,72	48,97
CaO	0,00	0,04	0,00	0,00
Na_2O	0,00	0,00	0,00	0,00
K_2O	0,00	0,00	0,00	0,00
ZnO	0,00	0,17	0,00	0,11
NiO	0,00	0,36	0,34	0,19
total	**100,2**	**100,3**	**100,1**	**100,0**
Si	1,001	1,002	1,000	1,002
Ti	0,000	0,000	0,004	0,000
Al	0,000	0,000	0,000	0,000
Cr	0,005	0,000	0,000	0,001
Fe^{+2}	0,200	0,207	0,206	0,196
Mn	0,004	0,004	0,000	0,005
Mg	1,786	1,771	1,779	1,788
Ca	0,000	0,001	0,000	0,000
Na	0,000	0,000	0,000	0,000
K	0,000	0,00	0,000	0,000
Zn	0,000	0,003	0,000	0,002
Ni	0,000	0,011	0,010	0,004
total	**2,996**	**2,998**	**2,999**	**2,996**

1 olivine in peridotites (lherzolites); 3-3 contact with orthopyroxene; 3-5 contact with clinopyroxene; 4-3 contact with spinel.

The rhombic pyroxene have narrow variation of composition: Fs_{15-18} En_{81-84} $Wo_{0.8-1.5}$ and contain aluminum Al_2O_3 2.41 to 3.64% and a low content of titanium (0.01 to 0.18% TiO_2). They correspond to the composition of enstatite.

Monoclinic pyroxenes in ultramafites have a composition with a relatively narrow variation: Fs_{5-7} En_{47-49} Wo_{45-46} and they are classified as diopsides. The content of aluminum in the monoclinic pyroxene is 2.52 to 5.87% Al_2O_3 and concentration of titanium and chromium are as follows: from 0.14 to 0.49% TiO_2, Cr_2O_3 0.21 to 0.59% (table 7). High values are determined for the loss on ignition in Vijaka area (6.28 to 10.49%), confirms the impression of a strong alteration that affected the original chemistry of ultramafic rocks (Morimoto, 1988).

Spinels are typical accessory minerals of lherzolites. They were developed starting from hypidiomorphic to allotriomorphic. The chemical composition of spinels varies greatly. The most common of them is Al-spinel, which is spotted in over 45% of analyzed peridotite rocks. Something subordinated is Al chromium spinel (over 35%) while the chromium hercinite is subordinate (18%). Their distribution with respect to the different varieties is as follows: Al-spinels and Al chromium spinels in particular often come in lherzolites (table 8).

Al chromium spinels are of low TiO_2 (0.06 to 0.09 wt.%) with concentrations NiO (0.45 to 0.57) and a narrow range of magnesistion 77.30 to 77.96 and chromium content from 10.92 to 15, 62. In Al spinel, magnesium is in the range of magnesium (Mg # = 100 * / (Mg + Fe^{2+}) = 53.69 to 71.51) with little share variation (Cr # = 100 * / (Cr + Al) = 6,17- 9.32). The concentration of nickel has been increased and is 0.18 to 0.90% and the content of titanium is small 0.0 to 0.02% TiO_2.

In areas of normal contact between ultramafites and amphibolite, appears subordinated colorless edenite hornblende with less chromium and magnesiohornblende. The concentrations of aluminum and calcium depend on the modal content of pyroxene and amphibole. The content of TiO_2 is low.

Calcium content in the olivine, is typical for olivines of high-pressure layered peridotite. This is not the primary feature but is the result of the redistribution of calcium between olivine and interkumulus minerals on subsolidus temperatures.

The distinction between the mantle rocks and ultramafite cumulate rocks was given by Irvine & Findlay (1972), who used the NiO vs Cr_2O_3 diagram for discrimination. Most mantle peridotites with spinel are have NiO value 0.2% .

Table 6. Selected chemical analyzes in orthopyroxene peridotites-lherzolites (wt. % and formula calculation based on 6 O).

	3-4	2-8	2--12	3-2
SiO_2	55,29	56,16	55,72	55,81
TiO_2	0,00	0,00	0,00	0,00
Al_2O_3	3,64	2,72	3,20	2,41
Cr_2O_3	0,17	0,24	0,00	0,06
Fe_2O_3	0,00	0,00	6,97	0,00
FeO	6,75	6,78	0,00	7,30
MnO	0,18	0,20	0,21	0,00
MgO	32,84	33,26	33,59	33,89
CaO	0,49	0,42	0,28	0,46
Na_2O	0,01	0,00	0,06	0,00
K_2O	0,05	0,01	0,00	0,00
NiO	0,39	0,10	0,19	0,29
total	**99,81**	**99,92**	**100,22**	**100,22**
Si	1,919	1,943	1,931	1,932
Ti	0,000	0,000	0,000	0,000
Al	0,148	0,110	0,130	0,098
Cr	0,004	0,006	0,000	0,001
Fe^{+3}	0,000	0,000	0,181	0,000
Fe^{+2}	0,196	0,196	0,000	0,211
Mn	0,005	0,005	0,006	0,000
Mg	1,699	1,715	1,735	1,748
Ca	0,018	0,015	0,010	0,017
Na	0,000	0,000	0,004	0,000
K	0,002	0,00	0,000	0,000
Ni	0,010	0,002	0,005	0,008
total	**4,001**	**3,992**	**4,002**	**4,015**

3-4 orthopyroxene contact with olivine; 2-8 contact with serpentine; 2-12 and 3-2 contact with clinopyroxenes.

Table 7. Selected chemical analyzes of clinopyroxene in peridotites-lherzolites (wt. % and formula calculation based on 6 O).

	3-7	4-7
SiO_2	51,87	53,37
TiO_2	0,49	0,14
Al_2O_3	4,70	2,52
Cr_2O_3	0,59	0,21
Fe_2O_3	1,29	1,48
FeO	1,63	1,24
MnO	0,11	0,17
MgO	15,72	16,91
CaO	22,30	23,30
Na_2O	1,12	0,77
K_2O	0,00	0,00
NiO	0,16	0,00
total	99,98	100,11
Si	1,892	1,942
Ti	0,013	0,003
Al	0,202	0,108
Cr	0,017	0,006
Fe^{+3}	0,035	0,040
Fe^{+2}	0,049	0,037
Mn	0,003	0,005
Mg	0,854	0,917
Ca	0,871	0,908
Na	0,079	0,054
K	0,00	0,00
Ni	0,004	0,00
Ni	0,004	0,00
total	4,019	4,020

3-7 and 4-7 contact with olivine.

Table 8. Selected chemical analyzes of spinel in peridotites-lherzolites (wt. % and formula calculation based on 32 O).

	1	2-2	3-1	3-2	4-2
SiO_2	0,11	0,16	0,15	0,05	0,09
TiO_2	0,00	0,21	0,09	0,06	0,00
Al_2O_3	58,98	23,93	55,80	56,97	56,98
Cr_2O_3	7,83	36,33	11,00	10,41	9,70
Fe_2O_3	2,84	8,91	2,15	2,20	2,67
FeO	9,88	14,96	10,00	10,37	9.69
MnO	0,13	0,91	0,31	0,00	0,29
MgO	19,73	12,96	19,11	19,34	19,32
CaO	0,17	0,03	0,06	0,00	0,09
Na_2O	0,18	0,00	0,13	0,00	0,18
K_2O	0,04	0,22	0,00	0,23	0,00
ZnO	0,02	0,55	0,43	0,00	0,07
NiO	0,24	0,13	0,45	0,57	0,49
total	**100,12**	**99,30**	**99,70**	**100,20**	**99,60**
Si	0,023	0,040	0,032	0,010	0,019
Ti	0,000	0,040	0,014	0,009	0,000
Al	14,32	7,055	13,79	13,96	14,03
Cr	1,275	7,156	1,824	1,712	1,608
Fe+3	0,440	1,685	0,340	0,345	0,390
Fe+2	1,701	3,12	1,75	1,80	1,69
Mn	0,023	0,194	0,055	0,00	0,052
Mg	6,058	4,516	5,976	5,997	6,009
Ca	0,038	0,009	0,013	0,00	0,020
Na	0,072	0,00	0,053	0,00	0,073
K	0,010	0,055	0,00	0,062	0,00
Zn	0,00	0,102	0,067	0,00	0,011
Ni	0,040	0,026	0,076	0,095	0,082
total	**24,001**	**24,000**	**24,000**	**23,999**	**23,999**

CONCLUSION

Selected samples of peridotites in the Krivaja-Konjuh massif southern edge were used to conducted optical researches by polarization microscopy, chemical analysis of macro elements, trace elements and rare earth by X-ray fluorescence spectroscopy, and chemical analysis of minerals by electron microprobe.

Vijaka amphibolites are related to the Krivaja-Konjuh ultramafite massif and these amphibolites are frequently layered in their highest parts with ultramafite pointing to their genetic relationships. It is evident that Vijaka amphibolite complex is part of the Dinarides Ophiolite zone in which they are involved with related Krivaja-Konjuh ultramafite massif.

Peridotite-lherzolites are thoroughly investigated by optical, chemical analysis and electron microprobe. The results of chemical research of these peridotites showed quite uniform modal composition of these rocks, which is characterized by a high content of MgO, low CaO and high content of MgO: FeO (about 5 and more), which is in accordance with the contents of the main components of the research results spinel lherzolites in the Krivaja-Konjuh ultramafic massif.

Based on CIPW normative system they have uniform composition with a very small variation in the content of the diopside with a slightly larger variation in the content of olivine. The content of CaO and NiO in olivine indicate olivines from crustal peridotites. The rhombic pyroxenes, according to their composition correspond to enstatites and monoclinic pyroxenes to diopsides. Spinelles in peridotites are Al spinels and Al chromium spinels.

High values determined for losses on ignition peridotite confirm virtual impression of strongly altered the original chemistry of ultramafite rocks.

REFERENCES

Ćirić, B. (1954). Neka zapažanja o dijabaz rožnjačkoj formaciji Dinarida. *Ves. Zav. geol. geof. istr.*, 20, 31 – 88.

Dimitrijević, M.D., Dimitrijević, M.N. (1973). Olistrome melange in the Yugoslavian Dinarides and late Mesozoic plate tectonics. *Journ. Geology*, 81, 328 – 340.

Faul, U., H., Garapić, G., Lugović, B. (2014): Subcontinental rift initiation and ocean-continent transitional setting of the Dinarides and Vardar zone: Evidence from the Krivaja-Konjuh Massif, Bosnia and Herzegovina. *Lithos* 202-203:283-299.

Frey, F. A. (1984). Rare earth element abundances in upper mantle rocks. In: Henderson, P. (ed.): *Rare earth elements geochemistry*, Elsevier, 153-203.

Irvine, T. N., Frinday, T. C. (1972): Alpine-type peridotite with particular reference to the Bay of Islands Complex.-In: The ancient oceanic lithosphere, 97-128, *Publ. Earth Physics Branch*, Ottawa, Canada.

Katzer, F. (1906): Istorijsko razvijanje i današnje stanje geoloških proučavanja Bosne i Hercegovine, *Glas. Zem. Muzeja BiH* 18, 37 –68.

Lanphere, M., Coleman, R., Pamić, J. & Karamata, S. 1975, Age of amphibolites associated with alpine peridotites in the Dinaride Ophiolite zone, Yugoslavia. Earth Plan. Scie. Lett., 26, 271-276.

Lugović, B., Altherr, R., Raczek, I., Hofmann, A. W., Majer, V. (1991): Geochemistry of peridotites and mafic igneous rocks from the Central Dinaridic Belt, Yugoslavia. Contrib. *Mineral. Petrol*., 106, 201-216.

Majer, V., Kreuzer, J., Harre, W., Seidel, E., Altherr, R., Okrusch, M. (1979): Petrology and geochronology of metamorphic rocks from Banija, Yugoslavia. *Inter. Ophiol. Symp., Abstracts*, 46-47, Nicosta.

Majer, V., Kreuzer, J., Harre, W., Seidel, E., Altherr, R., Okrusch, M. (1979): Petrology and geochronology of metamorphic rocks from Banija, Yugoslavia. *Inter. Ophiol. Symp., Abstracts*, 46-47, Nicosta.

Majer, V., Kreuzer, J., Harre, W., Seidel, E., Altherr, R., Okrusch, M. (1979): Petrology and geochronology of metamorphic rocks from Banija, Yugoslavia. *Inter. Ophiol. Symp., Abstracts*, 46-47, Nicosta.

Morimoto, N. (1988): Nomenclature of pyroxenes.- *Fortschr. Miner.*, 66, 2, 237-252.

Operta, M., Pamić, J., Balen, D., Tropper, P. (2003): Corundum-bearing amphibolites from metamorfic sole of the Krivaja – Konjuh ultramafic massif from the Dinaride Zone, Bosnia, Springer LINK *Mineralogy and Petrology*, 77(3-4) 287-295.

Operta, M., Salihović, S. (2003): Rezultati istraživanja amfibola iz amfibolitskih stijena u okolini Vareša, *Zbornik radova Rudarsko-geološko-građevinskog fakulteta u Tuzli*, XXVI, 67-73, Tuzla.

Operta, M. (2006): Geološke i mineraloško – petrografske karakteristike amfibolita u području Vijake kod Vareša, *Glasnik Zemaljskog muzeja PN-sveska* 32, str. 7-45, Sarajevo. UDK 54/59 (058). ISSN 0581-7528.

Operta, M. Hyseni, S., Balen, D., Salihovic, S., Durmishaj, B. (2011): Garnet group minerals from the amphibolite facies metamorphic rocks of Krivaja-Konjuh ultramafic massif in Bosnia and Herzegovina. *ARPN Journal of Engineering and Applied Sciences (JEAS)*, Vol. 6. ISSN 1819-6608.

Operta, M., Hyseni, S. (2012): Krivaja-Konjuh Ophiolite Complex in Bosnia and Herzegovina Addition to Study on Mineral Composition of Metamorphic Rocks, IJET, *International Journal of Engineering & Technology*, Volume 2, No.4, 653-663. ISSN 2049-3444.

Pamić, J. (1964): Magmatske i tektonske strukture u ultramafitima Bosanske serpentinske zone. *Poseb. Izdanje Geol. glas.*, knj.2, 1 – 108, Sarajevo.

Pamić, J., Sunarić-Pamić, O., Olujić, J., Antić, R. (1977): Petrografija i petrologija krivajsko-konjuškog ofiolitskog kompleksa I njegove osnivne geološke karakteristike. *Acta. Geol*., 9, 39-135.

Pamić, J. (1978): *Krivajsko – konjuški kompleks*. Geologija BiH, IV, "Geonžinjering" - Sarajevo, 99 – 135.

Pamić, J., Desmons, J. (1989): A complete ophiolite sequense in Rzav, area of Zlatibor and Varda ultramafic massifs, *The Dinaride ophiolite zone*, 13 – 32.

Pearce, J. A., Cann, J. R. (1973): Tectonic setting of basic volcanic rocks determined using trace element analyses.-*Earth. Planet. Sci. Lett*., 19, 290-300.

Šegvić, B. (2010): PhD: Petrologic and geochemical characteristics of the Krivaja-Konjuh ophiolite complex (NE Bosnia and Herzegovina) - petrogenesis and regional geodynamic implications. University of Heidelberg, Germany.

Trubelja, F., Marchig, V., Burgath, K. P., Vujović, Ž. (1995): Origin of the Jurassic Tethyan Ophiolites in Bosnia: A Geochemical Approach to Tectonic Setting, *Geol. croat*, Zagreb, 49 – 66.

Summary/Sažetak

Na odabranim uzorcima ultramafitskih stijena peridotita na južnom obodu krivajsko – konjuškog masiva provedena su detaljna optička istraživanja polarizacionim mikroskopom, hemijske analize makroelemenata, mikroelemenata i rijetkih zemalja rentgenskom fluorescentnom spektroskopijom, te hemijske analize minerala elektronskom mikrosondom. Peridotiti-lerzoliti su detaljno ispitani optičkim, hemijskim analizama i elektronskom mikrosondom. Rezultati hemijskih istraživanja ovih peridotita su pokazali dosta ujednačen modalni sastav ovih stijena, koji se odlikuje visokim sadržajem MgO, niskim sadržajem CaO i visokim sadržajem MgO:FeO (oko 5 i više). Bazirano na CIPW normativnom sistemu ujednačenog su sastava sa vrlo malim variranjem u sadržaju diopsida sa nešto većim variranjem u sadržaju sadržaju olivina. Sadržaj CaO i NiO u olivinu ukazuju na olivine iz krustalnih peridotita. Rompski pirokseni po sastavu odgovaraju enstatitu a monoklinski pirokseni su po sastavu diopsidi. Spineli u peridotitima su Al spineli i Al hromni spineli. Visoke vrijednosti određene za gubitke žarenjem peridotita potvrđuju virtualan dojam o snažno izmjenjenom izvornom hemizmu ultramafitskih stijena.

Glasnik hemičara i tehnologa Bosne i Hercegovine

Bulletin of the Chemists and Technologists of Bosnia and Herzegovina

2017

48

35-40

Print ISSN: 0367-4444
Online ISSN: 2232-7266

UDC: _____

Original Scientific Paper

Application of Aloe Vera as Green Corrosion Inhibitor for Aluminum Alloy Types AA8011 and AA8006 in 3.5% NaCl

Bikić F.[a], Kasapović D.[a], Delijić K.[b], Radonjić D.[b]

[a]*University of Zenica, Faculty of Metallurgy and Material Sciencies, Travnička cesta 1, Zenica, B&H*

[b]*University of Montenegro, Faculty of Metallurgy and Technology, Cetinjski put, 81000 Podgorica, Montenegro*

Article info
Received: 10/04/2017
Accepted: 19/06/2017

Keywords:
Aluminum Alloy Types AA8011 and AA8006
Inhibitor Aloe Vera
3.5% NaCl linear polarization
Tafel extrapolation

***Corresponding author:**
E-mail: farzet_bikic@yahoo.com

Abstract: This paper presents testing data on application possibilities of Aloe Vera as green corrosion inhibitor for aluminum alloy types AA8011 and AA8006 in 3.5% NaCl. Electrochemical DC linear polarization method has been used in the first phase of testing process, with the goal of determining the optimal concentration of Aloe Vera as inhibitor of mentioned alloys in 3.5% NaCl, by polarization resistance value. During first testing process, only one aluminum alloy type AA8011 was used. By adding the inhibitor in 3.5% NaCl, the polarization resistance increases, and the highest result was recorded in Aloe Vera concentration of 5 cm^3dm^{-3}. During second phase of testing, the inhibition effect of optimal Aloe Vera concentration was tested for aluminum alloy type AA8011 and AA8006 in 3.5% NaCl by curves of Taffel extrapolation method. The results of conducted tests show that Aloe Vera in concentration of 5 cm^3dm^{-3} can be used as green inhibitor for aluminum alloys type AA8011 and AA8006 of the Al-Fe-Si-Mn system, in 3.5% NaCl at room temperature (20 ± 2 ºC). All tested samples of aluminum alloy in 3.5% NaCl solution with the presence of inhibitor show significant shifting of Open Circuit Potential (E_{OCP}) towards positive values in respect with Open Circuit Potential (E_{OCP}) of treated aluminum alloy samples in 3.5% NaCl solution without inhibitor presence. Likewise, most of the samples treated in 3.5% NaCl solution with the presence of inhibitor lead to decrease of corrosion current density in relation to samples tested in 3.5% NaCl solution without inhibitor presence.

INTRODUCTION

The growing concern about the environment preservation has led to the setting of stricter provisions regarding the use of chemicals that can have a harmful impact on the environment, which led to a reduction of a number of effective corrosion inhibitors. Uses of non-toxic and natural products as corrosion inhibitors have become important because of the advantages of their environmentally friendly and biodegradable in nature, readily availability, renewable sources, and ecological aspects and can be synthesized by simple procedure with low cost (Gaber et al. 2008, Afidah et al. 2008). Environmentally friendly inhibitors are biodegradable substances which do not contain heavy metals or other toxic components (Amitha et al. 2012). Lately, research of plant extracts is an area of high interest when it comes to corrosion inhibitors. Aloe Vera is an important medicinal plant which belongs to the family of Liliacea (Rajendran et al. 2007). The leaf of Aloe Vera contains over 240 nutritional and medicinal ingredients. Chief among these are polysaccharides, glycoproteins, vitamins, mineral and enzymes (Ekpendu et al. 2004). Aloe Vera as commonly called is organic in nature and can be used in the production of green corrosion inhibitors. This paper tested application possibilities of Aloe Vera as green corrosion inhibitor for aluminum

alloys type AA8011 and AA8006 of the Al-Fe-Si-Mn system, in 3.5% NaCl. Aluminum alloys have proved to high quality metal material for many purposes, and by use, they are located immediately after the iron alloy, with continued growth in production and application (Delijić 2016, Birbilis 2011, Davis 1999). AA8000 series represents a special group of Al-alloys whose typical representatives are the AA8006 and AA8011. These alloys are suitable for the process of a continuous casting strips - cold rolling, could be deformed by rolling to form foil dimensions and successfully used in the packaging industry, microelectronics and heat exchangers (Zhong-wei et al. 2012). For their use in the packaging industry, eventual corrosion appearance at these alloys can be entirely controlled by use of green inhibitor that is non toxic to the human body.

EXPERIMENTAL

A commercial product of Aloe Vera with 66.3% of fresh Aloe Vera leaf juice was used as inhibitor in conducted testing. The testing of application possibilities of Aloe Vera as green corrosion inhibitor was conducted on aluminum alloys type AA8011 and AA8006 of the Al-Fe-Si-Mn system, intended for deformation shaping. Continuously casted strips of examined alloys, thickness 7 mm, are produced in industrial conditions on device "3C" at a speed of 1 m/min, and a casting temperature of 690° C. One part of continuously casted sample strips was annealed homogenously in the laboratory at a temperature of 580 ° C with the effective annealing time of 6 hours in an electric laboratory furnace with internal air circulation. Homogenized and non-homogenized samples of continuously casted alloys are deformed by cold rolling on a laboratory rolling stand, in same deformation conditions, for production of thin strips of 0.5 mm thickness, representing the material for production of thin strips and foils by subsequent cold rolling. Chemical composition of tested alloys are shown in Table 1.

Table 1. Chemical composition of test alloys, by weight % (the rest is Al)

Alloy tags	**Fe**	**Si**	**Mn**	**Mg**	**Cu**	**Zn**
AA8011	0.74	0.52	0.077	0.001	0.062	0.051
AA8011*	0.66	0.58	0.37	0.003	0.002	0.034
AA8006	1.34	0.14	0.43	0.012	0.002	0.035

Table 2 shows the used aluminum alloy sample tags depending on the manner of processing.

Table 2. Used aluminum alloy sample tags

Alloy tags	Sample tags	
	Initial state: continuously casted strips Deformed state	Initial state: homogenized continuously casted strips Deformed state
AA8006	1DX	1CX
AA8011*	2DX	2CX
AA8011	4DX	4CX

Investigations were conducted in the corrosion cell according to ASTM G5, on instrument potentiostat/galvanostat PAR 263A-2, with the software PowerCORR®. Basic solution used for testing was 3.5% NaCl, and the testing was conducted at a room temperature (20 ± 2 °C). Electrochemical DC linear polarization method has been used in the first phase of testing process. Linear polarization method implies scanning of working electrode potential on the order of ± 20 mV material polarization in relation to its Open Circuit Potential (E_{OCP}), at the speed of 0.2 mVs^{-1}. Final result of the above method is polarization resistance (Rp). By polarization resistance, our goal was to determine the optimal concentration of Aloe Vera as inhibitor of mentioned aluminum alloys in 3.5% NaCl. Aluminum alloy type AA8011, tag 4DX, was used for testing purposes. During second phase of testing, the inhibition effect of optimal Aloe Vera concentration was tested for aluminum alloy type AA8011 and AA8006 in 3.5% NaCl by curves of Taffel extrapolation method. Taffel extrapolation method implies scanning of working electrode potential on the order of ± 250 mV in relation to its Open Circuit Potential (E_{OCP}), at the speed of 0.2 mVs^{-1}.

RESULTS AND DISCUSSION

Table 3 show polarization resistance (Rp) testing results depending on inhibitor Aloe Vera concentration in 3.5% NaCl.

Table 3. Results of polarization resistance of aluminum alloy tag 4DX depending on inhibitor Aloe Vera concentration in 3.5% NaCl

Concentration of the inhibitor (cm^3dm^{-3})	Rp (Ω)
0	2208.704
1	13 679.302
2.5	14 394.375
3.5	12 077.83
4.5	29 895.970
5	**75 371.998**
6	18 053.171
6.5	14 203.357

Table 3 results show that optimal concentration of used Aloe Vera inhibitor is 5 cm^3dm^{-3}. At that inhibitor concentration, the polarization resistance amounts to 75 371.998 Ω. Solution without inhibitor shows smaller polarization resistance and amounts to 2208.704 Ω. Table 4 and Figures 1-6 show Open Circuit Potential (E_{OCP}) value and corrosion current density ($i_{cor.}$) of aluminum alloy samples type AA8011 and AA8006 treated in 3.5% NaCl solution with and without inhibitor presence. The inhibitor was added in the determined optimum concentration of 5 cm^3dm^{-3}.

Table 4. Values of Open Circuit Potential (E_{OCP}) and corrosion current density ($i_{cor.}$) of aluminum alloy samples treated in 3.5% NaCl solution with inhibitor (5 cm^3dm^{-3} of Aloa Vera) and without inhibitor presence

Alloy tags	Sample tags	E_{ocp}(mV)	Corrosion current density, $i_{cor.}$ (μAcm^{-2})
AA8006	1DX	-899.525	$4.393 \cdot 10^1$
	$1DX_{(with\ inh.)}$	-720.418	7.82
AA8011*	1CX	-1010.039	$1.746 \cdot 10^1$
	$1CX_{(with\ inh.)}$	-742.966	3.912
	2DX	-945.102	3.239
	$2DX_{(with\ inh.)}$	-724.389	8.47
	2CX	-756.438	6.028
	$2CX_{(with\ inh.)}$	-755.792	$4.081 \cdot 10^1$
AA8011	4DX	-791.438	5.625
	$4DX_{(with\ inh.)}$	-738.508	2.616
	4CX	-1004.118	7.993
	4CX (with inh.)	-746.762	2.605

Table 4 results show that all tested aluminum alloy samples treated in 3.5% NaCl solution with the presence of inhibitor significantly shift Open Circuit Potential (E_{OCP}) towards positive values in respect with Open Circuit Potential (E_{OCP}) of treated aluminum alloy samples in 3.5% NaCl solution without inhibitor presence. The shifting of Open Circuit Potential (E_{OCP}) towards positive values demonstrates that Aloe Vera in concentration of 5 cm^3dm^{-3} can be used as green inhibitor for aluminum alloys type AA8011 and AA8006 of the Al-Fe-Si-Mn system, at room temperature.

Figures 1-6 show Taffel polarization curves of aluminum alloys type AA8011 and AA8006 treated in 3.5% NaCl solution with and without inhibitor presence. All Figures show that tested aluminum alloy samples treated in 5% NaCl solution with the presence of 5 cm^3dm^{-3} concentration of inhibitor significantly shift Open Circuit Potential (E_{OCP}) towards positive values in respect with Open Circuit Potential (E_{OCP}) of treated aluminum alloy samples in 3.5% NaCl solution without inhibitor presence.

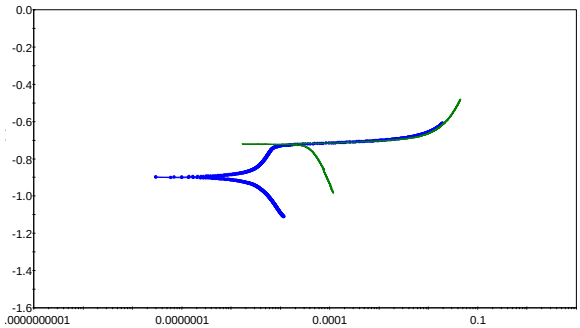

Figure 1. Taffel curves of Al-alloy sample tag 1DX
1 – sample treated in 3.5% NaCl solution with inhibitor presence (5 cm^3dm^{-3} of Aloa Vera)
2 – sample treated in 3.5% NaCl solution without inhibitor presence

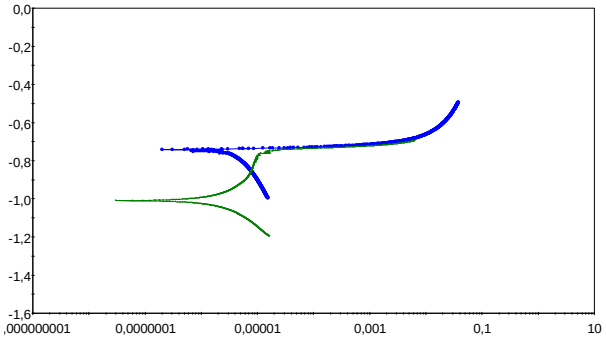

Figure 2. Taffel curves of Al-alloy sample tag 1CX
1 – sample treated in 3.5% NaCl solution with inhibitor presence (5 cm^3dm^{-3} of Aloa Vera)
2 – sample treated in 3.5% NaCl solution without inhibitor presence

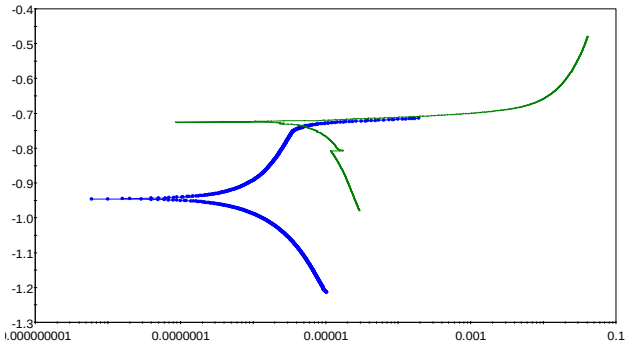

Figure 3. Taffel curves of Al-alloy sample tag 2DX
1 – sample treated in 3.5% NaCl solution with inhibitor presence (5 cm^3dm^{-3} of Aloa Vera)
2 – sample treated in 3.5% NaCl solution without inhibitor presence

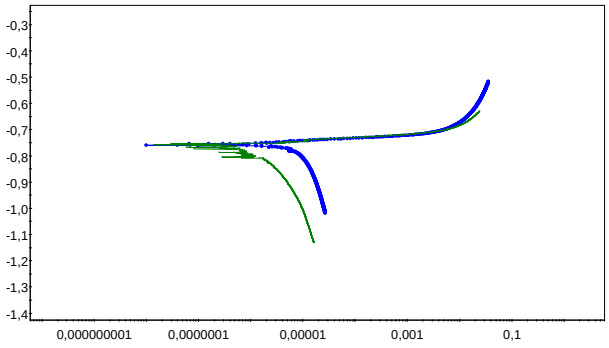

Figure 4. Taffel curves of Al-alloy sample tag 2CX
1 – sample treated in 3.5% NaCl solution with inhibitor presence (5 cm^3dm^{-3} of Aloa Vera)
2 – sample treated in 3.5% NaCl solution without inhibitor presence

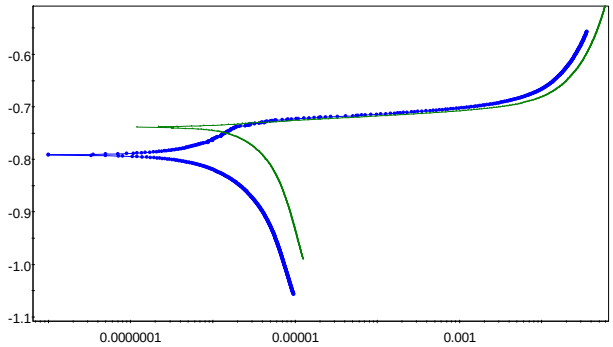

Figure 5. Taffel curves of Al-alloy sample tag 4DX
1 – sample treated in 3.5% NaCl solution with inhibitor presence (5 cm^3dm^{-3} of Aloa Vera)
2 – sample treated in 3.5% NaCl solution without inhibitor presence

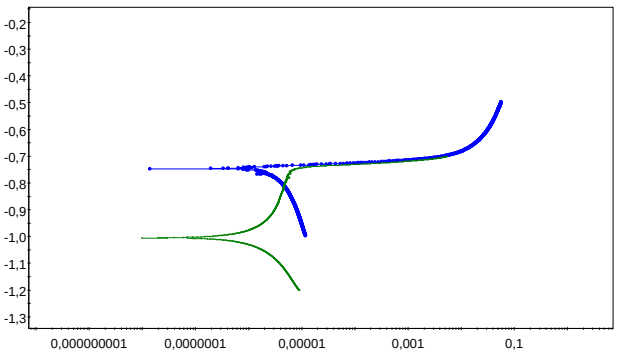

Figure 6. Taffel curves of Al-alloy sample tag 4CX
1 – sample treated in 3.5% NaCl solution with inhibitor presence (5 cm^3dm^{-3} of Aloa Vera)
2 – sample treated in 3.5% NaCl solution without inhibitor presence

Likewise, most of the samples treated in 3.5% NaCl solution with the presence of inhibitor lead to decrease of corrosion current density in relation to samples treated in 3.5% NaCl solution without inhibitor presence, with the exception of aluminum alloy sample type AA8011* (table 4).

CONCLUSIONS

Aloe Vera can be used as green corrosion inhibitor for aluminum alloy types AA8011 and AA8006 of the Al-Fe-Si-Mn system, in 3.5% NaCl, at room temperature (20 ± 2 ºC), confirmed by following test results:

- The polarization resistance (Rp) of aluminum alloy sample type AA8011 tag 4DX, table 3, is the smallest for sample treated in 3.5% NaCl solution. By increasing the inhibitor, the polarization resistance increases. The highest polarization resistance was obtained for the solution of 3.5% NaCl with the addition an inhibitor of Aloe Vera in a concentration of 5 cm^3dm^{-3}. The stated concentration is optimal for the stated inhibitor.
- All tested aluminum alloy samples type AA8011 and AA8006 treated in 3.5% NaCl solution with inhibitor presence (table 4) significantly shift Open Circuit Potential (E_{OCP}) towards positive values in respect with Open Circuit Potential (E_{OCP}) of treated aluminum alloy samples in 3.5% NaCl solution without inhibitor presence.
- Most of the samples treated in 3.5% NaCl solution with the presence of inhibitor lead to decrease of corrosion current density in relation to samples treated in 3.5% NaCl solution without inhibitor presence, with the exception of aluminum alloy sample type AA8011* (table 4).

Acknowledgement
This paper was realized through the financial support of bilateral project BiH-MNE in 2016 and 2017. Abbreviation project: MetKorAl

REFERENCES

Gaber-Abdel A.M., E. Khamis, Abo-ElDahab H., Adeel Sh. (2008). *Mater. Chem. Phys*. 109 297–305.

Afidah A.R., Rocca E., Steinmetz J., Kassim M.J. (2008). *Corros. Sci*. 50 1546–1550.

Amitha Rani B. E. and Bharathi Bai J. Basu (2012). Green Inhibitors for Corrosion Protection of Metals and Alloys: An Overview, *International Journal of Corrosion*, doi:10.1155/2012/380217.

Rajendran A., Narayana.V and Gnanavel.I. (2007). Separation and Characterization of the phenolic Anthraquinones from Aloe Vera. *Journal of Applied Sciences Research*, 3 (11):1407-1415.

Ekpendu T. O. (2004). Nigerian ethnomedicine and medicinal plant flora: anti-ulcerplants of the Benue area of Nigeria. *West African Journal of Pharmacology and drug Research*, 19, 1-14.

Delijić K., Markoli B., Naglič I., Radonjić D., Bikić F. (2016). Uticaj metalurškog stanja i legirajućih elemenata na korozione i mehaničke osobine nekih Al-Mg, Al-Mn, Al-Mg-Si i Al-Fe-Si legura, XVIII YuCorr, April 12-15, Tara Mountain, Serbia, *Proceedings*, ISBN 978-86-82343-24-0, 41-53.

Birbilis N., Muster T. (2011). Corrosion of Aluminum Alloys, *Corrosion Mechanisms in Theory and Practice, Third Edition, CRC Press*, 705-736.

Davis J. R. (1999). Corrosion of aluminum and aluminum alloys, *Materials Park, OH, ASM International*.

Zhong-wei Chen, Shi-shun Li, Jing Zhao (2012).Homogenization of twin-roll cast A8006 alloy, *Trans. Nonferrous Met. Soc. China*, 221280−1285.

Summary/Sažetak

U ovom radu su prikazani rezultati ispitivanja mogućnosti primjene Aloe Vera kao zelenog inhibitora legura aluminija tipa AA8011 i AA8006 u 3.5% NaCl. U prvoj fazi ispitivanja korištena je elektrohemijska DC metoda linearne polarizacije, gdje se preko vrijednosti polarizacijskog otpora željelo vidjeti koja je to optimalna koncentracija Aloe Vera kao inhibitora navedenih legura aluminija u 3.5% NaCl. Pri tome je korištena samo jedna legura aluminija tipa AA8011. S dodatkom inhibitora u 3.5% NaCl dolazilo je do povećanja polarizacijskog otpora, a najveći polarizacijski otpor je zabilježen kod dodatka Aloe Vera u koncentraciji 5 cm^3dm^{-3}. U drugoj fazi ispitivanja, metodom ekstrapolacije Tafelovih krivih ispitivan je efekat inhibicije utvrđene optimalne koncentracije inhibitora Aloe Vera na legure aluminija tipa AA8011 i AA8006 u 3.5% NaCl. Rezultati provedenih ispitivanja pokazuju kako se Aloe Vera u koncentraciji 5 cm^3dm^{-3} može koristiti kao zeleni inhibitor legura aluminija tipa AA8011 i AA8006 iz sistema Al-Fe-Si-Mn, u 3.5% NaCl na sobnoj temperaturi (20 ± 2 ºC). Kod svih ispitivanih uzoraka legura aluminija tretiranih u otopinama 3.5% NaCl s prisustvom inhibitora došlo je do značajnog pomijeranja potencijala otvorenog kruga (E_{OCP}) u pozitivnije vrijednosti u odnosu na E_{OCP} uzoraka tretiranih u otopinama 3.5% NaCl bez prisustva inhibitora. Također, kod većine uzoraka tretiranih u otopinama 3.5% NaCl s prisustvom inhibitora došlo je do smanjenja gustine struje korozije u odnosu na uzorke tretirane u otopinama 3.5% NaCl bez prisustva inhibitora.

Glasnik hemičara i tehnologa Bosne i Hercegovine

Bulletin of the Chemists and Technologists of Bosnia and Herzegovina

2017

48

41-44

Print ISSN: 0367-4444
Online ISSN: 2232-7266

UDC: _____

Original Scientific Paper

Zn-Ni alloy coating made of chloride electrolyte

Dautbašić A.*, Ćatić S., Ćatić O.

Faculty of Technology, University of Tuzla

Article info
Received: 13/06/2017
Accepted: 29/06/2016

Keywords:
chloride electrolytes, deposition, coatings, Zn-Ni alloy, salt spray chamber

***Corresponding author:**
E-mail:dautbasic.a@bih.net.ba
Phone: 00387-35-206-329

Abstract: Electrodeposition coating based on Zn-Ni alloys was made of chloride electrolyte which contains 142.56 g/dm^3 $NiCl_2x6H_2O$; 109.03 g/dm^3 $ZnCl_2$; 30.9 g/dm^3 H_3BO_3; 223.65 g/dm^3 KCl; 40.99 g/dm^3 CH_3COONa. As the result coatings of different sizes and different amount of Ni in each coating were prepared. The samples were tested in salt spray chambers according to BS EN ISO 10289:2001standard. The best results showed coatings which were over 10 μm thick and which contained up to 15% of Nickle. There were no signs of corrosion even after 2160 hours of being in salt spray chambers.

INTRODUCTION

Resistance of zinc coatings towards the corrosion processes is well known so these coatings were the first choice of protection for a long time during the production of the steel constructions. As technology developed and demands for thinner coatings but with much higher corrosion stability increased, zinc coatings were not satisfactory enough anymore. Research showed that alloy coatings based on zinc and other elements of iron triads can satisfy these conditions very well. There are many factors influencing features of deposited coatings based on double and in recent time even triple alloys based on zinc. Those factors are mostly concentration of metal ions, chemical composition of electrolytes that caused deposition and current density. [Esih 2010; Gamburg 2011; Vujičić 2002]

In this paper, coatings based on Zn-Ni alloys made of chloride electrolytes were tested. Depending on conditions (current density and deposition time), coatings of different sizes and with different amount of Ni in each coating were made.[Kanani 2005; Ramesh Bhat 2011; Eliaz 2014; Gou 2008] So far research showed that it is possible to get coatings based on Zn-Ni alloys which have corrosion characteristics, out of chloride electrolytes. [. Jović 2009; Bajat 2009; Roventi 2000]

Depending on the amount of Ni in alloy and the thickness, coatings were exposed to test in salt spray chambers and characterized according to standard BS EN ISO 10289:2001. [Stupnišek-Lisac 2007; BS EN ISO 10289:2001; EN ISO 9227].

EXPERIMENTAL

For electrochemical deposition of Zn-Ni based coatings chloride electrolyte was used. In table 1.The composition of chloride electrolyte is showed in Table 1.

Table 1. Chemical composition of electrolytes for deposition of coating Zn-Ni alloys

	$NiCl_2x6H_2O$	$ZnCl_2$	H_3BO_3	KCl	CH_3COONa
mol/dm^3	0.6	0.8	0.5	3	0.5

Electrolyte used is prepared using chemicals of p.a. purity. Tiles from plane construction steel were used as working electrodes for deposition of Zn-Ni based coatings. Electrode of high cleanliness Nickle (99.9%) was used as an auxiliary electrode during deposition of alloys. Relation between the surface of working and auxiliary electrode was 1: 2. Before the deposition, working electrodes were processed with abrasive paper, granulation 800 and 1200, degreased in NaOH solution then in ethanol and etched in 10% HCl solution. Between every phase of preparation, electrodes were washed with distilled water. Electrochemical cell for

deposition was laboratory glass of 500 cm^3 of volume. Current density which is used for deposition was 1; 2 and 3 A/dm^2, the temperature of solution was 35^0C and pH was 4.5. Time of deposition was 10, 15, 20 and 35 minutes to get the coatings of different sizes and with different amounts of Ni. Chemical composition thickness of Zn-Ni alloys were done in SurTec Eurosjaj d.o.o. Konjic, na Fischerscope® XRAY XDL-B laboratory. The results are showed in table 2.

Table 2. The thickness of Zn-Ni alloy and the amount of Ni in coating

Sample label	Sample label in salt chamber	Working conditions	Thickness of coating, μm	Amount of Ni in coating, %
1R	49	$i=2A/dm^2$ $\tau=20$ min	5.805	10.79
4R	50	$i=1A/dm^2$ $\tau=20$ min	9.326	11.93
2P	47	$i=2A/dm^2$ $\tau=20$ min	8.126	12.13
1K	43	$i=1A/dm^2$ $\tau=20$ min	5.273	13.60
2K	45	$i=2A/dm^2$ $\tau=20$ min	10.180	14.34
3K	46	$i=3A/dm^2$ $\tau=20$ min	12.62	17.89
1KT	40	$i=2A/dm^2$ $\tau=10$ min	5.036	11.27
2KT	41	$i=2A/dm^2$ $\tau=15$ min	7.111	11.49
6KT	42	$i=2A/dm^2$ $\tau=35$ min	14.97	14.86

Testing in salt spray chamber was done in SurTec-Eurosjaj d.o.o. Konjic. Chamber is JW-150-NS Salt Spray Chamber type. Testing lasted for 2160 hours. Conditions of testing in chambers were following : test space temperature was 35 °C; moisturizer of compressed air temperature was 45-50°C; compressed air pressure was 7-1,4 bars; solution was 5% NaCl; condensate pH in 25^0C was 6,8 while electrical conductivity of distilled water in 25°C was < 20 μS/cm.
After testing, the samples were taken out of salt chamber and visually evaluated according to BS EN ISO 10289:2001 standard. Samples 42 and 45 obtained after the testing in salt spray chambers are showed in P1 and the results are showed in Table 4.

Figure 1. Samples without appearance of corrosion after 2160 hours in salt spray chamber

RESULTS AND DISCUSSION

As it is seen in picture 1. and table 4., samples 40, 41, 48, 49 and 50. (40/1KT, 41/2KT, 48/3P 49/1R and 50/4R) did not satisfy the salt spray chamber test. The red corrosion appeared much earlier than the expected for this type of coating after 720 hours of testing. Although the Ni part in Zn-Ni alloy coating is satisfying and that is 8-15%, the coating thickness is small which is the cause of apperance of red corrosion much earlier than expected.
The rest of the samples satisfied the salt spray chamber test according to norms of DIN EN ISO 9227 NSS standard. For example, the sample (45/2K) which has 14,34% Ni and the coating thickness was 10,180 μm, did not show the appearance of red corrosion even after 2160 hours, so, according to BS EN ISO 10289:2001 standard, it has the assessment of protection and look (Rp/RA) 10/8sC.

According to standard, the rest of the samples that satisfied the salt spray chamber test are also described.
Sample 42 shows the appearance of white corrosion after 720 hours of testing but on on the surface area smaller than 0,25%. There were no visible defects. It is mostly caused by corrosion products made of anodic coating. The appearance of red corrosion is not noted even after 2160 hours of being in salt spray chamber. According to the assessment of protection and look Rp/ RA was 10/8sC. Sample 46 shows the appearance of white corrosion after 720 hours and on the surface area smaller than 1%. There are no visible defects. The amount of corrosion products was moderate. It is mostly about corrosion product made of anodic coating. The appearance of red corrosion is not noted even after 2160 hours of being in salt spray chamber. According to the assessment of protection and look Rp/RA was10/6mE.
Sample 43 shows the appearance of white corrosion after 480 hours and in that time it does not show any visible defects on coating. After 846 hours it shows visible defect and the appearance od red corrosion in the area of small drilled hole on the top of the electode. The amount of corrosion products is moderate. Corrosion products reach the base that started to peel. According to the assessment of protection and look Rp/RA was3/2mF.
Sample 47 shows the appearance of white corrosion after 720 hours and in that time it did not show any visible defects on coating. After 1176 hours it showed visible defect and the appearance of red corrosion in the area of small drilled hole on the top of the electrode and edges of the tested sample. The amount of corrosion products was moderate. Corrosion products reached the base but they were only on the top of the metal. There was no

peeling. According to the assessment and look Rp/RA equaled 6/5mE

Table 4. The test results from salt spray chamber

Sample	Thickness of coating, μm	Amount of Ni in coating, %	Start of the test	End of the test	White corrosion (hours)	Red corrosion (hours)	Assessment of protection and look
40/1KT	5,036	11,27	28.09.2015	05.10.2015	168	192	-
41/2KT	7,111	11,49	28.09.2015	06.10.2015	96	192	-
42/6KT	14,97	14,86	28.09.2015	28.12.2015	720	2160 (no corrosion)	10/8sC
43/1K	9,273	13,60	28.09.2015	03.11.2015	480	864	3/2mF
45/2K	10,180	14,34	28.09.2015	28.12.2015	720	2160 (no corrosion)	10/8sC
46/3K	12,62	17,89	28.09.2015	28.12.2015	720	2160 (no corrosion)	10/6mE
47/2P	8,126	12,13	28.09.2015	16.11.2015	720	1176	6/5mE
48/3P	5,951	13,71	28.09.2015	08.10.2015	120	240	-
49/1R	2,805	10,79	28.09.2015	02.10.2015	48	96	-
50/4R	9,326	11,93	28.09.2015	06.10.2015	96	192	-

CONCLUSION

Samples with Ni part of 8-15%, which had the red corrosion appear earlier than the expected for this type of coating, after 720 hours of testing did not passed the testing despite the the thickness of the coating As resault red corrosion appearaed much earlier than expected. The rest of the samples that had the thickness of Zn-Ni alloy coating higher than 10 μm and the needed part of Ni 15%, fully satisfied the salt spray chamber test. That means they did not show any signs of red corrosion appearance in the testing time of 2160 hours.

REFERENCES

Bajat J.B., Prevlake legura cinka, savez inženjera i tehničara za zaštitu materijala Srbije, Beograd 2009.

BS EN ISO 10289:2001 Methods for corrosion testing of metallic and other inorganic coatings on metallic substrates- Rating of test specimens and manufactured articles subjected to corrosion test.

Eliaz N., Venkatakrshna K., Chitharanjan A., Electroplating and characterization of Zn-Ni, Zn-Co and Zn-Ni-Co alloys, Departmant of Chemistry, National Institute of Technology Karnataka,India, 2014.

EN ISO 9227, Corrosion tests in artifical atmospheres- Salt sprey test (ISO 9227:2006).

Esih I., Osnove površinske zaštite, FSB Zagreb, 2010.

Gamburg Y.D., Zangari G., Theory and Practice of Metal Electrodeposition, Springer-New York, 2011.

Gou S.P., Sun I.W., Electrodeposition behavior of nickel and nickel-zinc alloys from the zinc chloride-1-ethyl-methylimidazolium chloride low temperature molten salt, Electrochim. Acta 53, 2008.

Institut za multidisciplinarna istraživanja Univerziteta u Beogradu (2009).

Jović V. D., Elezović N., Elektrohemijsko taloženje i karakterizacija legura,

Kanani N., Electroplating, Elsevier Science Ltd., 2005.

Ramesh Bhat S., Udaya Bhat K., Chitharanjan Hegde A., Corrosion Behaviour of Electrodeposited Zn-Ni, Zn-Co and Zn-Ni-Co Alloys, Anal.Bioanal. Electrochem., Vol.3, No. 3., 2011.

Roventi G., Fratesi R., Della Guardia R.A., Barucca G., Normal and anomalous codeposition of Zn-Ni allys from chloride bath, J. Appl. Electrchem., 2000.
Stupnišek-Lisac E.: "Korozija i zaštita konstrukcijskih materijala", Fakultet kemijskog inženjerstva i tehnologije, Zagreb, 2007.
Vujičić Vladimir – Korozija i tehnologija zaštite materijala, Beograd 2002.

Summary/Sažetak

Izvedena je elektrodepozicija prevlaka na bazi legura Zn-Ni iz hloridnog elektrolita sastava 142,56 g/dm^3 $NiCl_2x6H_2O$; 109,03 g/dm^3 $ZnCl_2$; 30,9 g/dm^3 H_3BO_3; 223,65 g/dm^3 KCl; 40,99 g/dm^3 CH_3COONa. Dobivene su prevlake različite debljine i sadržaja Ni u prevlaci. Uzorci su ispitivani u slanoj komori prema standardu BS EN ISO 10289:2001. Najbolje rezultate su pokazale prevlake debljine preko 10 μm i sadržajem nikla do 15%. Nisu pokazivali pojavu korozije ni nakon 2160 sati provedenih u slanoj komori.

Glasnik hemičara i tehnologa Bosne i Hercegovine

Bulletin of the Chemists and Technologists of Bosnia and Herzegovina

2017

48

45-50

Print ISSN: 0367-4444
Online ISSN: 2232-7266

UDC: _____

Original Scientific Paper

Electrodeposition of polyaniline films on stainless steel and their voltammetric behavior in corrosive environments

Gutić, S.*, Cacan, M., Korać, F.

University of Sarajevo, Faculty of Science, Department of Chemistry, Zmaja od Bosne 33-35, 71000 Sarajevo, B&H

Article info
Received: 29/06/2017
Accepted: 29/06/2017

Keywords:
Electropolymerization, conducting polymers, corrosion protection

***Corresponding author:**
E-mail: sgutic@pmf.unsa.ba
Phone: +-387-61-337636

Abstract: Polyaniline films were electrodeposited on the stainless steel substrates from aniline solutions with different acids. Kinetic of the film growth is discussed in terms of corrosion behavior of steel substrates in pure acids. Wide passive region in sulfuric and phosphoric acid enables initial oxidation of aniline and consequent deposition of polymer, without concurrent dissolution of alloy. On the other hand, in hydrochloric acid substrates actively dissolute at potentials necessary for aniline oxidation. However, formation of polymeric deposits is possible even in this case, probably due to the inhibition effect of aniline or oligoanilines formed during initial periods of anodic polarization. All deposited films exhibit electroactive behavior in low pH medium, while totally lose their ability for redox transitions in higher pH.

INTRODUCTION

Intrinsically conducting polymers (ICPs), sometimes referred as the synthetic metals, are organic semiconductors with unique physical and chemical properties, the most prominent being easy route of transition between (semi)conducting and insulating state, followed by significant change in structure, morphology and other physical properties. Typical materials from this class can be obtained by simple chemical or electrochemical polymerization of cheap monomers such as aniline, pyrrole, tiophene and ethylenedioxytiophene to give stable polymeric structures of polyaniline, polypyrrole, polytiophene and poly(ethylenedioxytiophene), respectively, in form of bulk product or in form of films deposited on different substrates, depending on the method of preparation. Also, different nanostructures can be prepared by relatively simple procedures.

Number of studies about protective performance of conducting polymer coatings discuss polymer protective performance in terms of its ability to help the formation and stabilization of passive layer on protected metallic surface (Wallace *et al.*, 2009; Inzelt, 2008; Tallman and Bierwagen, 2007; Lu *et al.*, 1998). However, protection mechanism can also include other processes, such as complexation of metallic ions with polymer or release (in some cases on-demand) of corrosion inhibitors, while simple mechanical protection should also be considered.

Electrochemical preparation of conducting polymers enable control of polarization rate and polymer film thickness, while obtained films good electrical contact with the protected substrate (Tallman and Bierwagen, 2007). However, electropolymerization on active substrates is connected with some difficulties, due to the fact that common conducting polymers are obtained by polymerization at positive potentials, at which substrate dissolution occurs. In some cases oxide layers formed on these potentials can improve polymer adhesion. On the other hand, formation of nonconducting passive layer leads to impeded electron transfer and totally inhibits polymer growth.

Electrodeposition of polyaniline on active substrates is performed in acidic electrolytes with the addition of some inhibitors or passivating agents such as oxalates (Huelser and Beck, 1990; Sazou, 2001; Yalçinkaya *et al.*, 2010; Tan and Blackwood, 2003) and salycylates (Petitjean *et al.*, 1999). Lacroix et al. (Lacroix *et al.*, 2000) and Nguyen et al. (Nguyen *et al.*, 1999) obtained adherent electrodeposited films on mild steel from neutral $LiClO_4$ electrolyte. Aniline polymerization from alkaline electrolyte give polymeric deposit that can't be transformed into the emeraldine form of polyaniline (Troch-Nagels *et al.*, 1992). Another interesting approach

for the preparation of polyaniline coating on active metals is two-step deposition in which polyaniline is coated onto the thin polypyrrole film previously deposited on the active substrate surface (Lacroix *et al*, 2000). According to different authors, electrodeposition of polyaniline on active substrates from the acidic electrolytes can be performed from sulfate (Troch-Nagels *et al.*, 1992; De Berry, 1985) and phosphate (Moraes and Motheo, 2006; Moraes *et al.*, 2003) solutions.

In this paper we present our results for the electropolymerization of aniline on the stainless steel substrates from different acidic media and voltammetric behavior of the deposits in corrosive environment with different pH.

EXPERIMENTAL

All electrochemical measurements, including the cyclovoltammetric polymerization of aniline, were performed in standard three electrode cell connected to Princeton Applied Research Potentiostat/Galvanostat 263A controlled by PowerCV software, with Ag/AgCl($KCl_{saturated}$) as reference, platinum foil as counter and sample as the working electrode. All potentials are given with respect to Ag/AgCl reference (0.197 mV vs. SHE). Steel samples (68.287wt% Fe; 16.96wt% Cr; 11,03wt% Ni; <4wt% Mo, Mn, Si, C, S, P) were cut in form of flag, with the geometric surface area of 2 cm^2 in contact with the electrolyte, polished with emery paper and aluminium oxide and cleaned with acetone before any measurement or deposition.

Electropolymerization was performed from 0.1 mol dm^{-3} aniline solutions that contained different acids: 1 mol dm^{-3} H_2SO_4, 3 mol dm^{-3} H_3PO_4 and 1 mol dm^{-3} HCl. For the purpose of making reference materials, anilline was electropolymerized from all three electrolytes onto the platinum substrates as well. Also, electrochemical behaviour of steel was evaluated in all three acids without aniline. After the deposition, all obtained samples were left in 1 mol dm^{-3} ammonia solution, in order to achieve total deprotonation and transition into the insulating emeraldine base form. Voltammetric behavior of the obtained deposits was evaluated in 0.5 mol dm^{-3} solutions NaCl with different pH values varying from 0.19 to 6.80.

RESULTS AND DISCUSSION

Figure 1 shows linear polarization response of steel samples in 1 mol dm^{-3} sulfuric and hydrocholric acid and 3 mol dm^{-3}phosphoric acid. Open circuit potential is ca. -0.50 V for HCl, -0.44 for H_3PO_4 and -0.40 V for H_2SO_4. In sulfate and phosphate medium passivity is pronounced up to 1.0 V, with the onset of secondary passivation at 1.25 V, while active dissolution begins at 1.7 V. In the hydrochloric acid, however, passivity window is quite narrow and active dissolution starts at 0.5 V. This results imply that hydrochloric acid is not an adequate medium for the electropolimerization, considering that oxidation of aniline to its radical cation (first step of aniline electropolimerization) occurs at potentials higher than 1.0 V, which is potential at which corrosion of substrate in HCl(aq) occurs at significant rate.

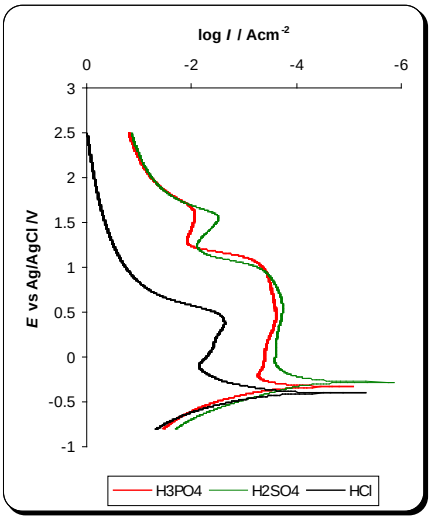

Figure 1. Polarization curves for steel substrates in different aqueous acids, recorded at 1 mV s^{-1}.

Nevertheless, electropolymerization by cyclic voltammetry was performed from all three acids on steel as well as on the platinum, in order to get some insight into the kinetics of the film formation. Recorded cyclic voltammograms are given in Figure 2. Regardless of the electrolyte acid, electropolymerization on platinum is reflected by typical, well defined voltammograms where the main electropolymerization features, such as initial oxidation current and currents from polyaniline redox processes, are clearly visible. However, comparing peak currents for the same cycle number reveals some differences in the film deposition rate, which is in accordance with observations of other authors (Duić and Mandić, 1992; Wei *et al.*, 1995], where deposition rate also decrease in order H_2SO_4 > H_3PO_4 > HCl. Slower deposition rate leads to the formation of thin films (for the same number of cycles) and significantly affects film morphology (Tallman and Bierwagen, 2007). Growth of electroactive polymer film on steel substrates is clearly visible for the sulfuric and phosphoric acid electrolytes (Figure 2), where characteristic redox transitions of polyaniline can still be observed on the cyclic voltammograms, together with the currents emerging from the formation of passive layers. However, pronounced potential shift of the polyaniline current peaks towards the more negative and positive values for the reduction and oxidation sweep respetively indicate sluggish electron transport, probably due to the poor electronic conductivity of the passive layer.

Polyaniline film formation from the hydrochloric acid electrolyte differs significantly from the described cases with sulfuric and phosphoric acid, as we expected based on the polarization behavior (Figure 1). During the first seven cycles (upper voltammogram for PANI-HCl on steel, Figure 2) oxidation current at 0.65 V decrease and shift to 0.6 V, while no visible deposit is formed. This current arises from the active dissolution of steel, which significantly inhibits deposition of polymer. However, at the eighth cycle slight increase of the oxidation current at 0.15 V can be observed. As cycling continues, this current becomes more prominent while polymer deposit

becomes visible. One of the plausible explanations for the observed decrease in dissolution currents and the onset of polymer film growth in HCl can be inhibition of dissolution by aniline and its oligomers, formed during the initial voltammetric cycles.

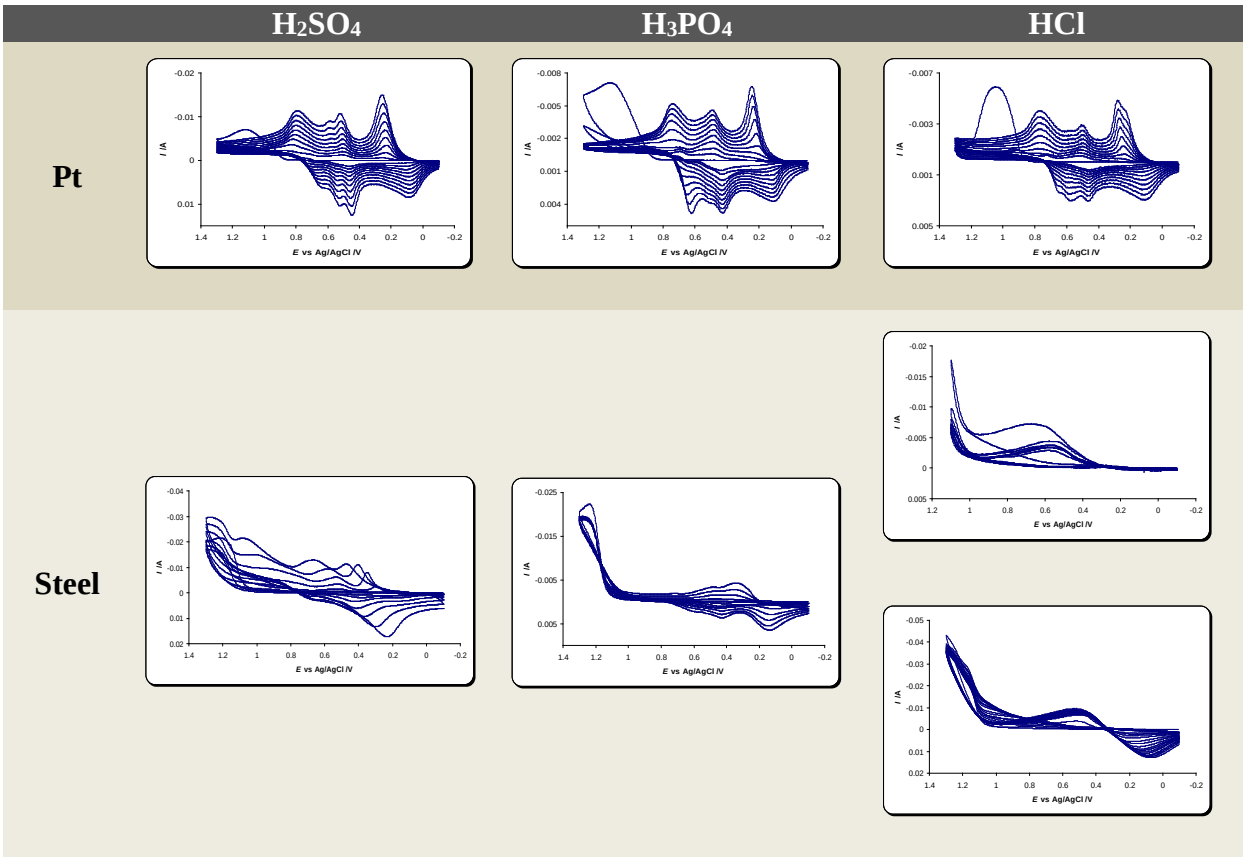

Figure 2. Cyclic voltammograms recorded during electropolymerization of aniline from different acids on platinum and stainles steel. Upper voltammogram for PANI-HCl on steel (right column) represents first seven cycles, while lower voltammogram refers to higher cycle numbers.

During electropolymerization polyaniline deposits in form of emeraldine salt (the only conductive form), which is protonated form of polyaniline with the same number of amine and imine nitrogen atoms in polymer chain, where the acidic anion acts as a counter-ion that keeps polymer electrically neutral. Deprotonation of this form (which is usually called *dedoping*) in order to get emeraldine base is performed after polymerization in 1 mol dm^{-3} aqueous ammonia. Sulfate, phosphate and chloride anions are removed from polyaniline prepared in this manner leaving space for the protonation (doping) with components of the corrosion solutions to give the conducting form, emeraldine salt. Deprotonation of polyaniline is followed by noticeable color change, as can be seen in Figure 3.

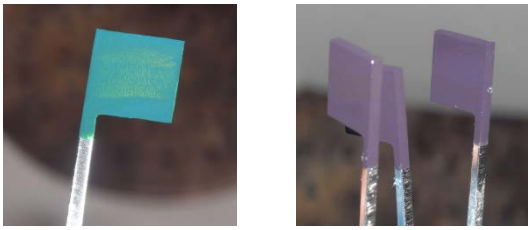

Figure 3. Polyaniline films before (left) and after (right) deprotonation

Figure 4 shows electrochemical behavior of polyaniline film in 0.5 mol dm^{-3} sodium chloride solutions with varying pH values, electrodeposited from sulfuric acid on steel. At low pH values all voltammograms exhibit voltammetric response typical for polyaniline: two well defined oxidation peaks on 0 and 0.5 V due to the redox transformation from leucoemeraldine to emeraldine and emeraldine to pernigraniline, respectively, and their corresponding reduction peaks. However, with the increasing of pH those currents gradually fade to finally give the voltammetric response without any observable faradaic current, indicating complete loss of electrochemical activity of polyaniline. This behavior is expected because protonation constants of amine and imine nitrogens dictate the total deprotonation of emeraldine salt at pH > 4, leaving insulating, redox inactive emeraldine base.

All samples were also linearly polarized up to 1.8 V in acidic chloride solution, in order to assess the impact of polyaniline coating on passivating processes on steel. As can be seen from the polarization curves in Figure 5, polyaniline coatings have almost the same current-potential response, regardless of the acid used for electropolymerization. Comparing polarization curve for steel in hydrochloric acid, shown in Figure 1, with curves curves in Figure 5 leads to the conclusion that polyaniline widens passive window of steel in acidic chloride solutions, which can be ascribed to the inherent redox

activity of polyaniline in acidic medium. This observation gives the possibility that polyaniline does not act as a physical barrier but actually protects underlying material in more complex manner, by keeping it in passive form.

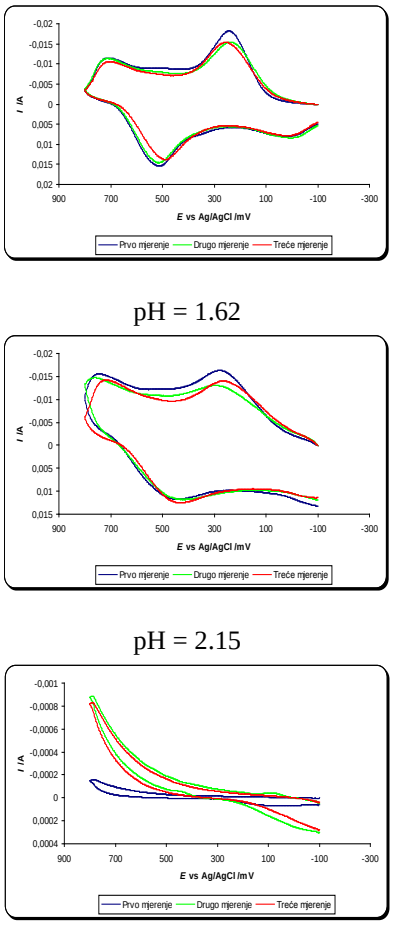

Figure 4. Cyclic voltammograms of polyaniline films in 0.5 mol dm^{-3} sodium chloride solutions with different pH, deposited from H_2SO_4 electrolyte on steel substrate.

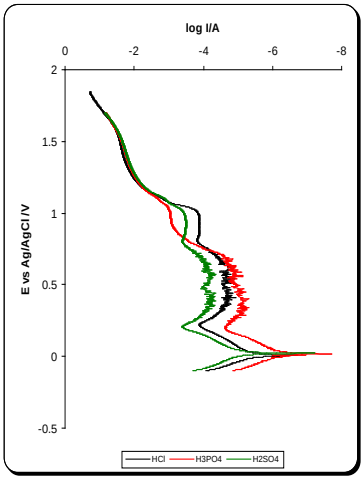

Figure 5. Polarization behavior of polyaniline coated steelsamples in acidic sodium chloride solution (pH = 0.19)

CONCLUSION

Electrochemical polymerization of aniline on stainless steel substrate was successfully performed from all three electrolytes, with the highest rate of deposition achieved in sulfuric acid. Polymerization from hydrochloric acid is hindered and followed by simultaneous dissolution of steel, which is slower after the formation of first visible polymer deposits.

Beside obvious differences in polymerization processes all coatings have similar electrochemical performance. Open circuit potentials for all PANI-modified samples in acidic sodium chloride solutions have values that fit into the passive window of steel substrates in the same solution, which indicates the possibility that polymer coating improves stability of the passive layer. However, the same cannot be concluded for the higher pH sodium chloride environments, where the redox behavior of polyaniline is hindered or totally prevented.

REFERENCES

DeBerry, D.W. (1985). Modification of the Electrochemical and Corrosion Behavior of Stainless Steels with an Electroactive Coating. *J Electrochem Soc*, *132*, 1022.

Duić,Lj., Mandić, Z. (1992). Counter-Ion and pH Effect on the Electrochemical Synthesis of Polyaniline. *J Electroanal Chem*, *335*, 207.

Huelser, P., Beck, F., (1990). Electrodeposition of Polypyrrole Layers on Aluminium from Aqueous Electrolytes. *J Appl Electrochem*, *20*, 596.

Inzelt, G. (2008). *Conducting Polymers – A new era in electrochemistry*, Springer-Verlag.

Lacroix, J.C., Camalet, J.-L., Aeiyach, S., Chane-Ching, K.I., Petitjean, J., Chauveau, E., Lacaze, P.C. (2000). Aniline Electropolymerizationm on Mild Steel and Zinc in a Two Step Process. *J Electroanal Chem*, *481*, 76.

Lu, W.K., Basak, S., Elsenbaumer, R. (1998). Corrosion Inhibition of Metals by Conducting Polymers In Skotheim, T.A., Elsenbaumer, R.L. *Handbook of Conducting Polymers* (2nd edition) (pp. 881–920) Marcel Dekker, Inc.

Moraes, S.R., Huerta-Vilca, D., Motheo, A.J. (2003). Corrosion Protection of Stainless Steel by Polyaniline Electrosynthesized from Phosphate Buffer Solutions. *Prog Org Coat*, *48*, 28.

Moraes, S.R., Motheo, A.J. (2006). PAni-CMC: Preparation, Charaterization and Application to Corrosion Protection. *Mol Cryst Liq Cryst*, *448*, 261.

Nguyen, T.D., Camalet, J.L., Lacroix, J.C., Aeiyach, S., Lacaze, P.C. (1999). Polyaniline Electrodeposition from Neutral Aqueous Media: Application to the Deposition on Oxidizable Metals. *Synth Met*, *102*, 1388.

Petitjean, J., Aeiyach, S., Lacroix, J.C., Lacaze, P.C. (1999). Ultra-fast Electropolymerization of Pyrrole in Aqueous Media on Oxidizable Metals in a One-Step Process. *J Electroanal Chem*, *478*, 92.

Sazou, D. (2001). Electrodeposition of Ring Substitued Polyanilines on Fe Surfaces from Aqueous Oxalic Acid Solutions and Corrosion Protection of Fe. *Synth Met, 118,* 133.

Tallman, D.E., Bierwagen, G.P. (2007). Corrosion Protection Using Conducting Polymers. InSkotheim, T.A., Reynolds, J.R. (Eds.) *Handbook of Conducting Polymers: Conjugated Polymers – Processing and Applications* (3rd edition)(pp 15-1 – 15-53) Taylor & Francis Group.

Tan, C.K., Blackwood, D.J. (2003). Corrosion Protection by Multilayered Conducting Polymer Coatings. *Corr Sci, 45,* 545.

Troch-Nagels, G., Winand, R., Weymeersch, A., Renard, L. (1992). Electron Conducting Organic Coating of Mild Steel by Electropolymerization. *J Appl Electrochem, 22,* 756.

Wallace, G.G., Spinks, G.M., Kane-Maguire, L.A.P., Teasdale, P.R. (2009*). Conductive Electroactive Polymers – Intelligent Polymer Systems*(3rd Edition) Taylor & Francis Group.

Wei, Y., Wang, J., Jia, X., Yeh, J.-M. Spellane, P. (1995). Polyaniline as Corrosion Protection Coatings on Cold Rolled Steel. *Polymer 36,* 4535.

Yalçinkaya, S., Tüken, T., Yazici, B., Erbil, M. (2010). Electrochemical Synthesis and Corrosion Behaviour of poly(pyrrole-co-o-anisidine-co-o-toluidine). *Curr Appl Phys, 10,* 783.

Summary/Sažetak

Polianilinski filmovi su elektrodeponovani na supstratima od nehrđajućeg čelika iz rastvora anilina sa različitim kiselinama. Kinetika rasta polimernog filma je diskutovana u svjetlu krozoionog ponašanja čeličnih supstrata u čistim kiselinama. Široko pasivno područje u sulfatnoj i fosfatnoj kiselini omogućava početnu oksidaciju anilina i posljedičnu depoziciju polimera, bez pratećeg rastvaranja legure. S druge strane, u hloridnoj kiselini dolazi do aktivnog rastvaranja supstrata na potencijalima potrebnim za oksidaciju anilina. Međutim, formiranje polimernih depozita je moguće čak i u ovom slučaju, vjerovatno usljed inhibicijskog efekta anilina ili oligoanilina nastalih tokom početnog perioda anodne polarizacije. Svi dobijeni filmovi pokazuju elektroaktivnost u sredinama sa niskim pH vrijednostima, dok istu potpuno gube pri većim pH vrijednostima.

Glasnik hemičara i tehnologa Bosne i Hercegovine

Bulletin of the Chemists and Technologists of Bosnia and Herzegovina

2017

48

Print ISSN: 0367-4444
Online ISSN: 2232-7266

UDC: _____

Review

51-58

Many roles of melatonin: diversity and complexity of reaction pathways

Galijasevic, S.

School of Science and Technology, Sarajevo Medical School, Department of Medical Chemistry and Biochemistry Sarajevo, Bosnia

Article info
Received: 29/05/2017
Accepted: 14/06/2017

Keywords:melatonin, peroxidase, free radicals, inhibition, inflammation, myeloperoxidase, antioxidant, inflammatory enzymes

***Corresponding author:**
Semira Galijasevic
semira.galijasevic@ssst.edu.ba

Abstract: Melatonin (N-acetyl-5-methoxy tryptamine) is well known as a free radical scavenger and antioxidant involved in different biological and physiological regulation such as modulation of circadian rhythms, seasonal reproduction, retinal physiology and sleep regulation. Synthetic melatonin is available commercially, and its supplements have been used clinically to treat a variety of medical conditions such as jet lag, shift work and sleep disorders. Recent studies demonstrated that melatonin serves as an inhibitor of myeloperoxidase (MPO) under physiological-like conditions. Melatonin-dependent inhibition of MPO occurred with a wide range of concentrations that span various physiological and supplemental ranges. Myeloperoxidase is enzyme involved in leukocyte-mediated host defenses but plays a pathogenic role during chronic inflammatory conditions. MPO levels implicate inflammation in the walls of coronary arteries, which in turn, may indicate a risk for heart disease or heart attack. Thus, supplementary concentrations of melatonin can influence physiological and pathophysiological role of MPO. In addition, MPO modulates nitric oxide production, so melatonin can indirectly affects nitric oxide concentration. Amounting evidence shows new emerging role of melatonin and its metabolites beyond the classic one. This review focuses on newly discovered mechanistic pathways of melatonin activity that has to be taken into consideration when discussing pharmacological uses of melatonin.

INTRODUCTION

The neurological hormone melatonin (*N*-acetyl-5-methoxy tryptamine) was first isolated from pineal gland and identified in 1958 (Lerner, Case and Takahashi, 1958). Hormone role in circadian rhythm was detected soon after that (Amstrong *et al.*1986). In 1991, Ianas *et al.* reported free radical scavenging activity of melatonin but also observed prooxidant activity. Tan *et al.* in 1993 confirmed free radical scavenging activity of melatonin. Since then, a numerous *in vitro* and *in vivo* studies demonstrated ability of melatonin to scavenge reactive oxygen and nitrogen species including hydroxyl radical, superoxide ion, peroxy radicals, singlet oxygen, nitric oxide, peroxynitrate and its metabolites (Reiter *et al.*, 2008;Tan *et al,1993;* Galano *et al.*,2011). Later, important discovery of melatonin ability to stimulate some important antioxidative enzymes such as superoxide dismutase, glutathione peroxidase, and glutathione reductase followed (Hardeland, 2005) adding another beneficial role of melatonin in regards to oxidative stress. In addition, some research suggested that melatonin can inhibit hydrogen peroxide (H_2O_2)-induced lipid peroxidation and lipoprotein modification. However, the possible *in vivo* reaction pathways for these properties have yet to be identified (Hardeland, 2005 Schaffazick *et al.*, 2005). Classical role of melatonin has been confirmed many times showing melatonin involvement in different biological and physiological functions such as modulation of circadian rhythms (Dawson and Armstrong, 1996), seasonal reproduction (Dardente, 2012), retinal

physiology (Wiechmann and Sherry, 2013) and sleep regulation (Claustrat, 2005). Number of reviews explained, in detail, these functions (Pandi-Perumal *et al.*, 2006) including free radical scavenging activity but antioxidant ability of melatonin drew the most attention. Mitigating harmful effect of oxidative stress by melatonin looked promising for the treatment of a number of diseases although increased flux of free radicals is secondary effect rather than cause of a many pathophysiologies. Synthetic melatonin is available commercially, and its supplements have been used clinically in a variety of medical conditions such as jet lag, shift work, and circadian rhythm sleep disorders, cancer, longevity and antioxidant therapy, sepsis, and neurodegenerative disorders (Kostoglou-Athanassiou, 2013; Srinivasan *et al*., 2013).

However, melatonin is the substance that has not been regulated by the U.S. Food and Drug Administration, and as a dietary supplement is widely available in forms of different preparations with unknown concentrations of active substance. No data about safety and active dose is available. Due to the relatively low physiological levels of melatonin in human tissue, melatonin has been recommended as a supplement for a wide variety of conditions in doses ranging from 0.3 to 1000 mgs/day given for 1-4 weeks. In clinical studies, a wide range of melatonin doses have been used, including "low-dose" (0.1 to 1.0 mgs) for jet lag and insomnia in the elderly, “moderate-doses” (5 and 10 mgs), often taken by mouth 30 to 60 minutes prior to sleep time for disturbances in children with neuro-psychiatric disorders and bipolar disorder, or “high dose” (50 to 1200 mgs) for treating cancer and migraine headaches (Altun and Ugur-Altun, 2007).

One of the issues related to the melatonin beneficial effect is what can be considered as biological and pharmacological concentration. When analyzing this, several issues have to be taken into account:

a. Melatonin is produced in pineal and non pineal sites. Non pineal concentrations can reach micromolar levels while pineal melatonin is generally in pico to nanomolar range.
   However, melatonin is also synthesized non pineal sites such bone marrow (Conti *et al.*, 2000), gastrointestinal tract (Bubenik, 2002), leukocytes (Hardeland *et al.*,2011), lymphocytes (Calvo *et al.*,2013), skin (Slominski *et al.*, 2005), airway epithelium (Kvetnoy, 1999). Melatonin concentration in these cells is much higher than those normally found in the blood and it does not seem to be regulated by the photoperiod. Mounting evidence shows that extrapineal melatonin as a key paracrine signal molecule with significant role in intercellular interactions.
b. Pineal melatonin easily crosses into circulation what is not a case with nonpineal melatonin where only small concentrations are released in circulatory system.
c. Melatonin can be metabolized enzymatically and nonenzymatically in the presence of free radicals. Thus, total oxidative stress has effect on final catabolism of melatonin.
d. Melatonin catabolic products AMFK and AMK are also strong free radical scavengers but of different reactivity towards different free radicals.
e. Melatonin has an immunomodulatory effect and upregulates antioxidant and proinflammatory enzymes (Deng et al., 2006; Rodriguez et al.,2004)
f. Drug interactions also influence the bioavailability of melatonin. (Hartter et al., 2000)
g. Melatonin modulates inflammatory enzyme myeloperoxidase and through the interactions of MPO with nitric oxide synthase regulates production of nitric oxide. (Galijasevic et al., 2008; Galijasevic et al., 2003)
h. General conditions such as age, total health status, antioxidant levels, over the counter and prescribed medications affect outcome of the melatonin therapy

Considering the variety of reactions pathways that melatonin can be involved and multiplicity of intracellular effects in it is clear that its concentration significantly direct outcome of the study especially in a complex biological milieu. In addition, no detailed dose studies have ever been done in relationship with particular condition. Generally, classical view of melatonin as a cronobiotic and antioxidant molecule with submolar circulating concentrations still persists. However this approach is insufficient and several new reactions pathways deserve attention and additional research. A variety of melatonin actions is presented in Figure 1.

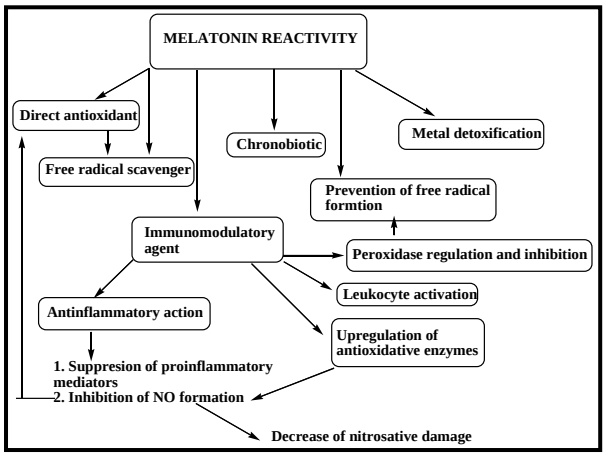

Figure 1. Multiple modes of melatonin actions

Reaction mechanism of melatonin

a. Catabolic pathways

Melatonin synthesized by the pineal gland is released into the bloodstream and then into other bodily fluids, including cerebral spinal fluid (CSF) (Rousseau *et al.*, 1999) saliva, (Vakkuri, 1985) and bile (Tan *et al.*,1999).

Both, endogenous and administered melatonin are generally considered to be metabolized in humans in the presence of cytochrome P450, forming 6-hydroxymelatonin (6-HMEL) followed by sulfate or glucuronide conjugation to 6-hydroxymelatonin sulfate or 6-hydroxymelatonin glucuronide and excreted in urine (Young*et al.,* 1985). However, melatonin is present in many tissues that do not have hepatic cytochromes P450, thus, tissue levels may not necessarily be a function of rates of hepatic metabolism or even directly related to plasma concentrations (Reiter *et al.,* 2003).

Second conversion pathway involves oxidation reaction e.g., by indoleamine 2,3-dioxygenase, myeloperoxidase, oxoferryl-Hb, hemin and a number of free radical such as $O_2^{\bullet-}$, $^{\bullet}OH + O_2^{\bullet-}$ $CO_3^{\bullet-}$,$^1O_2$, O_3, aromatic cation radicals and $O_2^{\bullet-}$, giving one of the most important melatonin metabolites, AFMK (*N*^{1}-acetyl-*N*^{2}-formyl-5-methoxykynuramine). In reaction with hydroxyl radical, melatonin can convert to c3-OHM (cyclic 3-hydroxymelatonin) that in the presence of another hydroxyl radical molecule forms AFMK. Deformylation of AFMK by hemoperoxidase and arylamine formamidase gives AMK (*N*^{1}-acetyl-5-methoxykyunaramine). Interestingly without administration of exogenous melatonin, serum levels of AFMK were undetectably low (Harthe *et al.,* 2003; Rozov *et al.,*2003). Several metabolites of melatonin have been detected in a different tissues, cells and urine (Tan *et al.,* 2003). AMFK and AMK are generally considered as major most important metabolites of melatonin, probably due to their strong free radical scavenging activities. Recent review pointed out that direct free radical scavenging activity may be relevant when concentrations of melatonin are high, and some of the oxidative reactions might be valid when done in isolate system, but questions about potency of this type of melatonin activity in biological systems remain to be investigated more (Hardeland *et al.,* 2008). The multiplicity of enzymatic and nonenzymatic catalysts capable of forming AFMK show the complexity of reactions mechanisms and difficulty to determine exact beneficial melatonin dose. Number of clinical studies showed excellent results in the treatment of different physiological conditions and disease. However, there are also a number of conflicting studies showing no or a little improvement after melatonin therapy. Study investigating efficacy and safety of exogenous melatonin for secondary sleep disorders and sleep disorders accompanying sleep restriction concluded that there is no evidence that melatonin is effective in treating secondary sleep disorders or sleep disorders accompanying sleep restriction, such as jet lag or shift work disorder. There is evidence that melatonin is safe with short term use, but additional studies are needed to determine its long-term safety (Buscemi *et al.,* 2006). Del Fabbro *et al.* tested results of prior studies that suggested that melatonin can attenuate weight loss, anorexia, and fatigue in patients with cancer. The primary purpose of their study was to compare melatonin with placebo for appetite improvement in patients with cancer cachexia. In cachectic patients with advanced cancer, oral melatonin, 20 mg, at night did not improve appetite, weight, or quality of life compared with placebo. Singer et al (Singer *et al.,* 2003) conducted a research to determine the safety and efficacy of 2 dose formulations of melatonin for the treatment of insomnia in patients with Alzheimer's disease. No statistically significant differences in objective sleep measures were seen between baseline and treatment periods for the any of the 3 groups: placebo, taking 2.5-mg slow-release melatonin, or 10-mg melatonin. Nonsignificant trends for increased nocturnal total sleep time and decreased wake after sleep onset were observed in the melatonin groups relative to placebo. Year before, Cardinalli *et al.* report the effect of melatonin (4-month-long treatment with 6 mg/day) in 45 AD patients with sleep disturbances. Melatonin improved sleep and suppressed sundowning, an effect seen regardless of the concomitant medication employed to treat cognitive or behavioral signs of AD. Melatonin treatment seems to constitute a selection therapy to ameliorate sundowning and to slow evolution of cognitive impairment in AD patients. Considerable evidence confirmed that melatonin can inhibit LDL oxidation that in turns plays an important role in the development of atherosclerosis [Reiter *et al.,* 2008]. One of the more detailed studies investigated *in vitro* protective effects of melatonin against oxidation of 1-palmitoyl-2-linoleoyl-sn-glycero-3-phosphocholine (PLPC). Liposomes and low-density lipoproteins conjugated dienes (CD) and hydroperoxides from cholesteryl esters (CEOOH) and phospholipids (PCOOH) were measured as indices of lipid peroxidation (Marchetti *et al.,* 2011).Melatonin was efficient in lowering lipid peroxidation in LDL, as shown by the decrease in the formation of CDs and hydroperoxides. Authors clearly mentioned that melatonin protections was based on free radical scavenging effect of melatonin since hydroxyl radical was directly involved in LDL oxidation. Another study performed in more complex experimental system showed that daily melatonin supplementation in mice increases atherosclerosis in proximal aorta. This study suggests that caution should be taken as regards high melatonin dosage in hypercholesterolemic patients (Tailleux *et al.,* 2002). Clearly, number of factors mentioned earlier in the text can influence the result of the studies. Multiplicity of reaction pathways and concentration of used melatonin and, in addition, age, physiology of pineal gland, oxidative stress, antioxidative and proxidative enzyme status when clinical studies are in question makes it difficult to obtain definitive answers on beneficial effect of melatonin. The possibility of additional undetected or concentration -dependent reaction mechanisms, either of melatonin or one if its metabolites, adds to the complexity of any type of studies.

b. Metal Chelator

Many studies have investigated link between metal-induced toxicity and carcinogenicity, and connected it to ability of metals to catalyze generation of reactive oxygen and nitrogen species in biological systems. Metal-mediated formation of free radicals results in modifications to DNA bases as well as can enhance lipid peroxidation. Biological studies showed that melatonin can protect against DNA oxidation and lower lipid peroxidation. (Reiter *et al*., 2008). Antioxidative activity of melatonin is generally accepted as one of the

mechanism that alleviates metal induced toxicity and oxidative changes on the system. Melatonin molecule being composed of a 5-methoxyindole group and an N-ethylacetamide group with nitrogen and oxygen atoms has also a potential ability to act as a metal chelator. The metal chelation ability of melatonin is mentioned marginally in literature reviews. In 1998, Limson *et al.* showed that melatonin formed complexes with aluminium (III), cadmium (II), copper (II), iron (III), lead and zinc suggesting metal detoxification role of melatonin in biological system. The metal chelating ability of melatonin was concentration dependent (Limson *et al.*, 1998; Gulcin *et al.*, 2002). Clearly, complex formation is dependent on amounts of available metal ions that can vary in different tissues and on melatonin concentrations. As a result, different melatonin concentrations are necessary for the complete formation of stable complexes that have significant consequences if melatonin is used as a detoxification agent in biological systems. Interestingly, experiments with iron showed that melatonin can bind iron (III) not to iron (II) thus blocking generation of free radical via the Fenton reaction. Parmar *et al.* found that melatonin affords some protection to rat hepatocytes in the presence of copper. Electrochemical studies show that melatonin, in addition to binding Cu^{2+}, may provide protection against copper-mediated free radical damage by binding Cu^{1+}. Lack *et al.* showed that melatonin form complexes with lithium, potassium, sodium and calcium. The stability of the complexes formed between melatonin and the metals decreased with the metals as follows: $K^{+}>Li^{+}>Na^{+}>Al^{3+}>Ca^{2+}$ .Another study evaluated the metal chelating and hydrogen peroxide (H_2O_2) scavenging activity of melatonin (Gulcin *et al.*, 2003). The metal chelating activity increased with increasing concentrations of melatonin (20–60 μg/mL). Based on these results, it is concluded that melatonin is an effective metal chelating agent. Interestingly, most of the studies showed the ability of melatonin to bind metal ions but a definitive mechanism is not known yet. One possible mechanism, in a complex biological milieu, is simple scavenging activity of free radicals like hydroxyl radicals generated in vivo from the metal-catalyzed breakdown of hydrogen peroxide, according to the Fenton reaction (Liochev and Fridovich 2002). However, O'Halloran and co-workers recently reported that the upper limit of so-called "free pools" of copper was far less than a single atom per cell (Rae *et al.*, 1999). This data imply that Fenton like reaction when copper is present is not feasible under these conditions. Thus, possibility of direct interaction of melatonin with metal ions forming complexes is another valid mechanistic pathway. We recently showed by using UV and IR spectroscopy direct formation of Cu-Melatonin complex on solutions where hydrogen peroxides was not present thus excluding free radical formation (Galijasevic, 2013). This study is initial one, done with varying copper and melatonin concentrations in order to find conditions necessary for the complex formation. Further experiments in biological systems need to be done to test whether chelation reactions is possible in more complex system. Another interesting metal that has deleterious effect on cells is mercury. Study showed that a 24-hour exposure to 50 μg/L mercury induced significant cell cytotoxicity in neuroblastoma cells (Galijasevic *et al.*,2000). Treatment of cells with melatonin before administration of mercury greatly reduced the mercury-induced cytotoxicity. Mechanism is not known but authors suggested that either chelation activity is present or melatonin causing production of increased levels of intracellular antioxidants such as glutathione .It is not excluded that both these mechanisms could be operating simultaneously.

More detailed studies are needed in order to confirm metal chelating abilities of melatonin, including experimental conformation of formed complex, determination of ligand donor atoms and molecular geometry of formed complex. In addition, kinetic of complex formation and determination of complex electrochemical potentials would give definitive answer on mechanism of melatonin interactions with metals. However, those results would not imply that exact mechanism exist in biological systems, simply because of complexity of studied systems and melatonin antioxidant activity and as a new research shows different enzymes inhibitory activity.

c. Enzyme inhibitor

Myeloperoxidase (MPO) is one of the most abundant enzymes in neutrophils and monocytes, involved in leukocyte-mediated host defenses. It is also thought to play a pathogenic role under certain circumstances such as during inflammatory tissue injury and chronic inflammatory conditions (Nicholls and, Hazen, 2004). MPO has been recently reported to be useful for identifying inflammation in the walls of coronary arteries, which in turn may indicate a risk for heart disease or heart attack (Weiss, 1988). Thus, inhibiting MPO may be a key step in the prevention of pathophysiology of LDL oxidation. MPO uses H_2O_2 generated during a respiratory burst as co-substrate to form cytotoxic oxidants and diffusible radical species. Evidence suggests that MPO-mediated reactive oxidants can promote protein nitration, lipid peroxidation, amine chlorination, and thiol nitrosylation. Recent review summarized catalytic cycle of MPO and corresponding inflammatory injury by a different mechanism (Arnhold and Flemming, 2010). At plasma levels of halides, chloride (Cl^{-}) is a major co-substrate for MPO and the cytotoxic oxidant, hypochlorous acid (HOCl), is produced. In addition to HOCl, MPO can generate a variety of reactive oxidant species, multiple distinct protein and lipid oxidation products, which have been identified in tissues associated with atherosclerosis and other inflammatory conditions (Shishehbor and Hazen, 2004). The ground state (secreted) form of the enzyme, reacts in a rapid and reversible manner with H_2O_2 to form Compound I. This redox intermediate oxidizes halides via a single two e^{-} oxidation step to their respective hypohalous acids. Alternatively, Compound I may oxidize multiple substrates through two sequential one e^{-} steps forming Compound II and ground state enzyme, respectively. Enhancement in peroxidase catalysis due to reduction of MPO-Compound II has been noted with a series of physiological reductants like superoxide ($O_2^{\bullet-}$), melatonin, tryptophan, nitric oxide (NO), and ascorbic acid (Lee *et al., 1991;* Hallingbäck *et al.*, 2006; Kettle

and Candaeis, 2000). Oxidation of melatonin was first observed by activated neutrophils in a reaction involving myeloperoxidase (Silva *et al.,* 2000). In order to clarify if melatonin is a substrate of MPO, Allegra et al investigated the oxidation of melatonin by MPO redox intermediates, compounds I and II (Allegra *et al.,* 2001). Spectral and kinetic analysis revealed that both intermediates compound I and compound II oxidize melatonin via one-electron processes. Authors concluded that that the rate of oxidation of melatonin is dependent on the H_2O_2 concentration and is not affected by superoxide dismutase. Another study proposes that melatonin serves as potent inhibitor of MPO under physiological-like conditions (Galijasevic *et al.,* 2003). In the presence of Cl^-, melatonin inactivated MPO at two points in the classic peroxidase cycle through binding to MPO to form an inactive complex, melatonin-MPO-Cl, and accelerating MPO compound II formation, an inactive form of MPO. Inactivation of MPO was mirrored by the direct conversion of MPO-Fe(III) to MPO compound II without any sign of compound I accumulation. This behavior indicates that melatonin binding modulates the formation of MPO intermediates and their decay rates. Melatonin-dependent inhibition of MPO occurred with a wide range of concentrations that span various physiological and supplemental ranges. More importantly, the oxidized form of melatonin, N^1-acetyl-N^2-formyl-5-methoxynuramine (AFMK) has no effect on MPO catalytic activity, but functions as a potent antioxidant due to its ability to serve as free radical scavenger. This interplay between MPO and melatonin may have a much broader application in biological systems. Thus, inactivation of MPO and its catalytic cycle can be controlled effectively by melatonin supplementation. Indeed, when the melatonin concentration is less than twice the H_2O_2 concentration, H_2O_2 consumption proceeds in a slower and linear manner and MPO returns to its ground state after melatonin oxidation. This behavior clearly demonstrates that MPO is capable of restoring its catalytic activity and rejoining the peroxidase cycle after melatonin exhaustion. On the other hand, when the melatonin concentration is greater than twice the H_2O_2 concentration, the initial slow phase of H_2O_2 consumption remains at the same rate through the progression of the reaction and ceases when H_2O_2 is completely consumed. Clearly, melatonin concentrations used in inflammatory event controls reaction pathways and inhibition of MPO activity that in turns regulates HOCl production and possible deleterious effect on the biological environment. Effect of melatonin inflammatory events by MPO inhibition has the broader consequences on pathophysiologies where nitric oxide is involved. Nitric oxide is directly involved in MPO catalytic mechanism by a number of different pathways modulating MPO activity and contributing to the detrimental effect of MPO system at the sites of enzyme expression. NO serves as both a ligand and a substrate for MPO, and the overall effect of NO on the catalytic activity depends on the affinity of MPO for NO vs. H_2O_2 and their concentrations. Another mechanism of interactions between MPO and iNOS suggest that the MPO system consumed NO released by iNOS during steady-state catalysis, thereby preventing the NO-induced inhibition attributed to the formation of the iNOS–nitrosyl complex. Thus, removal of NO from the iNOS milieu by the MPO system during steady-state catalysis causes a significant increase in iNOS catalytic activity. Myeloperoxidase, acting as a sink for NO efficiently activates iNOS preventing shutdown of the NO production system (Galijasevic et al., 2003). Numbers of studies have shown that melatonin influence the bioavailability of NO by inhibition of NO synthase activity (Aydogan *et al.,* 2006). Besides enzyme inhibition melatonin, AMFK, and AMK can scavenge NO and peroxynitrite. The highest reactivity towards radical nitrogen species has AMK, but its formation dependents on a number of factors mentioned earlier. Melatonin dose of 1 microM-1mM inhibits NO production in immunostimulated macrophages mainly by inhibiting the expression of iNOS. (Gilad *et al.,* 1998). Tested concentrations are very high even for a nonnpinela sites of melatonin production, and inhibition can only be achieved when pharmacological doses of melatonin are taken. Even in that case, it is not clear whether such concentrations can be achieved at the needed sites due to the variety of melatonin reaction pathways. Another study confirmed too that, besides its antixodant activity, melatonin inhibits peroxynitrite formation by inhibition of the enzyme nitric oxide synthase in some brain tissues (Leon *et al.,* 2004). Experiments in vivo showed that melatonin administration prevents sepsis-induced electron transport chain damage decreasing the activity and expression of INOS and mtNOS, thus reducing intramitochondrial nitric oxide (NO) and peroxynitrite (ONOO-) levels (Acuña-Castroviejo *et al.,* 2003). Melatonin improved vascular function in experimental hypertension, reducing intimal infiltration and restoring NO production. Melatonin improved the NO pathway also in animal models for the study of diabetes and prevented NO down-regulation and adhesive molecules up-regulation in nicotine-induced vasculopathy (Rodella *et al.,* 2013). The question about most preferred reaction mechanism of melatonin still remains unanswered. Whether melatonin concentrations have an effect on a preferred mechanism is still unknown too. In addition, presence of myeloperoxidase at the sites of inflammation and interplay between MPO, NO and iNOS adds to the complexity of melatonin reactions pathways.

At the sites of inflammation melatonin can act as free radical scavenger of already formed NO and $ONOO^-$, inhibit NOS production, act as a substrate for MPO compounds I and II or inhibit MPO and block H_2O_2 consumption and modulate interplay between MPO and iNOS, thus indirectly affecting production of NO. Which mechanism will be predominating one, or what can act as an efficient switch between possible reaction pathways is not experimentally shown yet. Interactions of iNOS, MPO and free radicals at the sites of inflammation with melatonin are presented in Figure 2. Presented reaction pathways are not intended to be comprehensive and only major reactions are shown due to the clarity.

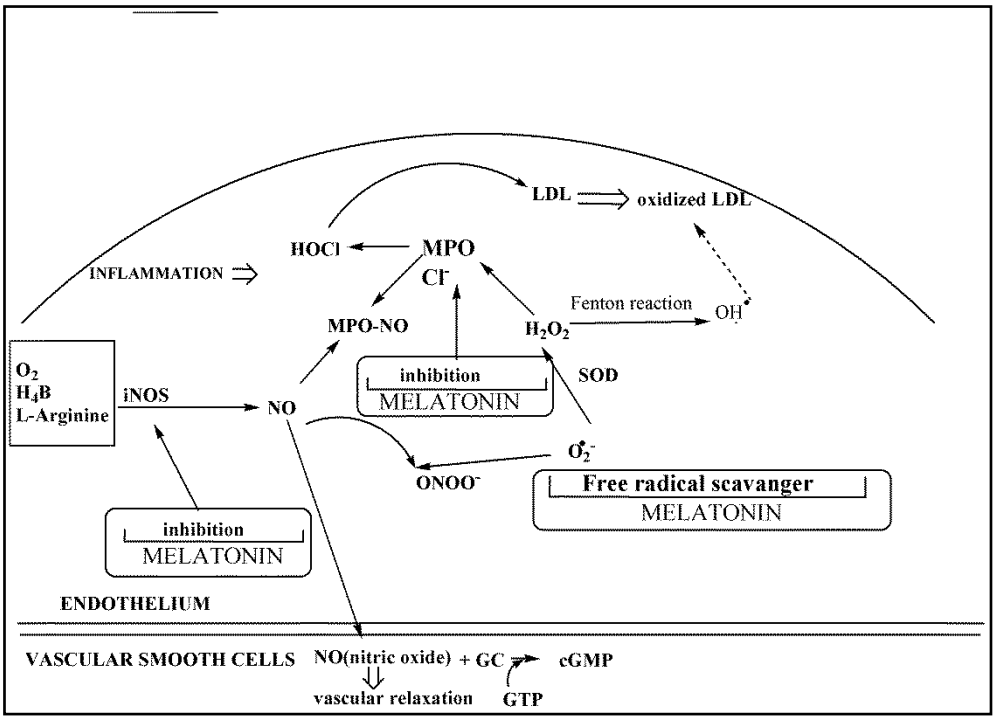

Figure 2. Involvement of melatonin multiple reaction pathways at the sites of inflammation. Melatonin can exert its effect by free radical scavenging, myeloperoxidase inhibition, nitric oxide syntahase inhibition or acting as a substrate for myeloperoxidase. Each action will result with a cascade of reactions with a different outcome

CONCLUSION

Melatonin like no other molecule drew attention as a natural supplement with a numerous beneficial effects. Most of these claims are based on a melatonin ability to scavenge harmful free radicals. Research shows that melatonin reactivity comprises many different reaction pathways. It is reasonable to conclude that different conditions of system that is treated melatonin and other reactants concentrations, and melatonin metabolites availability influence the final outcome. Some of the most reactions pathways such as modulation of inflammatory enzymes and possible metal detoxifications deserve more attention. Definitive dose-response studies are needed if beneficial effect of melatonin is going to be established. In addition, concentration and type of free radicals that can actually be scavenged by melatonin need to be tested and compared to the antioxidant present in the biological system Melatonin is remarkable molecule with a variety of biological roles showing a promising role in a treatment of variety conditions and diseases justifying additional systematic research.

ACKNOWLEDGEMENT

This work has been supported by Federal Ministry of Education and Science (Bosnia and Herzegovina) research grant awarded to S.G.

REFERENCES

Acuña-Castroviejo D., Escames G., León J., Carazo A., Khaldy H. (2003).Mitochondrial regulation by melatonin and its metabolites. *Adv Exp Med Biol* 527:549-557

Allegra M, Furtmüller P.G., Regelsberger G, Turco-Liveri M.L., Tesoriere L., Perretti M., Livrea M.A., Obinger C. (2001) Mechanism of reaction of melatonin with human myeloperoxidase. Biochem Biophys Res Commun. 282(2):380-6

Altun A, Ugur-Altun B. (2007) Melatonin: therapeutic and clinical utilization. *Int J Clin Pract.* 61(5):835-45

Arnhold J., Flemmig J.(2010).Human myeloperoxidase in innate and acquired immunity. Arch Biochem Biophys.; 500(1):92-106.

Armstrong S.M., Cassone V.M., Chesworth M.J. (1986). Synchronization of mammalian circadian rhythms by melatonin. *J Neural Transm*, Suppl 21: 375-394.

Aydogan S., Yerer M.B., Goktas A.(2006) Melatonin and nitric oxide. J Endocrinol Invest.; 29(3):281-7.

Bubenik G.A. (2002). Gastrointestinal melatonin: localization, function, and clinical relevance. *Dig Dis Sci.* 47:2336–2348

Buscemi N., Vandermeer B., Hooton N., Tjosvold L., Hartling L., Vohra S., Klassen T.P., Baker G. (2003) Efficacy and safety of exogenous melatonin for secondary sleep disorders and sleep disorders accompanying sleep restriction: meta-analysis. British Medical Journal 332(7538):385-93.

Cardinali D.P., Brusco L.I., Liberczuk C., Furio A.M. (2002).The use of melatonin in Alzheimer's disease. *Neuro Endocrinology Letters*. 23 Suppl 1:20-3.

Claustrat B, Brun J, Chazot G.(2005) The basic physiology and pathophysiology of melatonin. *Sleep Med Rev*.9,11–24.

Calvo J.R., González-Yanes C., Maldonado M.D. (2013) The role of melatonin in the cells of the innate immunity: a review. *Journal of Pineal Research.* 55(2):103-20

Conti A, Conconi S, Hertens E Skwarlo-Sonta K, Markowska M., Maestroni J.M. (2000). Evidence for melatonin synthesis in mouse and human bone marrow cells. *Journal Pineal Research*; 28: *193–202*.

Dardente H. (2012). Melatonin-dependent timing of seasonal reproduction by the pars tuberalis: pivotal roles for long daylengths and thyroid hormones. J *Neuroendocrinol.*, 24:249-266

Dawson D, Armstrong S.M. (1996). Chronobiotics--drugs that shift rhythms. *Pharmacol Ther, 69:15*-36.

Del Fabbro E., Dev R., Hui D., Palmer L, Bruera E. (2013).Effects of melatonin on appetite and other symptoms in patients with advanced cancer and cachexia: a double-blind placebo-controlled trial. *Journal of Clinical Oncology*. 31(10):1271-6.

Deng W.G., Tang S.T., Tseng H.P.,Wu K.K. (2006) Melatonin suppresses macrophage cyclooxygenase-2 and inducible nitric oxide synthase expression by inhibiting p52 acetylation and binding. *Blood.* 15;108(2):518-24

Galano A.D., Tan D.X., Reiter R.J. (2011). Melatonin as a natural ally against oxidative stress: a physicochemical examination. *Journal of Pineal Research.* 51, 1-16.

Galijasevic S., Abdulhamid I., Abu-Soud H.M. (2008) Melatonin is a potent inhibitor for myeloperoxidase Biochemistry.47;(8):2668-77.

Galijasevic S., Saed G.M., Diamond M.P., Abu-Spud H.M. (2003). Myeloperoxidase up-regulates the catalytic activity of inducible nitric oxide synthase by preventing nitric oxide feedback inhibition. *Proc Natl Acad Sci U S A.* 100(25):14766-71.

Galijasevic S., Ljevarevic V., Dugandzic V.(2013) International Turkish Congress on Molecular Spectroscopy (TURCMOS), Istanbul.

Gilad E., Wong H.R., Zingarelli B., Virág L., O'Connor M., Salzman A.L., Szabó C. (1998) Melatonin inhibits expression of the inducible isoform of nitric oxide synthase in murine macrophages: role of inhibition of NFκB activation. *FASEB Journal.* 12:685–693

Gulcin I., Buyukokuroglu M.E., Oktay M., Kufrevioglu O.I. (2002).On the in vitro antioxidant properties of melatonin. *Journal of Pineal Research*. 33:167-171

Gulcin I, Buyukokuroglu M.E., Kufrevioglu O.I.(2003). Metal chelating and hydrogen peroxide scavenging effects of melatonin. *Journal of Pineal Res*earch. 34: 278–281

Hallingbäck H.R., Gabdoulline R.R., Wade R.C. (2006).Comparison of the binding and reactivity of plant and mammalian peroxidases to indole derivatives by computational docking. *Biochemistry*; 45:2940-2950

Hardeland R. (2005).Antioxidative protection by melatonin – Multiplicity of mechanisms from radical detoxification to radical avoidance. *Endocrine*. 27:119–130.

Hardeland R., Cardinali D.P, Srinivasan V, Spence D.W., Brown G.M., Pandi-Perumal S.R. (2011) Melatonin - a pleiotropic, orchestrating regulator molecule. *Progress in Neurobiology*. 93:350-384.

Harthe C., Claudy D., De´chaud H. Vivien-Roels B., Pévet P., Claustrat B.(2003) Radioimmunoassay of N-acetyl-N-formyl-5-methoxykynuramine (AFMK): a melatonin oxidative metabolite. *Life Science*. 73:1587–1597.

Hartter S., Grozinger M,, Weigmann H., Röschke J., Hiemke C. (2000).Increased bioavailability of oral melatonin after fluvoxamine coadministration. *Clinical Pharmacology and Therapeutics.* 67:1–6.

Ianas O., Olinescu R., Badescu I.(1991). Melatonin involvement in oxidative processes. *Endocrinologie*. 29:147-153.

Kettle A.J., Candaeis L.P. (2000). Oxidation of tryptophan by redox intermediates of myeloperoxidase and inhibition of hypochlorous acid production. *Redox Rep.*; 5:179-84

Kostoglou-Athanassiou I. (2013) Therapeutic applications of melatonin. *Ther Adv Endocrinol Metab*. 4(1):13-24.

Kvetnoy I.M. (1999). Extrapineal melatonin: location and role within diffuse neuroendocrine system.*Histochem J*.31 (1):1-12.

Lack B., Daya S., Nyokong T.(2001) Interaction of serotonin and melatonin with sodium, potassium, calcium, lithium and aluminium. *Journal of Pineal Research.*31 (2): 102–108.

Lee H.C., Booth K.S., Caughey W.S, Ikeda-Saito M. (1991).Interaction of halides with the cyanide complex of myeloperoxidase: a model for substrate binding to compound I. Biochim. Biophys. Acta; 1076:317-320

Lerner A.B., Case J.D., Takahashi Y. (1958). Isolation of melatonin, a pineal factor that lightens melanocytes. J Am Chem Soc,80: 2587

Leon J., Acuña-Castroviejo D, Sainz R.M., Mayo J.C., Tan D.X., Reiter R.J. (2004).Melatonin and mitochondrial function. *Life Science*.75:765-790

Limson J., Tebello N., Oaya S. (1998). The interaction of melatonin and its precursors with aluminium, cadmium, copper, iron, lead, and zinc: An adsorptive voltammetric study *Journal of Pineal Research*. 15–21

Liochev S.I., Fridovich I. The Haber-Weiss cycle — 70 years later: an alternative view. (2002).*Redox report.* 7:55–57.

Marchetti C., Sidahmed-Adrar N., Collin F., Jore D., Gardès-Albert M., Bonnefont-Rousselot D. (2011) Melatonin protects PLPC liposomes and LDL towards radical-induced oxidation. *Journal of Pineal Research*. 51(3):286-96

Nicholls S.J., Hazen S.L.(2004). The role of myeloperoxidase in the pathogenesis of coronary artery disease. *Jpn J Infect Dis.*; 57: S21-2.

Olivieri G., Brack C., Müller-Spahn F., Stähelin H.B. (2000). Mercury Induces Cell Cytotoxicity and Oxidative Stress and Increases β-Amyloid Secretion and Tau Phosphorylation in SHSY5Y Neuroblastoma Cells. *J Neurochem*; 74: 231–236.

Pandi-Perumal S.R., Srinivasan V., Maestroni G.J, *,Cardinali D.P., Poeggeler B., Hardeland R...*(2006). Melatonin: Nature's most versatile biological signal*? FEBS Journal*, 273(13):2813-38.

Parmar P., Limson J., Nyokong T., Daya S. (2002).Melatonin protects against copper-mediated free radical damage J. Pineal Res; 32 (4) : 237–242.

Poeggeler B., Saarela S., Reiter R.J., Tan D.X., Chen L.D., Manchester L.C., Barlow-Walden L.R. Melatonin--a highly potent endogenous radical scavenger and electron donor: new aspects of the oxidation chemistry of this indole accessed in vitro. (1994). Ann N Y Acad Sci 738:419-20

Rae T.D., Schmidt P.J., Pufahl R.A., Culotta V, C., O'Halloran T.V. (1999).Undetectable intracellular free copper: the requirement of a copper chaperone for superoxide dismutase. *Science.*284:805–808

Reiter R.J, Tan D.X., Kim S.J.,Qi W.(2008) Melatonin as a pharmacological agent against oxidative damage to lipids and DNA. *Proc.West Pharmacol. Soc.*, 41: 229-236.

Reiter R.J., Tan D.X., Mayo J.C., Sainz R.M., Leon J., Czarnocki Z.(2003). Melatonin as an antioxidant:

biochemical mechanisms and pathophysiological implications in humans. *Acta Biochim Pol.* 50(4):1129-46.

Rousseau A., Petren S., Plannthin J., Eklundh T., Nordin C. (1999) Serum andcerebrospinal fluid concentrations of melatonin: a pilot study in healthy male volunteers. *Journal of Neural Transmission*. 106:883-888.

Rodella L.F., Favero G., Foglio E., Rossini C., Castrezzati S., Lonati C., Rezzani R. (2013)Vascular endothelial cells and dysfunctions: role of melatonin. *Front Biosci (Elite Ed)*. ; 5:119-29.

Rodriguez C., Mayo J.C., Sainz R.M., Antolín I, Herrera F., Martín V., Reiter R.J. (2004) Regulation of antioxidant enzymes: a significant role for melatonin. Journal of Pineal Research. 36: 1–9.

Rozov S.V., Filatova E.V., Orlov A.A., Volkova A.V., Zhloba A.R., Blashko E.L., Pozdeyev N.V.(2003) N1-acetyl-N2-formyl-5-methoxykynuramine is a product of melatonin oxidation in rats. Journal of Pineal Research. 35:245–250

Schaffazick S.R., Pohlmann A.R, de Cordova C.A., Creczynski-Pasa T.B., Guterres S.S.(2005) Protective properties of melatonin-loaded nanoparticles against lipid peroxidation. *International journal of pharmaceutics*; 289:209-13

Shishehbor M.H., Hazen S.L. (2004), Inflammatory and oxidative markers in atherosclerosis: relationship to outcome. *Curr Atheroscler Rep*.; 6:243-50.

Singer C., Tractenberg R.E., Kaye J., Schafer K., Gamst A., Grundman M., Thomas R., Thal L.J.(2003) A multicenter, placebo-controlled trial of melatonin for sleep disturbance in Alzheimer's disease. *Sleep.* 1l26(7):893-901.

Slominski A., Fischer T.W., Zmijewski M.A., Wortsman J., Semak I., Zbytek B., Slominski R.M., Tobin D.J. (2005).On the role of melatonin in skin physiology and pathology. *Endocrine*; 27:137–148.

Srinivasan V, Mohamed M, Kato H.(2012) Melatonin in bacterial and viral infections with focus on sepsis: a review. *Recent Pat Endocr Metab Immune Drug Discov.* 6(1):30-9.

Tailleux A, Torpier G, Bonnefont-Rousselot D., Lestavel S., Lemdani M., Caudeville B., Furman C., Foricher R., Gardes-Albert M., Lesieur D., Rolando C., Teissier E., Fruchart J.C., Clavey V., Fievet C., Duriez P. (2002).Daily melatonin supplementation in mice increases atherosclerosis in proximal aorta. *Biochemical and Biophysical Research Communication. 293(3):1114-23.*

Tan D.X., Chen L.D., Poeggeler B, Reiter R.J. Melatonin: a potent, endogenous hydroxylradical scavenger (1993) *Endocrine Journal*.1: 57-60.

Tan D., Manchester L.C., Reiter R.J., Qi W., Hanes M.A., Farley N.J. (1999).High physiological levels of melatonin in the bile of mammals. *Life Science.* 65:2523-2529.

Tan D.X., Manchester L.C., Terron M.P., Flores L.J., Reiter R.J .(2007*)* One molecule, many derivatives: a never-ending interaction of melatonin with reactive oxygen and nitrogen species? *Journal of Pineal Research*. 42(1):28-42.

Vakkuri O., (1985).Diurnal rhythm of melatonin in human saliva. *Acta Physiol Scand* 124: 409-412.

Young I.M., Leone R.M., Francis P, Stovell P., Silman R.E. (1985). Melatonin is metabolized to N-acetyl serotonin and 6-hydroxymelatonin in man. *The Journal of Clinical Endocrinology & Metabolism.* 60:114-119.

Young I.M., Leone R.M., Francis P, Stovell P., Silman R.E. (1985). Melatonin is metabolized to N-acetyl serotonin and 6-hydroxymelatonin in man. The Journal of Clinical Endocrinology & Metabolism. 60:114-119.

Summary/Sažetak

Melatonin (N-acetil-5-metoksi-triptamin) je poznat kao skupljač slobodnih radikala i antioksidans koji sudjeluju u različitim biološkim i fiziološkim regulacijama kao što su modulacija cikardijarnog ritma, sezonske reprodukcije, fiziologija retine i regulacija sna. Sintetski melatonin je komercijalno dostupan, a njegovi su dodaci klinički korišteni za liječenje različitih medicinskih stanja kao što su jet lag, smetnje u radu i poremećaji spavanja. Nedavne studije pokazale su da melatonin služi kao inhibitor mijeloperoksidaze (MPO) u fiziološkim uvjetima. Melatonin inhibira MPO pri različitim koncentracijama što može utjecati na fiziološku i patofiziološku ulogu MPO. Osim toga, MPO modulira proizvodnju nitrogen oksida, tako da melatonin može neizravno utjecati na koncentraciju nitrogen oksida. Brojni dokazi pokazuju novu ulogu melatonina i njegovih metabolita pored klasične uloge . Ovaj rad analizira novootkrivene mehanističke puteve aktivnosti melatonina koje treba uzeti u obzir pri primjeni melatonina u farmakološke svrhe.

INSTRUCTIONS FOR AUTHORS

GENERAL INFORMATION

Bulletin of the Chemists and Technologists of Bosnia and Herzegovina (Glasnik hemičara i tehnologa Bosne i Hercegovine) is a semiannual international journal publishing papers from all fields of chemistry and related disciplines.

Categories of Contributions

1. *Original Scientific Papers* – (about 10 typewritten pages) report original research which has not been published previously, except in a preliminary form. The paper should contain all the necessary information to enable reproducibility of the described work.
2. *Short Communications* – (about 5 typewritten pages) describing work that may be of a preliminary nature but which merits immediate publication.
3. *Notes* – (about 3 typewritten pages) report unpublished results of short, but complete, original research or describe original laboratory techniques.
4. *Reviews* – (about 30 typewritten pages) present a concise and critical survey of a specific research area. Generally, these are prepared by the invitation of the Editor.
5. *Book and Web Site Reviews* – (about 2 typewritten pages).
6. *Extended Abstracts* – (about 2 typewritten pages) of Lectures given at international meetings.
7. *Technical Papers* – (about 10 typewritten pages) report on applications of an already described innovation. Typically, technical articles are not based on new experiments.

Reviewing the Manuscript

All contributors are evaluated according to the criteria of originality and quality of their scientific content, and only those deemed worthy will be accepted for publication. To facilitate the reviewing process, authors are encouraged to suggest three persons competent to review their manuscript. Such suggestions will be taken into consideration but not always accepted.

The Editor-In-Chief and Editors have the right to decline formal review of a manuscript when it is deemed that the manuscript is:

1. on a topic outside the scope of the Journal;
2. lacking technical merit;
3. of insufficient novelty for a wide international readership;
4. fragmentary and providing marginally incremental results; or
5. is poorly written.

Proofs

When a manuscript is ready for printing, the corresponding author will receive a PDF-formatted manuscript for proof reading, which should be returned to the journal within one week. Failure to do so will be taken as the authors are in agreement with any alteration which may have occurred during the preparation of the manuscript.

Copyright

Subscribers may reproduce tables of contents or prepare lists of articles including abstracts for internal circulation within their institutions. Permission of the Publisher is required for resale or distribution outside the institution and for all other derivative works, including compilations and translations.

Professional Ethics and Publication Policy

The journal expects the Editors, Referees and authors to adhere to the well-known standards of professional ethics. Authors are responsible for the factual accuracy of their contributions. Submission of the paper commits the author not to submit the same material elsewhere. Referees should act promptly. If certain circumstances preclude prompt attention to the manuscript at the time it is received, the non-received manuscript should be returned immediately to the Editor or the Referee should contact the Editor for possible delay of the report submission date. The Editor accepts full responsibility for his decisions on the manuscripts.

PREPARATION AND SUBMISSION OF MANUSCRIPT

Cover Letter

Manuscripts must be accompanied by a cover letter in which the type of the submitted manuscript. It should contain:

1. full name(s) of the author(s),
2. mailing address (address, phone and fax numbers, e-mail) of the author to whom correspondence should be addressed,
3. title of the paper (concise, without any abbreviations),
4. type of contribution,
5. a statement that the article is original and is currently not under consideration by any other journal or any other medium, including preprints, electronic journals and computer databases in the public domain, and
6. the names, full affiliation (department, institution, city and country), and
7. e-mail addresses of three potential Referees.

Contributors from Bosnia and Herzegovina should provide the name and full affiliation of at least one Referee from abroad.

Authors are fully encouraged to use ***Cover Letter Template*.**

Manuscript preparation

The submitted articles must be prepared with Word for Windows. Manuscripts should be typed in English (either standard British or American English, but consistent throughout) with 1.5 spacing (12 points Times New Roman; Greek letters in the character font Symbol) in A4 format leaving 2.5 cm for margins. Authors are fully encouraged to use ***Manuscript Template***.

All contributions should be written in a style that addresses a wider audience than papers in more specialized journals. Manuscripts with grammar or vocabulary deficiencies are disadvantaged during the scientific review process and, even if accepted, may be returned to the author to be rewritten in idiomatic English. The authors are requested to seek the assistance of competent English language expert, if necessary, to ensure their English is of a reasonable standard. The journal maintains its policy and takes the liberty of correcting the English of manuscripts scientifically accepted for publication.

Tables and figures and/or schemes should not be embedded in the manuscript but their position in the text indicated. In electronic version (Word.doc document) tables and figures and/or schemes should follow the text, each on a separate page. Please number all pages of the manuscript including separate lists of references, tables and figures with their captions.

IUPAC and International Union of Biochemistry and Molecular Biology recommendations for the naming of compounds should be followed.

SI units, or other permissible units, should be employed. The designation of physical quantities should be in Times New Roman font. In text, graphs, and tables, brackets should be used to separate the designation of a physical quantity from the unit. Please do not use the axes of graphs for additional explanations; these should be mentioned in the figure captions and/or the manuscript (example: "pressure at the inlet of the system, kPa" should be avoided).

Percents and *per mills*, although not being units in the same sense as the units of dimensioned quantities, can be treated as such. Unit symbols should never be modified (for instance: w/w %, vol.%, mol.%) but the quantity measured has to be named, *e.g.* mass fraction, w=95 %; amount (mole) fraction, x=20 %.

Latin words, as well as the names of species, should be in *italic*, as for example: *i.e., e.g., in vivo, ibid, Artemisia annua* L., *etc*. The branching of organic compound should also be indicated in *italic*, for example, *n*-butanol, *tert*-butanol, *etc*.

Decimal numbers must have decimal points and not commas in the text (except in the Bosnian/Croatian/Serbian abstract), tables and axis labels in graphical presentations of results. Thousands are separated, if at all, by a comma and not a point.

Structure of the Manuscript

The manuscript must contain, each on a separate page, the title page, abstract in English, (abstract in Bosnian/Croatian/Serbian), graphical abstract (optional), main text,

list of references, tables (each table separately), illustrations (each separately), and legends to illustrations (all on the same page).

1. ***Title page*** must contain: the title of the paper (bold letters), full name(s) of the author(s), full mailing addresses of all authors (italic), keywords (up to 6), the phone and fax numbers and the e-mail address of the corresponding author.
2. A one-paragraph ***abstract*** written of 150–200 words in an impersonal form indicating the aims of the work, the main results and conclusions should be given and clearly set off from the text. Domestic authors should also submit, on a separate page, a Summary/Sažetak. For authors outside Bosnia and Herzegovina, the Editorial Board will provide a Bosnian/Croatian/Serbian translation of their English abstract.
3. Authors are encouraged to submit a ***graphical abstract*** that describes the subject matter of the paper. It should contain the title of the paper, full name(s) of the author(s), and graphic that should be no larger than 11 cm wide by 5 cm tall. Authors are fully encouraged to use ***Graphical Abstract Template.***
4. ***Main text*** should have the following form:
   - ***Introduction***should include the aim of the research and a concise description of background information and related studies directly connected to the paper.
   - ***Experimental*** section should give the purity and source of all employed materials, as well as details of the instruments used. The employed methods should be described in sufficient detail to enable experienced persons to repeat them. Standard procedures should be referenced and only modifications described in detail.
   - ***Results and Discussion***should include concisely presented results and their significance discussed and compared to relevant literature data. The results and discussion may be combined or kept separate.
   - The inclusion of a ***Conclusion***section, which briefly summarizes the principal conclusions, is highly recommended.
   - ***Acknowledgement*** (optional).
   - Please ensure that every ***reference*** cited in the text is also present in the reference list (and *vice versa*). Unpublished results and personal communications are not recommended in the reference list, but may be mentioned in the text. If these references are included in the reference list they should follow the standard reference style of the journal and should include a substitution of the publication date with either "Unpublished results" or "Personal communication" Citation of a reference as "in press" implies that the item has been accepted for publication. As a minimum, the full URL should be given and the date when the reference was last accessed. Any further information, if known (DOI, author names, dates, reference to a source publication, etc.), should also be given. No more than 30 references should be cited in your manuscript.

     In the text refer to the author's name (without initials) and year of publication (e.g. "Steventon, Donald and Gladden (1994) studied the effects..." or "...similar to values reported by others (Anderson, Douglas, Morrison, *et al.*, 1990)..."). Type the names of the first three authors at first citation. At subsequent citations use

first author *et al.* The list of references should be arranged alphabetically by authors' names and should be as full as possible, listing all authors, the full title of articles and journals, publisher and year.

Examples of ***reference style***:

a) Reference to a journal publication:
Warren, J. J., Tronic, T. A., Mayer, J. M. (2010). Termochemistry of proton-coupled electron transfer reagents and its implications. *Chemical Reviews*, *110 (12)*, 6961-7001.

b) Reference to a book:
Corey, E. J., Kurti, L. (2010). *Enantioselective chemical synthesis*. (1st Ed.) Direct Book Publishing, LLC.

c) Reference to a chapter in an edited book:
Moody, J. R., Beck II, C. M. (1997). Sample preparation in analytical chemistry. In Setlle, F. A. (Ed.), *Handbook of instrumental techniques for analytical chemistry*. (p.p. 55-72). Prentice Hall.

d) Reference to a proceeding:
Seliskar, C. J., Heineman, W.R., Shi, Y., Slaterbeck, A.F., Aryal, S., Ridgway, T.H., Nevin, J.H. (1997). *New spectroelectrochemical sensor*, in Proceedings of 37th Conference of Analytical Chemistry in Energy and Technology, Gatlinburg, Tenesee, USA, p.p. 8-11.

e) Patents:
Healey, P.J., Wright, S.M., Viltro, L.J., (2004).*Method and apparatus for the selection of oral care chemistry*, The Procter & Gamble Company Intellectual Property Division, (No.US 2004/0018475 A1).

f) Chemical Abstracts:
Habeger, C. F., Linhart, R. V., Adair, J. H. (1995). Adhesion to model surfaces in a flow through system. *Chemical Abstracts,* CA 124:25135.

g) Standards:
ISO 4790:1992. (2008). *Glass-to-glass sealings - Determination of stresses*.

h) Websites:
Chemical Abstract Service, www.cas.org, (18/12/2010).

- ***Tables*** are part of the text but must be given on separate pages, together with their captions. The tables should be numbered consequently in Latin numbers. Quantities should be separated from units by brackets. Footnotes to tables, in size 10 font, are to be indicated consequently (line-by-line) in superscript letters. Tables should be prepared with the aid of the Word table function, without vertical lines. Table columns must not be formatted using multiple spaces. Table rows must not be formatted using Carriage returns (enter key; ↵ key). Tables should not be incorporated as graphical objects.
- ***Figures and/or Schemes*** (in high resolution) should follow the captions, each on a separate page of the manuscript. High resolution illustrations in TIF or EPS format (JPG format is acceptable for colour and greyscale photos, only) must be uploaded as a separate archived (.zip or .rar) file.

Figures and/or Schemes should be prepared according to the artwork instructions.

- ***Mathematical and chemical equations*** must be numbered, Arabic numbers, consecutively in parenthesis at the end of the line. All equations should be embedded in the text except when they contain graphical elements (tables, figures, schemes and formulae). Complex equations (fractions, inegrals, matrix…) should be prepared with the aid of the Word Equation editor.

Artwork Instructions

Journal accepts only TIF or EPS formats, as well as JPEG format (only for colour and greyscale photographs) for electronic artwork and graphic files. MS files (Word, PowerPoint, Excel, Visio) are NOT acceptable. Generally, scanned instrument data sheets should be avoided. Authors are responsible for the quality of their submitted artwork.

Image quality: keep figures as simple as possible for clarity - avoid unnecessary complexity, colouring and excessive detail. Images should be of sufficient quality for the printed version, i.e. 300 dpi minimum.

Image size: illustrations should be submitted at its *final size* (8 cm for single column width or 17 cm for double column width) so that neither reduction nor enlargement is required.

Photographs: please provide either high quality digital images (250 dpi resolution) or original prints. Computer print-outs or photocopies will not reproduce well enough for publication. Colour photographs rarely reproduce satisfactorily in black and white.

The facility exist for color reproduction, however the inclusion of color photographs in a paper must be agreed with Editor in advance.

Reporting analytical and spectral data

The following is the recommended style for analytical and spectral data presentation:

1. ***Melting and boiling points***:
   mp 163–165°C (lit. 166°C)
   mp 180°C dec.
   bp 98°C
   Abbreviations: mp, melting point; bp, boiling point; lit., literature value; dec, decomposition.
2. ***Specific Rotation***:
   $[a]^{23}_{D}$ –222 (*c* 0.35, MeOH).
   Abbreviations: a, specific rotation; D, the sodium D line or wavelength of light used for determination; the superscript number, temperature (°C) at which the determination was made; In parentheses: *c* stands for concentration; the number following *c* is the concentration in grams per 100 mL; followed by the solvent name or formula.

3. ***NMR Spectroscopy***:
   ^{1}H NMR (500 MHz, DMSO-d_6) d 0.85 (s, 3H, CH_3), 1.28–1.65 (m, 8H, 4´CH_2), 4.36–4.55 (m, 2H, H-1 and H-2), 7.41 (d, *J* 8.2 Hz, 1H, ArH), 7.76 (dd, *J* 6.0, 8.2 Hz, 1H, H-1'), 8.09 (br s, 1H, NH).
   ^{13}C NMR (125 MHz, $CDCl_3$) d 12.0, 14.4, 23.7, 26.0, 30.2, 32.5, 40.6 (C-3), 47.4 (C-2'), 79.9, 82.1, 120.0 (C-7), 123.7 (C-5), 126.2 (C-4).
   Abbreviations: d, chemical shift in parts per million (ppm) downfield from the standard; *J*, coupling constant in hertz; multiplicities s, singlet; d, doublet; t, triplet; q, quartet; and br, broadened. Detailed peak assignments should not be made unless these are supported by definitive experiments such as isotopic labelling, DEPT, or two-dimensional NMR experiments.
4. ***IR Spectroscopy***:
   IR (KBr) n 3236, 2957, 2924, 1666, 1528, 1348, 1097, 743 cm^{-1}.
   Abbreviation: n, wavenumber of maximum absorption peaks in reciprocal centimetres.
5. ***Mass Spectrometry***:
   MS *m/z* (relative intensity): 305 (M^+H, 100), 128 (25).
   HRMS–FAB (*m/z*): $[M+H]^+$calcd for $C_{21}H_{38}N_4O_6$, 442.2791; found, 442.2782.
   Abbreviations: *m/z*, mass-to-charge ratio; M, molecular weight of the molecule itself; M^+, molecular ion; HRMS, high-resolution mass spectrometry; FAB, fast atom bombardment.
6. ***UV–Visible Spectroscopy***:
   UV (CH_3OH) l_{max} (log e) 220 (3.10), 425 nm (3.26).
   Abbreviations: l_{max}, wavelength of maximum absorption in nanometres; e, extinction coefficient.
7. ***Quantitative analysis***:
   Anal.calcd for $C_{17}H_{24}N_2O_3$: C 67.08, H 7.95, N 9.20. Found: C 66.82, H 7.83, N 9.16.All values are given in percentages.
8. ***Enzymes and catalytic proteins relevant data:***
   Papers reporting enzymes and catalytic proteins relevant data should include the identity of the enzymes/proteins, preparation and criteria of purity, assay conditions, methodology, activity, and any other information relevant to judging the reproducibility of the results[1]. For more details check Beilstein Institut/STRENDA (standards for reporting enzymology data) commission Web site (http://www.strenda.org/documents.html).

[1] For all other data presentation not mentioned above please contact Editor for instructions.

Submission Checklist

The following list will be useful during the final checking of an article prior to sending it to the journal
for review:

- E-mail address for corresponding author,
- Full postal address,
- Telephone and fax numbers,
- All figure captions,
- All tables (including title, description, footnotes),
- Manuscript has been "spellchecked" and "grammar-checked",
- References are in the correct format for the journal,
- All references mentioned in the Reference list are cited in the text, and *vice versa*.

Submissions

Submissions should be directed to the Editor by e-mail: ***glasnik@pmf.unsa.ba***, or ***glasnikhtbh@gmail.com***. All manuscripts will be acknowledged on receipt (by e-mail) and given a reference number, which should be quoted in all subsequent correspondence.

Glasnik hemičara i tehnologa Bosne i Hercegovine

Bulletin of the Chemists and Technologists of Bosnia and Herzegovina

Print ISSN: 0367-4444
Online ISSN: 2232-7266

Zmaja od Bosne 33-35, BA-Sarajevo
Bosnia and Herzegovina
Phone: +387-33-279-918
Fax: +387-33-649-359
E-mail: glasnik@pmf.unsa.ba
glasnikhtbh@gmail.com

Sponsors

Glasnik hemičara i tehnologa Bosne i Hercegovine

Bulletin of the Chemists and Technologists of Bosnia and Herzegovina

Print ISSN: 0367-4444
Online ISSN: 2232-7266

Zmaja od Bosne 33-35, BA-Sarajevo
Bosnia and Herzegovina
Phone: +387-33-279-918
Fax: +387-33-649-359
E-mail: glasnik@pmf.unsa.ba
glasnikhtbh@gmail.com

www.elektroprivreda.ba/stranica/te-kakanj

Federalno ministarstvo obrazovanja i nauke

www.fmon.gov.ba

Zahvaljujemo se **Federalnom ministarstvu obrazovanja i nauke** na finansijskoj pomoći za izdavanje ovog broja ***Glasnika hemičara i tehnologa Bosne i Hercegovine***.

Redakcija GLASNIKA-a